Modeling and Mitigating Cascading Failures in Interdependent Power Grids and Communication Networks

by

Marzieh Parandehgheibi
B.S., Sharif University of Technology (2009)
S.M., Massachusetts Institute of Technology (2012)

Submitted to the Department of Aeronautics and Astronautics
in partial fulfillment of the requirements for the degree of
Doctor of Philosophy
at the
MASSACHUSETTS INSTITUTE OF TECHNOLOGY
June 2016

Author .....
Department of Aeronautics and Astronautics
May 9, 2016

Certified by .....
Eytan Modiano
Professor of Aeronautics and Astronautics
Thesis Supervisor

Certified by .....
Munther Dahleh
Professor of Electrical Engineering and Computer Science

Certified by .....
Konstantin Turitsyn
Assistant Professor of Mechanical Engineering

Accepted by .....
Paulo C. Lozano
Associate Professor of Aeronautics and Astronautics
Chair, Graduate Program Committee

Modeling and Mitigating Cascading Failures in Interdependent Power Grids and Communication Networks

by

Marzieh Parandehgheibi

Submitted to the Department of Aeronautics and Astronautics
on May 9, 2016, in partial fulfillment of the
requirements for the degree of
Doctor of Philosophy

Abstract

Many of today's critical infrastructures are organized in the form of networks, which are dependent on one another. A particular example is the power grid and the communication network used to control the grid. While this dependence is beneficial during normal operation, as it allows for more efficient operation, it can be harmful when the networks are under stress. Indeed, in such interdependent network infrastructures, a cascade of failures may occur where power failures can lead to communication failures, which, in turn, lead to cascading power failures. Therefore, it is necessary to develop proper models and analytical tools to asses the robustness of interdependent networks to failures. In this thesis, we develop such models with emphasis on interdependent power grids and communication networks.

Initially, we focus on the abstract modeling of interdependent networks. In particular, we propose a new model for interdependent networks with known topologies, define and analyze metrics for assessing the robustness of such networks to cascading failures, and propose algorithms for robust design of interdependent networks.

Next, we focus on the interactions between power grids and communication and control networks. We model the cascading failures in the power grid using the power flow equations, and use the communication network to implement a control policy in the power grid which mitigates cascading failures in interdependent networks. Using this model, we show that the interdependent power grids are more robust than isolated ones.

Finally, we model the impact of communication loss on the performance of power grids under two different control scenarios. The first one is the emergency control mechanism where failures in the power grid should be monitored and mitigated by the control center. In this case, we investigate the impact of simultaneous communication failures on the performance of such control mechanisms. In particular, we propose new emergency control schemes for partial communication networks, and investigate the network parameters that are most effective in causing the cascade of failures from communication networks to the power grid. The second control mechanism is distributed frequency control in power grids. We show that the optimal solution

will not be achieved under communication link failures. We propose a novel control mechanism that uses the power dynamics instead of direct information from the communication network, and show that it achieves the optimal solution and is globally asymptotically stable. We also analyze the impact of discrete-time communication on the performance of distributed frequency control. We show that the convergence time increases as the time interval between two messages increases, and propose a new algorithm that uses the dynamics of the power grid to decrease the convergence time.

Thesis Supervisor: Eytan Modiano
Title: Professor of Aeronautics and Astronautics

Acknowledgments

I would like to sincerely thank my advisor Prof. Eytan Modiano for his invaluable support and constant guidance throughout my years at MIT. I would like to also thank my thesis committee members Prof. Konstantin Turitsyn and Prof. Munther Dahleh for their valuable advice and feedback on my work and all the fruitful discussions we had. This work was not possible without their help and support.

I would also like to thank my former and current lab-mates as well as members of LIDS and RLE for their friendship and encouragement over the past couple of years at MIT. In particular, I would like to thank Greg Kuperman, Sebastian Neumayer, Matt Johnston, Nathan Jones, Guner Celik, Kayi Lee, Hyang-Won Lee, Hulya Seferoglu, Jianan Zhang, Anurag Rai, Igor Kadota, Rajat Talak, Thomas Stahlbuhk, Qingkai Liang, Abhishek Sinha, Andrea Censi, Ali-Akbar Agha-Mohammadi, Yasin Yazicioglu, Rose Faghih and Arman Rezaee. I am also thankful to LIDS and AA staff especially Jennifer Donovan, Brian Jones, Roxana Hernandez, Rachel Cohen, Lynne Dell, Beth Marois, Jean Sofronas and Joyce Light for their prompt support and kind care.

I wish to express my deepest gratitude to my parents, Zahra and Saeed, for their endless love and support throughout my life. Thank you for believing in me, encouraging me to think big and chasing my dreams. I would also like to thank my parent-in-laws, Manijeh and Ahmad, for their constant kindness and support. I am also grateful to my brother, Ali, and my sister-in-law, Shabnam, who have always inspired me to pursue my goals and supported me during ups and downs of my life. Love you all!

Finally, I would like to thank my best friend, partner and husband, Hamed, for being with me and understanding me throughout this journey. I was very lucky to meet him at MIT for the first time and share the moments of my life with him here. I cannot wait to start the next phase of our life together.

This work was supported by NSF grant CNS-1017800, DTRA grants HDTRA-09-1-0050, HDTRA1-13-1-0021 and HDTRA1-14-1-0058, and by a grant from the

MIT/Masdar Institute Cooperative Program.

Contents

List of Figures

Chapter 1

Introduction

1.1 Motivation

Many of today's critical infrastructures are organized in the form of networks, which are dependent on one another. A particular example is the power grid and the communication network used to control the grid. While this dependence is beneficial during normal operation, as it allows for more efficient operation, it can be harmful when the networks are under stress. Indeed, in such interdependent network infrastructures, a cascade of failures may occur where power failures can lead to communication failures, which, in turn, lead to cascading power failures.

The monitoring and control of today's power grid relies on a Supervisory Control and Data Acquisition (SCADA) system. One of the main control operations is the Automatic Generation Control (AGC) which is used to match power supply with demand in the grid through frequency control. This is done both at the local (generator) level, and the wide-area level. AGC systems rely on communications in order to disseminate control information, and the lack of communications, or even delay in communications can cause AGC systems to malfunction and fail, leading to wide-scale power outages [3, 4].

In August 2003, lack of real-time monitoring and rapid control decisions for mitigating failures led to a catastrophic blackout which affected 50 million people in Northeast America. According to the final report of the 2003 blackout [1], this black-

out started with the loss of three transmission lines in Ohio. However, the operators did not realize these failures due to insufficient monitoring; thus, no remedial action was taken at that time which triggered a very fast cascade, and led to a full blackout in the Northeast United States and parts of Canada. The reports in [5] and [2] indicate that the reason for tripping of many generators and transmission lines was power imbalance in the control areas and lack of communication between the operators for mitigating the failures.

It is thus essential to design the communication and control network together with control policies that facilitate widespread monitoring of the power grid, and enables the power grid to react to rapid changes and unexpected failures in the network. Moreover, for cost and sustainability considerations, the communication equipment often receive the power for operation directly from the power grid. However, this creates a strong interdependency between the two networks, where the operation of the power grid is dependent on receiving control signal from the communication network, and the operation of the communication network is dependent on receiving power from the grid. Therefore, in the case a power blackout, power outages lead to communication failures which in turn lead to additional power outages.

1.2 The 2003 Blackout

In August 14, 2003, a massive blackout occurred in the northeast United States and Ontario, Canada, where 50 million people lost power for a significant amount of time. This blackout started with the loss of transmission lines in Ohio due to inadequate tree trimming.

The operators did not realize the failure of Ohio transmission lines due to insufficient monitoring; thus, no remedial action was taken at that time. In the subsequent hour, several transmission lines and generators tripped due to overheating of power lines and local generator controls. These initial failures triggered a very fast cascade, which occurred in less than 5 minutes and led to a full blackout in Northeast America. Table 1.1 shows the sequence of key failures over time [5].

Monitoring	
14:02	Transmission line disconnects in southwestern Ohio
15:05:41 - 15:41:33	Transmission lines disconnect between eastern Ohio and northern Ohio
15:45:33 - 16:08:58	Remaining transmission lines disconnect from eastern into northern Ohio
Control	
16:08:58 - 16:10:27	Transmission lines into northwestern Ohio disconnect, and generation trips in central Michigan
16:10:00 - 16:10:38	Transmission lines disconnect across Michigan and northern Ohio, generation trips off line in northern Michigan and northern Ohio, and northern Ohio separates from Pennsylvania
16:10:40 - 16:10:44	Four transmission lines disconnect between Pennsylvania and New York
16:10:41	Transmission line disconnects and generation trips in northern Ohio
16:10:42 - 16:10:45	Transmission paths disconnect in northern Ontario and New Jersey, isolating the northeast portion of the Eastern Interconnection
16:10:46 - 16:10:55	New York splits east-to-west. New England (except southwestern Connecticut) and the Maritimes separate from New York and remain intact
16:10:50 - 16:11:57	Ontario separates from NY west of Niagara Falls and west of St. Lawrence. Southwestern Connecticut separates from NY and blacks out.
16:13	Cascade Completed

Table 1.1: Key Failures in 2003 blackout in Northeast America

As can be seen from Table 1.1 and Figure 1-1, most of the failures occurred during a 5 minute period through a rapid succession of tie lines and generators tripping. As we discuss below, much of this failure cascade was a result of "inadequate situational awareness" and could have been prevented using reliable communications and control. In fact, according to the final report by NERC, although the first stage of failures occurred slowly, operators could not stabilize the power grid due to inadequate situational awareness.

In a subsequent stage, lack of control and a large power imbalance in the grid led to tripping of tie lines and generators. According to the report by NY-ISO [2], at 16:10:39 EDT, the tie lines between Pennsylvania and New York were highly loaded

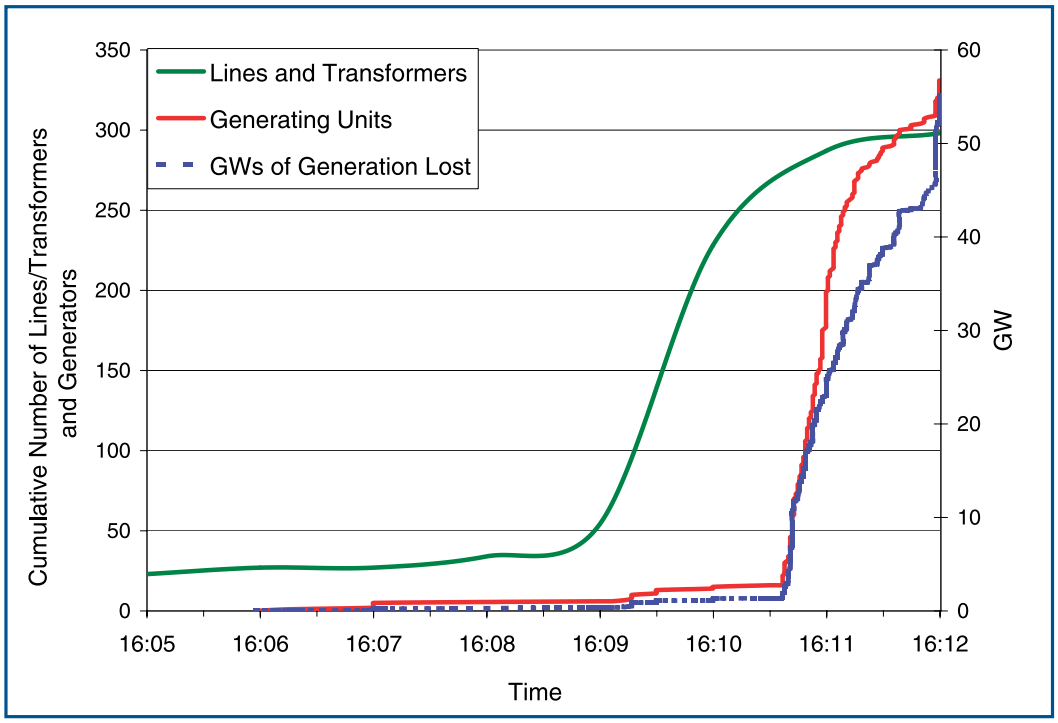

Figure 1-1: Rate of Line and Generator Trips During Blackout 2003 - source [1]

due to large power imbalance between the areas; these tile lines tripped within 6 seconds. One second later, the tie-lines between New England and New York became overloaded and tripped within two seconds. Finally, two seconds later, the tie lines between Ontario and New York tripped within less than one second. Figures 1-2 show the loss of tie lines connected to New York which led to a large amount of power loss in the area [2].

In addition, lack of proper monitoring and control led to the rapid tripping of generators. According to the final report on the 2003 Blackout, at least 265 power plants with more than 508 individual generating units shut down [1]. The NY ISO reported the detailed time scale of generators tripping [2]. The sequence of failures occurred in rapid succession over a period of 35 seconds: 16:11:04, 16:11:05, 16:11:06, 16:11:08, 16:11:09, 16:11:10, 16:11:13, 16:11:14, 16:11:17, 16:11:19, 16:11:22, 16:11:23, 16:11:27, 16:11:28, 16:11:38, 16:11:39.

Investigations show that the response of local protection devices was the cause

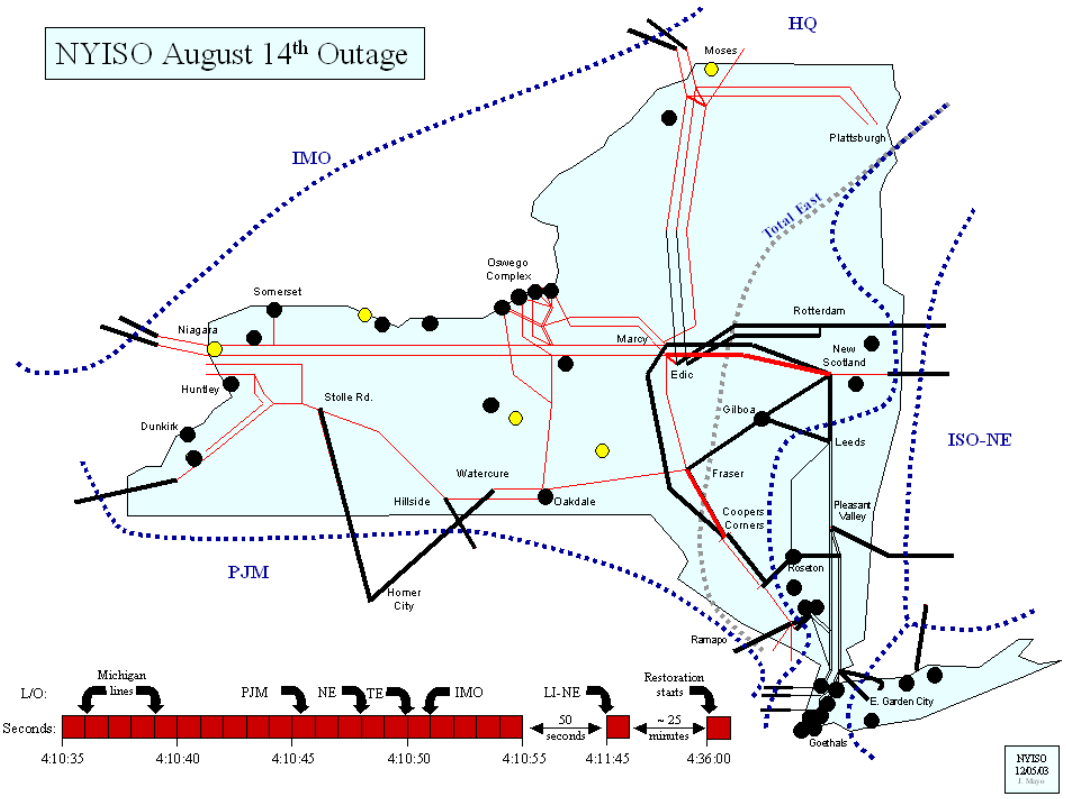

Figure 1-2: Failure of Tie lines between NYISO and PJM, NE-ISO, IMO - source [2]

of most of generators tripping. In fact, since there was no coordination between the generators and ISOs when applying the load shedding schemes, relays in generators did not tolerate the under/over frequency in the area and tripped. However, in the presence of a communication network between ISOs, a fast frequency wide-area controller could have changed the set points of generators, avoid the failures and help the grid to recover.

Another reason for tripping of some generators was the loss of power in local controllers. According to the final report, some generators received power from the grid in order to control their system. Since the grid could not supply the plant's in-house power needs reliably, the generators tripped and led to further power loss. This is a direct example of the cascading affect between communications and control even within the local control area.

1.3 Our Contributions

We now give an overview of the contributions of this thesis. Motivated by the 2003 blackout in Northeast America, we first propose a new abstract model for interdependent networks with known topologies. We define and analyze metrics for assessing the robustness of such networks to cascading failures, and propose algorithms for robust design of interdependent networks. Next, we focus on the case of power grids and communication networks. We model the cascading failures in the power grid using the power flow equations, and use the communication network to implement a control policy in the power grid which mitigates cascading failures in interdependent networks. Using this model, we show that interdependent power grids are more robust than isolated ones. Then, we model the impact of communication loss on the performance of power grid under emergency control, and investigate the network properties which are more effective in cascading the failures from communication networks to the power grid. Finally, we analyze the effect of communication loss on the performance of optimal distributed frequency control in power grids. In particular, we show that the optimal solution will not be achieved under communication link failures. We propose a novel control mechanism that uses the dynamics of the power grid instead of information from the communication network and prove that it achieves the optimal solution and is globally asymptotically stable. In the following, we describe our contributions throughout this thesis in more details.

1.3.1 Abstract Interdependency Model

In Chapter 2, we propose a new model for interdependent networks with "known" topologies. We consider two networks A and B, where every node in A is connected to source node S_A via a path in network A, and every node in B is connected to source node S_B via a path in B. In addition, the interdependency between networks A and B is described as follows. Every node in network A receives at least one incoming edge from a node in network B, and every node in network B receives at least one incoming edge from a node in network A. Figure 1-3 shows an example of

our interdependent network.

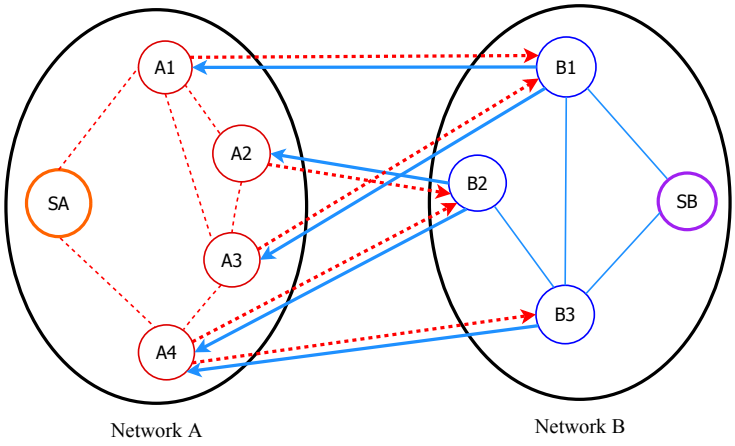

Figure 1-3: Interdependency Model - Dotted lines represent links of type A and solid lines represent links of type B. According to our model, a node in network A is operating if (a1) it is connected to source S_A via a path of operating nodes in A, and (a2) it is connected to at least one operating node in network B. Similarly, a node B is operating if (b1) it is connected to source S_B via a path of operating nodes in B, and (b2) it is connected to at least one operating node in network A.

We consider both unidirectional and bidirectional interdependent edges. In order to analyze the robustness of networks, we define several metrics for identifying the critical nodes in interdependent networks:

- Min-Node-Cut: minimum number of node removals in network A that lead to the failure of a single node in network B;
- Min-Total-Failure: minimum number of node removals from both networks that lead to the failure of entire network B;
- Min-Partial-Failure: minimum number of node removals from network A that lead to the failure of D nodes in network B.

We analyze the complexity of each metric for both cases of unidirectional and bidirectional networks. In particular, we prove that all metrics are NP-complete for networks with unidirectional interdependency. On the other hand, metrics Min-Node-Cut and Min-Total-Failure can be evaluated in polynomial time for networks

with bidirectional interdependency, where metric Min-Partial-Failure remains NP-complete under bidirectional interdependency. We propose several heuristics to approximate the NP-complete metrics.

Next, we prove that for any set of interdependent networks with similar physical properties, bidirectional interdependent networks are more robust than unidirectional interdependent networks. Moreover, we propose algorithms for explicit design of robust bidirectional interdependent networks [6, 7].

We analyze the abstract models of interdependent networks in Chapter 2; however, in reality, networks such as power grids and communication networks have more complex behaviors. In the next chapters, we focus on the interactions between these two networks.

1.3.2 Interdependent Power Grid and Communication Networks

In Chapter 3, we analyze the interdependency between power grids and communication networks by considering the power flow dynamics inside the power grid, and control mechanisms applied by the communication networks.

A simple model for analyzing the behavior of the power grid is the DC power flow model which has been widely used in the literature (see [8] for a survey on the power flow models). When a power node or line fails, its load is shifted to other elements of the grid. During this process, the flow in one or more lines may be pushed beyond their capacity which leads to the failure of the overloaded lines. Similarly, failure of these lines redistributes power and may lead to further “Cascading Failures".

In Chapter 3, we model the cascading failures inside the power grid using power flow equations. We also assume that each communication node requires a certain amount of power from the grid to operate; thus, lack of power would lead to failures in the communication network. Note that in reality, communication nodes can be supported by back up batteries or generators; thus, disconnection from the power grid may not lead to the failure of communication nodes.

Moreover, we propose an intelligent load shedding policy applied by the control and communication network to mitigate the cascade of failures inside the power grid. We simulate our model of interdependent power grid and communication networks, and show a counter-intuitive result where interdependent power grids are *more robust* than isolated ones (See Figure 1-4). This is due to the fact that although some power nodes will be lost due to interdependent cascade of failures, the cascading failures inside the power grid can be mitigated using the control scheme applied by the communication network [9].

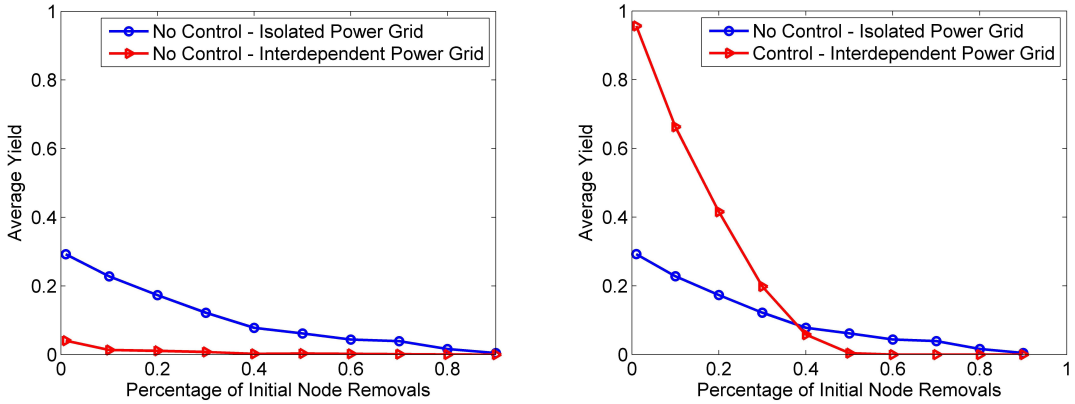

(a) No Control- Interdependent networks are more vulnerable.

(b) Control - Interdependent networks are more reliable.

Figure 1-4: Comparing yield of interdependent and isolated power grids. The yield (the ratio of served load to the initial load) in interdependent power grid and communication network without control is lower than the isolated power grid (Figure 1-4(a)). However, when intelligent control is applied to the interdependent network, the yield is higher than the isolated power grid (Figure 1-4(b)).

In Chapter 3, we use a simplistic assumption that a power node fails if it loses its connection to the communication networks. In the next two chapters of this thesis, we focus on two different control mechanisms inside the power grid, and investigate the impact of communication loss on their performances.

1.3.3 Modeling the Impact of Communication Loss on the Power Grid

There are many control mechanisms inside the power grid that serve different purposes. Some of these control mechanisms may not require a communication network,

such as the primary frequency controller, and some may require communication networks, such as the AGC or economic dispatch. However, each of these control mechanisms have different communication requirements. For example, AGC is updated every 2 to 4 seconds, whereas economic dispatch is updated every 10-15 minutes. Therefore, the effect of communication loss or delay on the performance of control mechanisms in the power grid should be analyzed separately.

In Chapter 4, we analyze the impact of communication failures on the emergency control of the power grid. Figure 1-5 shows an example of the case where simultaneous failures occur in both the power grid and communication networks. Therefore, the control center cannot control some parts of the power grid due to partial loss of communication. We design a centralized emergency control scheme under both full and partial communication network which mitigates the cascading failures in the power grid by shedding the minimum amount of load. We use our emergency control scheme to model the impact of communication loss on the power grid. We show that unlike previous models used in the literature, power nodes that have lost their connection to the communication network, and consequently the control center, do not always fail; i.e. the "point-wise" failure model is not appropriate. In addition, we show that the impact of communication loss is a function of several parameters such as the size and structure of the power and communication failure, as well as the operating mode of power nodes disconnected from the communication network [10,11].

In Chapter 5, we analyze the impact of communication failures on the performance of optimal distributed frequency control. We consider a consensus-based control scheme, and show that it does not converge to the optimal solution when the communication network is disconnected. We propose a new control scheme that uses the power dynamics to replicate the information not received from the communication network, and prove that it achieves the optimal solution under any single communication link failure. Figure 1-6 shows an example of disconnected communication network and the updated control scheme.

In addition, we show that this control improves cost under multiple communication link failures. In addition, we analyze the impact of discrete-time communication on

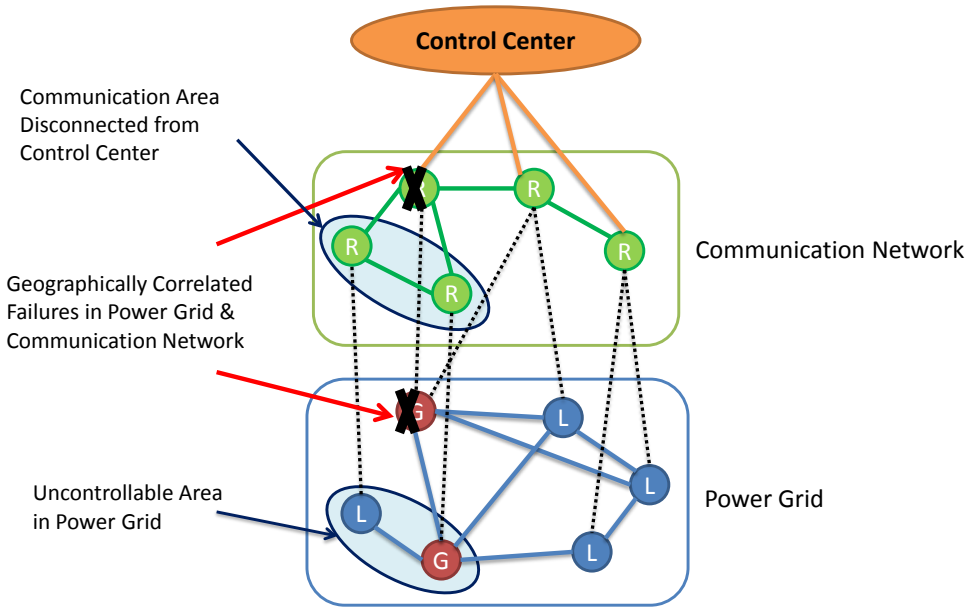

Figure 1-5: Dotted lines indicate dependency of power nodes on communication nodes. Power nodes that have lost their connection to the communication network become "uncontrollable". Note that uncontrollable nodes may operate fine using localized control, but cannot be controlled remotely because they are not reachable.

the performance of distributed frequency control. In particular, we show that the convergence time increases as the time interval between two messages increases. We propose a new algorithm that uses the dynamics of the power grid, and show through simulation that it improves the convergence time of the control scheme significantly [12].

1.4 Related Work

The concept of interdependency was first introduced by Rinaldi *et. al.* in [13], where the authors described different types of interdependencies as well as different types of failures that can occur in interdependent systems. In 2008, Rosato *et. al.* explored the impact of failures in the power grid on the performance of communication networks [14]. Moreover, the authors in [15, 16] studied the impact of power failures on multilayer communication networks whereas the authors in [17] studied the effect of geographically correlated failures on interconnected power-communication networks.

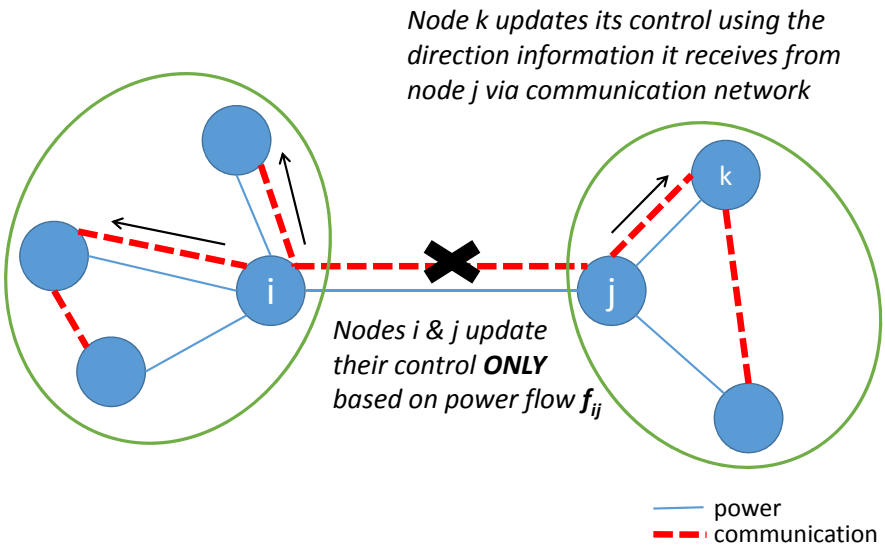

Figure 1-6: Power Grid and Communication Network - Solid lines are power lines and dashed lines are communication lines. When nodes i and j become disconnected, the optimal solution will not be achieved under the original distributed control. We design a new control where nodes i and j update their local control decision only based on the power flow between nodes i and j, and prove that the optimal solution can be achieved.

In 2010, Buldyrev *et. al.* developed the first mathematical model for describing interdependency between two networks [18]. They modeled each network as a random graph and assumed there exists a one-to-one interdependency between the two networks. They considered two networks A and B, where node in network A can operate if it is connected to the largest connected component in network A and its correspondent node in network B is also operating. Using percolation theory, they showed that failures spread more in interdependent networks than isolated networks; thus, interdependent networks are more vulnerable. Since then, there have been many follow-up works on the model by Buldyrev *et. al.*, studying the asymptotic behavior of random networks [19–22]. However, in reality networks are not random, and models and analytical tools are needed for studying networks with known topology.

There are very few papers on the interdependent networks with known topologies. In [23], the authors identified the most critical nodes by defining a new centrality measurement for interdependent networks. The authors of [24] and [25] extended the model to multilayer networks where different types of interdependency exist and a

node depends on multiple types of nodes for operation. They proposed ILP formulations to find the most vulnerable nodes under several network settings. Finally, in [26], the authors used the Moore-Penrose pseudo-inverse of the graph Laplacians to show some topological properties of the interdependency between networks.

This abstract model cannot describe the complex behavior of power grids and communication networks. In a power grid the flows are driven by Kirchoff's laws, and cannot be described by a network flow model. Thus, when a failure occurs in a power grid, the power flow is redistributed on the the rest of the network and some elements could overload and fail, leading to "Cascading Failures". The cascade of failures in the power grid is a very complex phenomena, and several models have been introduced for explaining its behavior (see for example [27–31]).

In order to prevent these failures, there are special remedial systems in the power grid that help to stabilize the grid during a disturbance. One of these remedial actions is changing the power injection at nodes (minimum load and generator shedding) so that grid's constraints are satisfied. A closely related problem in terms of formulation is the Optimal Power Flow (OPF) problem where the objective is minimizing the total cost of power generation. In our case, this can be replaced by the total cost of power loss. The OPF problem in the DC model is a well-studied problem with many extensions such as OPF with Transmission Switching [32].

The future power grid is going to integrate renewable energy resources. This will increase the fluctuations in the generation, and requires more reserve capacity to balance the power. One of the approaches to balancing power without having large reserve capacities is demand response, where loads are "adjustable" and participate in balancing the power. Since the number of loads is large, they cannot be controlled in a centralized manner. Thus, it is essential to use "distributed" control for demand response that incorporates all three stages of traditional frequency control.

Recently, there have been many attempts to develop distributed frequency control mechanisms. In particular, in [33], the authors designed a distributed frequency controller which balances the power under unknown changes in the amount of generation and load, and compared its performance with a centralized controller. In [34],

the authors proposed a primary control mechanism, similar to the droop control, for microgrids leading to a desirable distribution of power among the participants, and proposed a distributed integral controller to balance the power. These results are extended in [35], where the authors used a similar averaging-based distributed algorithm to incorporate all three stages of frequency control in microgrids. Finally, in [36], the authors proposed a similar consensus-based algorithm for optimal frequency control in transmission power grid.

Chapter 2

Abstract Modeling of Interdependent Networks

In this chapter, we study the robustness of interdependent networks where two networks are said to be interdependent if the operation of one network depends on the operation of the other one, and vice versa. We propose a new model for analyzing interdependent networks with known topology under both unidirectional and bidirectional interdependencies. We define several metrics for finding the most critical nodes in such interdependent networks, evaluate their complexity and propose heuristics for NP-complete metrics. Finally, we introduce two closely related definitions for robust design of interdependent networks; propose algorithms for explicit design, and demonstrate the relation between robust interdependent networks and expander graphs.

2.1 Introduction

Many of today's infrastructures are organized in the form of networks and are becoming increasingly interdependent. For example, the power grid and communication networks have a cyber-physical interdependency where the power nodes depend on the control signals coming from the communication nodes and communication nodes operate using the power coming from the power nodes. As another example, the power grid and gas networks have a physical-physical interdependency where the

compressors in gas networks require power from the power grid to transmit gas and the gas generators in the power grid require gas to generate power.

Although interdependency is required for the operation of both networks under normal conditions, if a failure happens inside one of the networks it can cascade to the other network. For example, if a failure occurs inside the power grid, some of the communication nodes will lose their power and fail. As a result, new power nodes lose their control and fail which can lead to the failure of additional communication nodes. Thus, a cascade of failures can occur between the two networks due to the strong interdependency.

The concept of interdependency was first introduced by Rinaldi *et. al.* in [13], where the authors described different types of interdependencies as well as different types of failures that can occur in interdependent systems. In 2010, Buldyrev *et. al.* developed the first mathematical model for describing interdependency between two networks [18]. They modeled each network as a random graph and assumed there exists a one-to-one interdependency between the two networks. They consider two networks A and B, where node in network A can operate if it is connected to the largest connected component in network A and its correspondent node in network B is also operating. Using percolation theory, they showed that failures spread more in interdependent networks than isolated networks; thus, interdependent networks are more vulnerable. Using this model, Parshani *et al.* showed that reducing the dependency between the networks makes them more robust to random failures [19]. In [37], the robustness of a slightly different version of interdependent networks was investigated where mutually dependent nodes have the same number of connectivity links. A discussion of follow-up works on Buldyrev's model can be found in [20].

The robustness of interdependent networks under targeted attacks was studied in [21]. The stability of interdependent spatially embedded networks, and the impact of geographical attacks on the robustness of two interdependent spatially embedded networks was studied in [38] and [39], respectively. Moreover, in [40], the notion of interdependency was generalized to more than two networks, and the ability of networks to tolerate certain structural attacks was investigated.

There have also been some efforts on designing robust interdependent networks. The authors in [41] proposed a strategy based on “betweenness" centrality measures to make a minimum number of nodes resilient such that the overall robustness of networks is increased. In [42] a dynamic enhancing model was studied, where the authors defined a healing process, where an interdependency link is formed with some given probability. They showed that there is a threshold for this probability where catastrophic failures occur below the threshold and do not occur above the threshold. Finally, the authors in [22] showed that the robustness of interdependent networks depends on the allocation of the interdependency links, and characterized an optimum allocation against random attacks.

As described above, most of the literature on interdependency follows the model of [18], and relies on the asymptotic behavior of random networks. However, in reality networks are not random, and models and analytical tools are needed for studying networks with known topology.

In this chapter, we propose a new model for interdependent networks, and we consider two types of interdependency links: bidirectional and unidirectional. We propose several metrics for identifying the impact of failures in one network on the vulnerability of the other one due to interdependency, analyze the complexity of our metrics, and propose algorithms for approximating them.

Next, we prove that interdependent networks with bidirectional edges are more robust than those with unidirectional edges, and propose two closely-related definitions for robust interdependent networks: (1) a lexicographic definition which guarantees that networks robust to large failures are also robust to small failures, and (2) a relative definition which guarantees that the ratio of the size of the initial failure to the size of the final failure is large.

Finally, we propose explicit algorithms for robust design of networks under the first definition and showed the relation of robust interdependent networks with expander graphs under the second definition.

The rest of this chapter is organized as follows. In Section 2.2, we introduce our model for interdependent networks. In Section 2.3, we introduce two closely-related

metrics for vulnerability assessment of interdependent networks, and in Sections 2.4 and 2.5, we analyze these metrics in networks with unidirectional and bidirectional interdependency, respectively. In Section 2.6, we compare the robustness of these two interdependency models. Next, in Section 2.7, we introduce two definitions for robust networks and propose algorithms for allocating the interdependency links in order to obtain the most robust bidirectional interdependent networks. Finally, in Section 2.8, we discuss the robustness of interdependent networks with general topologies, and conclude in Section 2.9.

2.2 Model

Consider network A with N_1 nodes and a set of robust source nodes S_A[1] where every node in A is connected to at least one source node in S_A via a path in network A. Similarly, network B has N_2 nodes and a set of robust source nodes S_B where every node in B is connected to at least one source node in S_B via a path in B. Without loss of generality, we assume that each network has exactly one source node, where one can replace all source nodes in S_A (S_B) with one dummy node called S_A (S_B). In addition, there exists an interdependency between nodes in networks A and B as follows: every node in network A receives at least one incoming edge from a node in network B, and every node in network B receives at least one incoming edge from a node in network A. See Figure 2-1 for an example of our interdependent network.

According to our model, a node in network A is operating if (a1) it is connected to source S_A via a path of operating nodes in A, and (a2) receives an incoming edge from at least one operating node in network B. Similarly, a node B is operating if (b1) it is connected to source S_B via a path of operating nodes in B, and (b2) receives an incoming edge from at least one operating node in network A. Note that condition (a2) guarantees the connection of node A to source S_B, as well. This is due to the fact that an operating node of type B should be connected to S_B. Similarly, condition (b2) guarantees the connection of node B to source S_A.

[1]We assume that source nodes do not fail.

It is worthwhile to note the critical difference between the interdependent networks and isolated networks which makes the analysis of interdependent networks more complex. According to our model, in interdependent networks, every node of type A will be operational if it is receiving incoming edges from both type A and type B nodes; however, its outgoing edge will be "only" of type A. Therefore, although each operational node is connected to both sources S_A and S_B via two paths, the type of nodes in each path also matters.

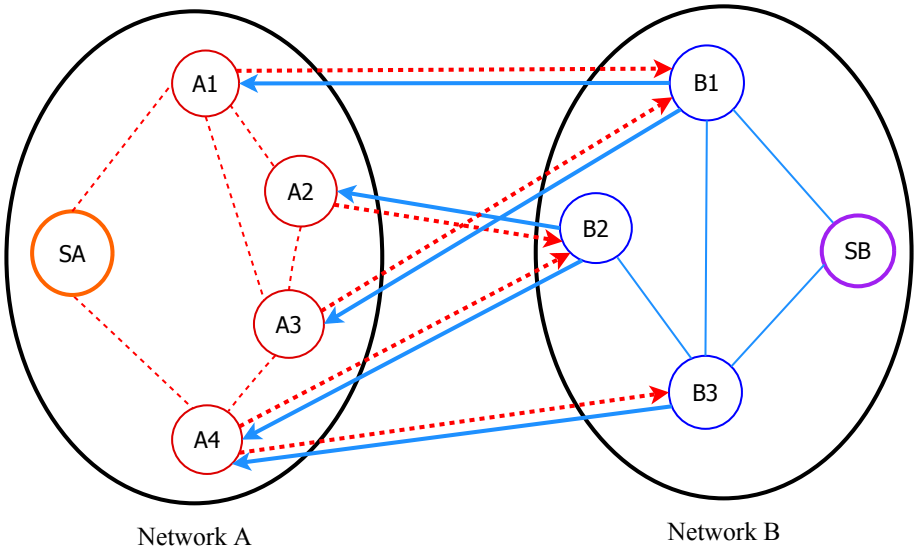

Figure 2-1: Interdependency Model - Dotted lines represent links of type A and solid lines represent links of type B.

This network can be seen as an abstract model of power grid and communication networks interdependency. Suppose network A is the power grid and network B is the control and communication network. Sources in network A are the generators and nodes are the substations, and every substation receives its power from the generator via a path. Moreover, sources in network B are the control centers and nodes are the routers, and every router receives the control signals from the control center via a path. Finally, every router has at least one incoming edge from the power grid to receive power, and every substation has at least one incoming edge from the communication network to receive control signals.

2.2.1 Effect of a Single Failure

We start with an example demonstrating that a single failure can cascade multiple times within and between networks A and B (Figure 2-2). Suppose that initially node A_4 fails (Step 1). As a result, all the edges attached to A_4 fail, and node B_3 loses its connection to network A and fails (Step 2); Consequently, node A_1 and A_3 lose their connection to network B, and node B_2 loses its connection to source S_B, and all fail (Step 3). Finally node B_1 loses its connection to network A, and substation A_2 loses its connection to source S_A, and both fail (Step 4).

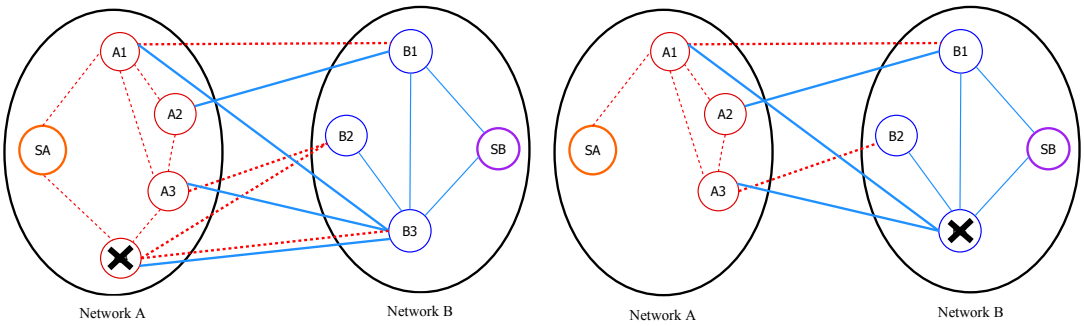

(a) Step1 - A_4 fails, initially

(b) Step2 - B_3 fails

(c) Step3 - A_1, A_3 and B_2 fail

(d) Step4 - B_1 and A_2 fail

Figure 2-2: Cascade of a single failure in an interdependent model

In this chapter, the interdependent networks A and B have special *star topologies*; i.e. every node is directly connected to the source in that network. In a star topology, failure of a node in network A cannot disconnect other nodes in network A from source S_A; and similarly, failure of a node in network B cannot disconnect other nodes in network B from source S_B. Therefore, any cascading failure in the system would be *only* due to the interdependency between the networks. We consider this topology as it gives us the opportunity to investigate the impact of interdependency

on the robustness of networks. Then, we extend our analysis to networks with acyclic topologies; i.e. trees.

2.2.2 Types of Interdependency

One can consider both unidirectional and bidirectional interdependencies. In unidirectional interdependency, interdependent edges are unidirectional; i.e. if node i in network A supports node j in network B, it is not necessarily supported by node j. In bidirectional interdependency, interdependent edges are bidirectional; i.e. if node i in network A supports node j in network B, it is also supported by node j (See Figure 2-3).

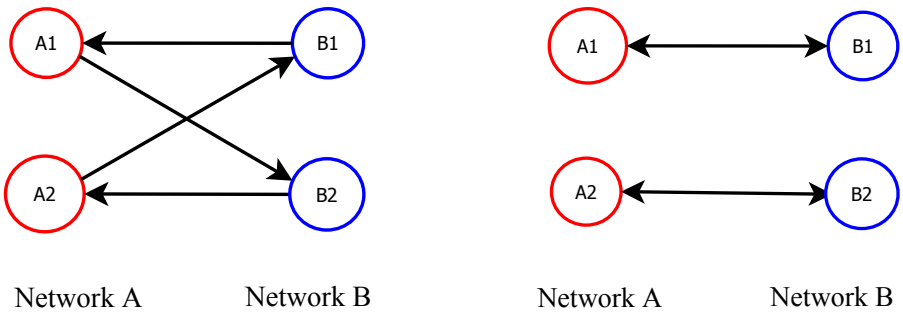

(a) Unidirectional Interdependency (b) Bidirectional Interdependency

Figure 2-3: Graph structure under different interdependency models

The main difference between the cascade of failures in these two networks is the fact that in unidirectional networks, a failure can cascade in multiple stages, whereas in a bidirectional network, a failure cascades only in one stage [2] (See [6] for more details). Later, we will see that the bidirectional interdependent networks are more robust than the unidirectional interdependent networks due to this difference.

2.3 Metrics

In order to find the most influential nodes in an interdependent network, we define two closely related metrics.

[2]Suppose failure cascades from i_1 to i_2 to i_3; i.e. two stages. This means that node i_2 has two neighbors ; i.e. two incoming edges; thus, loss of neighbor i_1 does not lead to the failure of node i_2

Definition 1. Metric $\mathcal{MR}(D)$ denoting the minimum number of node removals from network A which causes the failure of D *arbitrary* nodes in network B.

Definition 2. Metric $\mathcal{MRB}(D)$ denoting the minimum number of node removals from *both* networks which causes the failure of D *arbitrary* nodes in network B.

Note that metric $\mathcal{MR}(D)$ for $D = 1$ can be interpreted as the Min-Node-Cut; i.e. the minimum number of node removals in network A that lead to the failure of a single node in network B. In addition, metric $\mathcal{MR}(D)$ for $D = N_2$ can be interpreted as the Min-Total-Failure; i.e. the minimum number of node removals from network A that lead to the failure of entire network B. Finally, metric $\mathcal{MR}(D)$ for arbitrary values of D can be interpreted as the Min-Partial-Failure; i.e. the minimum number of node removals from network A that lead to the failure of D nodes in network B. The same interpretation holds for the metric $\mathcal{MRB}(D)$.

2.4 Unidirectional Interdependency

In the this section, we consider the interdependent networks with unidirectional interdependent edges. First, we analyze the complexity of metrics. Then, we formulate them as ILP formulations; and finally, we propose heuristic algorithms for evaluating them.

2.4.1 Complexity

We will start with evaluating a special case of $\mathcal{MRB}(D)$ where $D = N_2$; i.e. minimum node removals from both networks that lead to the failure of the entire network B. Note that failure of all nodes in network B leads to the failure of all nodes in network A, too. In the following we show that evaluating $\mathcal{MRB}(D = N_2)$ is in fact a hitting cycle problem, and prove that it is an NP-complete problem. In order to do so we start with the following lemmas:

Lemma 1. A network with one or more operating nodes has at least one cycle of operating nodes.

Proof. We prove by contradiction that no node in a network can operate if there is no cycle in the network. Suppose that there is no cycle, i.e. all nodes are connected through one or more paths. First, remove all of the non-operating nodes; hence, the remaining nodes are operating, and the network is still acyclic. Now consider the starting node of one of the paths which is either a node in network A (A_i) or a node in network B (B_j). This starting node does not have any incoming edges; therefore, it cannot operate which is a contradiction with the assumption of nodes being operating.

Now we show that existence of at least one cycle is sufficient to have an operating node. In a bipartite graph, every node in network A (network B) in a cycle receives an incoming edge from a node in network B (network A) in that cycle; thus, the nodes in that cycle can operate. If all the other nodes of the network receive an incoming edge directly or through a path starting from a node in that cycle, those nodes will be operating, too.

□

Lemma 2. To stop the operation of any cycle, one of the nodes in the cycle should be removed (Cycles are Stable Components, i.e. the operation of nodes inside the cycle is not affected by the failure of outside nodes).

Proof. By definition, every substation (router) in the bipartite graph remains operating if it has an incoming edge from an operating router (substation). Every node in a cycle receives at least one incoming edge from the nodes inside that cycle; therefore, the removal of nodes outside the cycle will not affect the operation of the nodes inside that cycle. As a result, to stop the operation of a cycle, one of its nodes must be removed. □

Note that stopping the operation of a cycle is not equivalent to stopping the operation of all the nodes inside the cycle. If the nodes inside a cycle are isolated from the other nodes, removing exactly one node from the cycle will stop all of them from operating. However, if nodes inside a cycle receive incoming edges from other

nodes outside of the cycle, more node removals are needed to cause the failure of all of the nodes in that cycle.

Lemma 3. For the failure of the entire network, at least one node from every cycle should be removed .

Proof. By contradiction - Suppose that there exists a cycle so that none of its nodes are removed. By lemma 2, all of the nodes inside that cycle remain operating, which contradicts the assumption of total failure. □

Theorem 1. The minimum number of nodes that hit all of the cycles in a bipartite graph is the optimal solution for the $\mathcal{MRB}(D = N_2)$ problem.

Proof. Immediate from lemma 3. □

Corollary 1. Finding the $\mathcal{MRB}(D = N_2)$ in star networks with unidirectional interdependency is NP-complete.

Proof. By Theorem 1, evaluating metric $\mathcal{MRB}(D = N_2)$ is a hitting cycle problem which is equivalent to the well-known problem of Feedback Vertex Set (FVS). By definition, FVS in a graph finds the smallest set of nodes so that their removal makes the graph acyclic; and it is known to be NP-complete for general graphs [43]. Moreover, Yannakakis proved that FVS is NP-complete for bipartite graphs [44]. Therefore, evaluating $\mathcal{MRB}(D = N_2)$ which is finding FVS in bipartite graphs is also NP-complete. □

Corollary 2. Finding the $\mathcal{MRB}(D)$ in star networks with unidirectional interdependency is NP-complete for any arbitrary value of D.

Proof. Since $\mathcal{MRB}(D = N_2)$, which is a special case of this problem, is NP-complete. □

An alternative version of the problem is the minimum number of *edges* needed to be removed to cause a total failure. Similar to lemmas 2 and 3, to stop the operation of any cycle, one should remove one of its edges, and to have a total failure, at least one edge from every cycle should be removed. Consequently, we have the following results:

Theorem 2. The minimum number of edges that hit all of the cycles is the optimal solution for the Edge-$\mathcal{MRB}(D = N_2)$ problem.

Corollary 3. Finding the minimum edge removals for total failure in the star networks with unidirectional interdependency is NP-complete.

Proof. By Theorem 2, minimum edge removals problem is the edge version of the hitting cycle problem which is exactly equivalent to the well-known problem of Feedback Edge Set (FES). Similar to FVS, FES finds the smallest set of edges whose removals make the graph acyclic, and it is known to be NP-complete for general graphs [43]. Furthermore, Guo *et al.* proved that FES is NP-complete for bipartite tournaments [45]. Since finding FES in bipartite tournaments is a special case of the our problem, it is also NP-complete. □

2.4.2 Formulation

It was shown in lemma 3 that finding the $\mathcal{MRB}(D = N_2)$ is a hitting cycle problem. Next, we present a cycle-based Integer Linear Programming (ILP) formulation for this problem, assuming that all of the cycles are given. Let N be a $n \times 1$ binary vector so that each component N_j takes values 1 if node j is removed and 0 otherwise. Let matrix $A \in R^{m \times n}$ be a mapping between the m cycles and n nodes, where $A_{ij} = 1$ if cycle i contains node j and $A_{ij} = 0$ otherwise. Let e be a $m \times 1$ vector of ones. Our problem can be formulated as follows.

$$\text{minimize} \quad \sum_{j=1}^{n} N_j \tag{2.1}$$

$$\text{subject to} \quad A \times N \geq e \tag{2.2}$$

$$N_j \in \{0, 1\}, \quad j = 1, \cdots, n \tag{2.3}$$

In this formulation, the objective is to minimize the number of node removals. Every row i of constraint (2.2) requires that at least one of the removed nodes should hit cycle i. In the following, we develop heuristics to solve the problem.

2.4.3 Heuristics

Since computing the $\mathcal{MRB}(D = N_2)$ is computationally difficult, we consider approximation algorithms that give a near-optimal set of node removals in polynomial time. As explained in Section 2.4, the node removal problem is equivalent to a hitting cycle problem. Thus, if we have the set of all cycles in the graph, we can apply a greedy algorithm devised for solving the hitting set problem [46]. The input to the algorithm is the set of cycles (each cycle is defined as the set of nodes it contains), and the set of nodes in the graph. This cycle-based algorithm is an iterative algorithm that works as follows. In each iteration, it removes the node that is shared among maximum number of cycles, updates the set of cycles, and repeats until no cycle remains.

This cycle-based algorithm needs the set of all cycles as input; however, in general, a graph may have an exponential number of cycles. To overcome this deficiency, we devise a new algorithm that relies on the degree of the nodes instead of the cycles. The input to the algorithm is the adjacency matrix of the graph. The algorithm is iterative: Each iteration starts with a pruning stage in which the algorithm removes all of the edges that do not belong to a cycle. In the next stage of the iteration, it removes the node that has the maximum outgoing degree. Next, the algorithm removes all nodes that fail as a result of the cascading effect of that removal. Finally, the algorithm updates the adjacency matrix of the graph and repeats the iteration until no node remains.

In the following, we compare the performance of these algorithms with the optimal solution. We consider a random bipartite graph with N nodes on each side. Note that we use random graphs to analyze our algorithms, but they apply to any deterministic graph. Since enumerating all the cycles requires exponential time, we keep the size of N small, and limit the graph to have small cycles. To do that, instead of randomly generating edges, we randomly generate cycles of size 6 or smaller until all the nodes have at least one incoming edge. For each value of N, we generate 100 random graphs and then apply our algorithms to each graph in order to find the minimum node removals. Moreover, for the optimal solution, we solve the hitting cycle problem

as given by (2.1)-(2.3) using CPLEX. As can be seen from Figure 2-4, on average, the degree-based algorithm gives a slightly larger number of nodes compared with the cycle-based algorithm and the optimal solution; however, it is very fast as it does not need to enumerate all of the cycles.

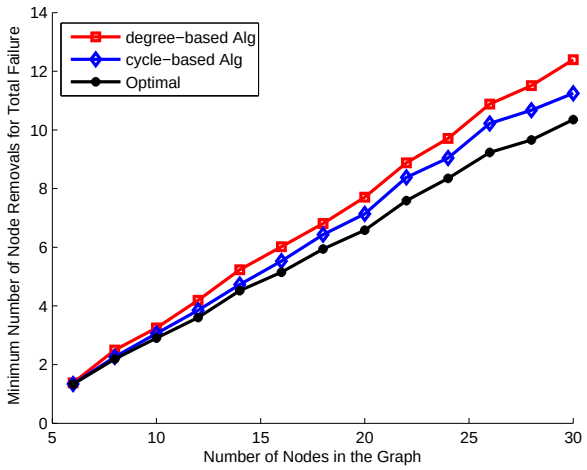

Figure 2-4: Comparing different algorithms with optimal solution

2.5 Bidirectional Interdependency

In this section, we will analyze the robustness of interdependent networks with bidirectional interdependent edges.

We start by showing that for any given set of final failures, the set of initial removals can be found in polynomial time.

Lemma 4. In bidirectional interdependent networks with star topologies, the smallest set of nodes in network A whose removals lead to the failure of a *given* set of D nodes, namely Y_D, in network B is the set of direct neighbors of nodes in Y_D, namely $\mathcal{N}(Y_D)$.

Proof. This is due to the fact that in bidirectional interdependent networks with star topologies, failures cascade only in one stage. □

Note that by Lemma 4,

$$\mathcal{MR}(D) = \min\{\mathcal{N}(Y_D) : \forall Y_D \in B, |Y_D| = D\} \tag{2.4}$$

By Lemma 4, It is easy to see that in bidirectional interdependent networks with star topology, metric $\mathcal{MRB}(D)$ can be obtained directly from metric $\mathcal{MR}(D)$ via equation 2.5. Thus, it is enough to only focus on evaluating metric $\mathcal{MR}(D)$

$$\begin{aligned}\mathcal{MRB}(D) &= \min\{\mathcal{MR}(D-1)+1, \mathcal{MR}(D)\} \\ &= \min_{i=0,\cdots,D}\{\mathcal{MR}(i)+D-i\} \end{aligned} \tag{2.5}$$

Next, we analyze the complexity of metrics in bidirectional interdependent networks; then, provide ILP formulations; and finally, we present heuristic algorithms to evaluate the metrics. It's worth noting that all the analysis in the rest of this section are focused on "bidirectional" interdependent networks with "star" topology unless mentioned otherwise.

2.5.1 Complexity

In this section, we show that evaluating $\mathcal{MR}(D)$ and $\mathcal{MRB}(D)$ are NP-complete problems in general; however, for certain values of D, they can be solved in polynomial time.

Theorem 3. For arbitrary values of D, finding the $\mathcal{MR}(D)$ in a bidirectional interdependent network with star topology is an NP-complete problem.

Proof. The proof is based on a reduction from the problem of balanced complete bipartite subgraph which is known to be NP-complete [43]. Consider graph G as a bidirectional interdependent network. According to Lemma 4, nodes in set $Y \in B$ fail if *all* of their direct neighbors, namely nodes in $X \in A$, are removed. Note that nodes in X can have direct neighbors other than nodes in Y; i.e. nodes in set $B \setminus Y$ (See Figure 2-5(a)). Finding $\mathcal{MR}(D)$ in graph G is equivalent to finding the smallest set X whose removal leads to the failure of set Y with at least D nodes.

In order to prove the hardness of finding $\mathcal{MR}(D)$, we construct a new bipartite graph G' as the complement of graph G where all of the interdependent edges are

removed, and all disjoint pairs are connected with a bidirectional edge (See Figure 2-5(b)). Since there is no connection between nodes in sets Y and $A \setminus X$ in graph G, subgraph $(Y, A \setminus X)$ forms a complete bipartite graph (biclique) in G'. Therefore, finding $\mathcal{MR}(D)$ is equivalent to finding the largest set $A \setminus X$ where $(A \setminus X, Y)$ is a biclique and Y contains at least D nodes.

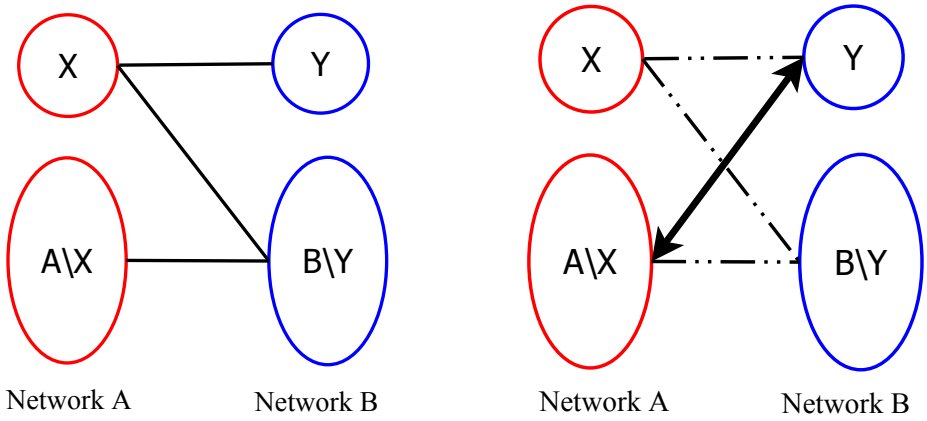

(a) Graph G (b) Graph G'

Figure 2-5: Graph Topologies in Proof of Theorem 3

Next we show that finding such biclique is an NP-complete problem. The proof of hardness is based on a reduction from the problem of balanced complete bipartite subgraph which is known to be NP-complete [43].

Definition 3. *Balanced Complete Bipartite Subgraph:* Given a bipartite graph $G = \{V, E\}$ and a positive integer $K \leq |V|$, are there two disjoint subsets $V_1, V_2 \subset V$ such that $|V_1| = |V_2| = K$ and any pair of nodes in (V_1, V_2) be an edges in E?

Next, we show that if we can solve our problem in graph G for every value D, then we can solve the Balanced Complete Bipartite Subgraph problem in graph G' for every value $K = D$ as follows. Suppose that $\mathcal{MR}(D)$ can be evaluated in graph G in polynomial time. Thus, for every value of D, we can find the largest $A \setminus X$ subgraph of G' in polynomial time so that $(A \setminus X, Y)$ is complete and $|Y| \geq D$. If $|A \setminus X| \geq D$, there exists a complete bipartite graph of size D in graph G', and if $|A \setminus X| < D$, there exists no complete bipartite graph of size D in G'. Therefore, we can decide if there exists a balanced complete bipartite subgraph of size $K = D$ in

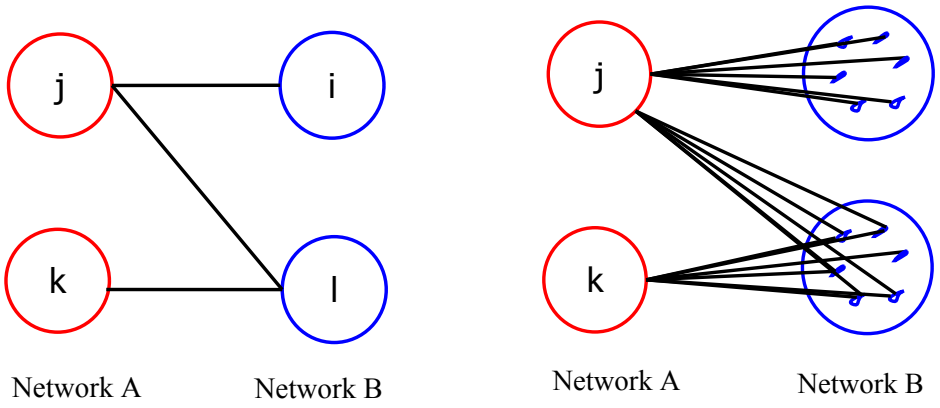

(a) Subnetwork G (b) Subnetwork G'

Figure 2-6: Conversion of subnetwork G to subnetwork G'

G' in polynomial time which is a contradiction. Thus, our problem is NP-complete.

□

Corollary 4. For arbitrary values of D, finding the $\mathcal{MRB}(D)$ in a bidirectional interdependent network with star topology is an NP-complete problem.

Proof. The proof is based on a reduction from NP-complete problem $\mathcal{MR}(D)$ (Theorem 3). For an arbitrary bipartite network G, construct network G' as follows. Replace every node $i \in B$ with a cluster of W nodes, where W is a very large number ($W > N_1 + N_2$). For every node $j \in A$ connected to node $i \in B$ in network G, connect $j \in A$ in network G' to all W nodes replacing $i \in B$ (See Figure 2-6). Now it is enough to show that if metric $\mathcal{MRB}(D)$ can be evaluated in polynomial time for network G', metric $\mathcal{MR}(D)$ can also be evaluated in polynomial time for network G, which is a contradiction to Theorem 3.

Suppose one can evaluate $\mathcal{MRB}(D)$ in network G' for failure of $D' = WD$ nodes in B in polynomial time. It is easy to see that for any removal of nodes $X \in A$ in network G leading to D failures in B, removal of the same exact nodes from A in network G' leads to the failure of $D' = DW$ nodes in B and vice versa. This is due to the fact that in network G', all edges between every $j \in A$ and a cluster of W node in B are mapped according to edges in graph G. Moreover, since $W > N_1 + N_2$, all removals will be only from network A. Thus, $\mathcal{MRB}(D)$ for $D' = DW$ failures in network G' is exactly the same as $\mathcal{MR}(D)$ for D failures in network G.

□

Proposition 1. $\mathcal{MR}(D)$ can be found in polynomial time for values of $D = k$ and $D = N_2 - k$ where k is a constant. In particular, for $D = 1$, $\mathcal{MR}(D)$ is the minimum degree of nodes in network B, and for $D = N_2$, $\mathcal{MR}(D)$ is the size of network A; i.e. N_1.

Proof. By Lemma 4, $\mathcal{MR}(D) = \min\{\mathcal{N}(Y_D) : \forall Y_D \in B\}$. For $D = k$ and $D = N_2 - k$, the number of combinations of Y_D is polynomial in D (i.e., $C(N_2, k) = C(N_2, N_2 - k) = O(N_2^k)$); thus, $\mathcal{MR}(D)$ can be found in polynomial time.

For $D = 1$, clearly the target node in network B is the one with the minimum number of neighbors in network A; thus, $\mathcal{MR}(D)$ is the minimum degree of nodes in network B.

For $D = N_2$, we prove our claim by contradiction. Suppose node $i \in A$ has not been removed. Since failures cascade only in one stage, removal of no set of nodes in network A can lead to the failure of node $i \in A$. Thus, i remains an operating node, which means that it is connected to at least one node $j \in B$. Therefore, node $j \in B$ is operating, too; i.e. $D < N_2$ which is a contradiction. □

Proposition 2. $\mathcal{MRB}(D = N_2)$ can be found in polynomial time.

Proof. As discussed before, in bidirectional interdependent networks, edges are cycles of length two, and hitting cycles of length two guarantees hitting cycles of larger size. On the other hand, hitting at least one node in every cycle of size two is equivalent to finding the minimum vertex cover in bipartite graphs. By K*ö*nig's Theorem, finding the minimum vertex cover in bipartite graph is equivalent to maximum matching, which is polynomially solvable [47]. Thus, finding the minimum node removals from both networks to cause the failure of the entire network is polynomially solvable. □

Next, we show that not only one cannot evaluate the exact value of $\mathcal{MR}(D)$ in polynomial time (unless $\mathcal{P} = \mathcal{NP}$), one cannot approximate this metric in polynomial time.

Theorem 4. There exists no PTAS to provide an r-approximation for the $\mathcal{MR}(D)$ for some values of $r > 1$.

Proof. The proof is based on the inapproximability of the balanced biclique problem [48, 49]. The details can be found in Appendix 2.10.1. □

In the following, we formulate the problem as an ILP and then, show several heuristics that provide nearly-optimal approximations for metric $\mathcal{MR}(D)$ in practice.

2.5.2 Formulation

Here, we provide an ILP formulation for evaluating metric $\mathcal{MR}(D)$. Let N_1 denote the number of nodes in network A and N_2 denote the number of nodes in network B. Moreover, let X denote the set of binary variables associated to the nodes in network A where $X_i = 1$ if node i is removed, and $X_i = 0$ otherwise. Similarly, let Y denote the set of binary variables associated to the nodes in network B where $Y_j = 1$ if node j fails due to the cascading effect, and $Y_j = 0$ otherwise. Our formulation is as follows.

$$\min \quad \sum_{i=1}^{N_1} X_i \tag{2.6a}$$

$$\text{s.t.} \quad Y_j \leq X_i \quad (i,j) \in E \tag{2.6b}$$

$$\sum_{j=1}^{N_2} Y_j \geq D \tag{2.6c}$$

$$X_i, Y_j \in \{0,1\} \tag{2.6d}$$

Here, the objective is to minimize the number of node removals from network A. Constraint (2.6b) shows that node Y_j from network B fails if all of its direct neighbors in network A are removed. Moreover, constraint (2.6c) enforces the failure of at least D nodes in network B.

2.5.3 Heuristics

In this section, first we propose three heuristics and then, compare their performances using simulation results.

Greedy Algorithm

The first algorithm is a Greedy approach that only uses the adjacency matrix of the network, and works as follows.

	Greedy Algorithm
1	Initialize the removal and failure sets as $R = \phi$ and $F = \phi$;
2	Select the node with minimum degree in network B, and add it to F; If there are several nodes with minimum degree, select one randomly;
3	Remove all nodes in network A that are attached to the node selected in Step 2. Add these nodes to set R;
4	Remove all the edges attached to the nodes in F and R. Update degrees;
5	Repeat previous steps until $\|F\| = D$;
6	Return $\|R\|$.

In each iteration, the greedy algorithm removes the minimum number of nodes from network A required for the the failure of one additional node in network B. Therefore, after at most D iterations, removal of nodes in set R leads to the failure of D nodes in network B; i.e. set F.

Proposition 3. In the worst case, the solution of greedy algorithm is no more than D times the optimal solution.

Proof. By contradiction - Suppose that $\mathcal{MR}(D) = X$; thus, the degree of each node in the optimal failure set in network B is at most X. Moreover, suppose that the greedy algorithm returns a removal set of size X' where $X' > DX$. Thus, greedy algorithm has selected a node in network B with degree of larger than X. This is contradiction to the fact that greedy starts by selecting nodes in network B with minimum degree, and there are at least D nodes with degree smaller than or equal to D.

Next, we show that this bound can be tight. Consider a bipartite graph where network A has $X(D+1)$ nodes divided into $D+1$ batches of equal sizes, and network

B has $2D$ nodes divided into two batches of equal sizes. Connect each node i in the first batch of network B to all the X nodes in the i^{th} batch in network A. Moreover, connect all of the D nodes in the second batch in network B to all of the X nodes in the last batch in network A (See Figure 2-7). It is easy to see that $\mathcal{MR}(D) = X$ where the greedy algorithm could select XD nodes. This is due to the fact that all nodes in network B have degree X. Thus, greedy algorithm could select all nodes from the first batch in network B which requires XD removals from network A.

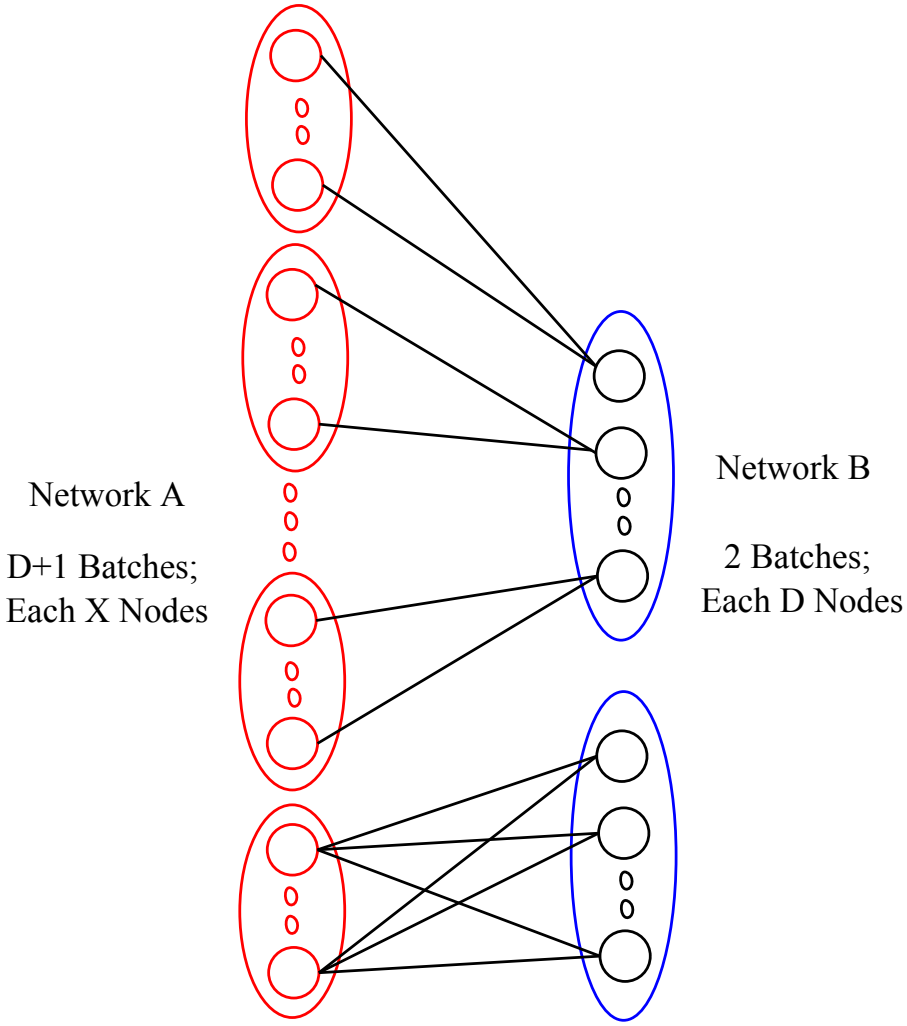

Figure 2-7: A scenario where worst-case bound of greedy algorithm is tight.

□

Note that in the example of Proposition 3, all nodes in network B have equal

degrees, and the greedy algorithm selects one of them randomly. Therefore, although this algorithm could achieve the worst-case solution, the probability of this event is $(1-\frac{D}{2D})(1-\frac{D-1}{2D-1})\cdots(1-\frac{1}{D+1})$ which becomes very small as D increases. Later, in the simulation section, we will show that the greedy algorithm has a good performance in most scenarios.

Randomized Rounding

The second algorithm is a modified randomized rounding. Randomized rounding is a widely used technique to solve difficult integer optimization problems. In general, it solves the Linear Program (LP) relaxation of the original ILP formulation, and rounds the solution randomly. In our case, we relax the constraint (2.6d) so that X and Y can take any real value in range $[0, 1]$.

Let X_i^* and Y_j^* be the optimal values of the relaxed LP problem. Our randomized rounding algorithm works as follows.

	Randomized Rounding
1	Initialize the removal and failure sets as $R = \phi$ and $F = \phi$;
2	Select each node $Y_j \in B$ with probability Y_j^*, and add it to set F;
3	Repeat step 2 until $\|F\| = D$; i.e. D nodes fail;
4	Find all the nodes in network A that are attached to the nodes in the failure set F. Add all these nodes the set of removals R;
6	Return $\|R\|$.

In this algorithm, we select nodes from network B randomly and independently until D nodes are selected for the failure set F. Clearly, nodes with larger values of Y_j^* have a higher chance to be part of set F. Later, we will see in the simulation section that for networks that Y_j^* has values close to either 1 or 0, the randomize rounding algorithm provides a nearly-optimal solution.

Simulated Annealing

Simulated Annealing is a random search strategy that can be used to find the near optimal solutions for integer problems [50]. Here, we propose two versions of the SA where the difference is in selecting the neighbors.

The first algorithm selects a random neighbor R' of current removal set R by adding, removing or replacing nodes in R, and then checking for feasibility; i.e. checking if the new removal set R' leads to the failure of D nodes in network B. If the neighbor set R' is feasible and has smaller or equal number of nodes, algorithm moves to R' with probability 1. If R' is feasible but larger; i.e. has an additional node $i \in R' \backslash R$, the algorithm moves to R' with some positive probability proportional to the degree of node i such that neighbors with larger degree nodes are more likely to be selected.

Let $d(i)$ denote the degree of node i. The details of first SA algorithm are as follows.

	Simulated Annealing 1
1	Start with an initial set of node removals $R = R_0$ from A that lead to the failure of D nodes in B; Set initial temperature T, final temperature T_F, and reduction parameter $r \in (0, 1)$;
2	Repeat the followings for L times: a) Pick a neighbor of R, namely R', by either adding, removing or replacing one random node in R; b) set $\Delta = 1$, if $\|R'\| > \|R\|$; and set $\Delta = -1$, otherwise; c) If R' is feasible; i.e. removal of nodes in R' leads to the failure of D nodes in B, move to the new neighbor according to the following rules: i) if $\Delta = -1$, set $R = R'$ and $F = F'$; ii) if $\Delta = 1$, set $R = R'$ and $F = F'$ with probability $exp(-\frac{1}{T}(1 - \frac{d(i)}{\sum_{i=1}^{N_1} d(i)}))$;
3	Set $T = rT$;
4	Repeat steps 2 and 3 until $T < T_F$;
5	Return $\|R\|$.

Next, we propose another Simulated annealing algorithm which selects a random neighbor F' of failure set F such that $|F'| \geq D$. This guarantees that the removal set R' associated to failure set F' is always feasible. Under this selection, if R' has smaller or equal number of nodes than R, the algorithm moves to the new neighbor; otherwise, it moves to the larger neighbor with some positive probability proportional to the increase in size of removal set, where larger R' has lower probability to be selected. The details of algorithm is as follows.

In practice, we initialize both simulated annealing algorithms with the solution of

Simulated Annealing 2

1 Start with an initial set of node removals $R = R_0$ from A that lead to the failure of D nodes in B; Set initial temperature T, final temperature T_F, and reduction parameter $r \in (0, 1)$;
2 Repeat the followings for L times:
  a) Pick a *feasible* neighbor of F, namely F', according to the following rules:
    i) if $|F| = D$, either add or replace a random node in F (call it F'), and find the set of removals R' for failure of F';
    ii) if $|F| > D$, randomly add or remove a node from F (call it F'), and find the set of removals R' for failure of F';
  b) set $\Delta = 1$, if $|R'| > |R|$; and set $\Delta = -1$, otherwise;
  c) Move to the new neighbor according to the following rules:
    i) if $\Delta = -1$, set $R = R'$ and $F = F'$;
    ii) if $\Delta = 1$, set $R = R'$ and $F = F'$ with probability $exp(-\frac{|R'|-|R_0|}{T})$;
3 Set $T = rT$;
4 Repeat steps 2 and 3 until $T < T_F$;
5 Return $|R|$.

greedy algorithm to have a good starting point. In addition, instead of returning the final removal set, the algorithm returns the smallest $|R|$ found during all iterations.

Comparison

In this section, we compare the performances of our algorithms by running simulations over a set of networks. We also obtain the optimal solution by solving the ILP formulation given by equations (2.6a)-(2.6d) using CPLEX. The ILP can be solved for small networks; thus, we can compare the performance of our algorithms with the optimal solution.

Since the networks in this section have bipartite topologies, we generate random bipartite graphs according to the Molloy and Reed model, where every pair of nodes are randomly connected based on the degree of all nodes (See [51] for more details). Here, we consider networks with two types of degree distributions: Type (1) all N nodes on both sides have a binomial degree distribution with average k[3], and Type (2) half of nodes in each side has a binomial degree distribution with average k_1 and

[3]We also generated random regular bipartite graphs with degree k; since the behavior of regular graphs was very close to graphs with binomial distribution, we do not show the simulation results

the other half has a binomial distribution with average k_2.

Figures 2-8(a)-2-8(d) show the performances of our algorithms for type(1) networks of size $N = 100$ and average degrees $k = 1, \cdots, 4$. It can be seen that for $k = 1$, the randomized rounding is nearly optimal. However, as k increases, its performance degrades. This is due to the fact that for small degree networks, the optimal solution of the relaxed LP achieves values close to 0 or 1. Thus, approximating these values will give a nearly optimal solution. However, as the degree increases, the values of variables in the relaxed LP are no longer close to 0 or 1; thus, the approximation of these values is no longer close to the optimal solution.

Moreover, as k increases, the performance of the greedy algorithm improves. The reason is that in networks with small degrees, there are fewer nodes in network B that have common neighbors in A. Therefore, the greedy algorithm has a lower chance to find them. However, when the degree increases, more nodes share neighbors; thus, the greedy algorithm performs better (See Proposition 3 for a more detailed argument).

Finally, as expected both simulated annealing algorithms perform better than greedy algorithm. This is due to the fact that the starting point of the simulated annealing algorithm is selected to be the output of the greedy algorithm.

Figures 2-9(a)-2-9(d) show the runtime of the algorithms for the same set of networks. It can be seen that greedy and randomized rounding are very fast, and the runtime for the optimal solution becomes prohibitive as the size of the network increases. Moreover, it can be seen that the first simulated annealing algorithm has an almost constant run time for all values of average degree k and final failures D, whereas the runtime of the second simulated annealing algorithm remains constant for all values of average degree k, but increases as D increases.

We also analyze the performances of our algorithms for the same set of networks but larger values of D. Figures 2-10(a)-2-10(d) show that the behavior of the algorithms remains the same, and the the first simulated annealing algorithm performs nearly-optimal.

Next, we analyze the performances of our algorithms for type(2) networks of size $N = 100$ and average degrees of $k_1 = 2$ and $k_2 = 20$. It can be seen from Figure

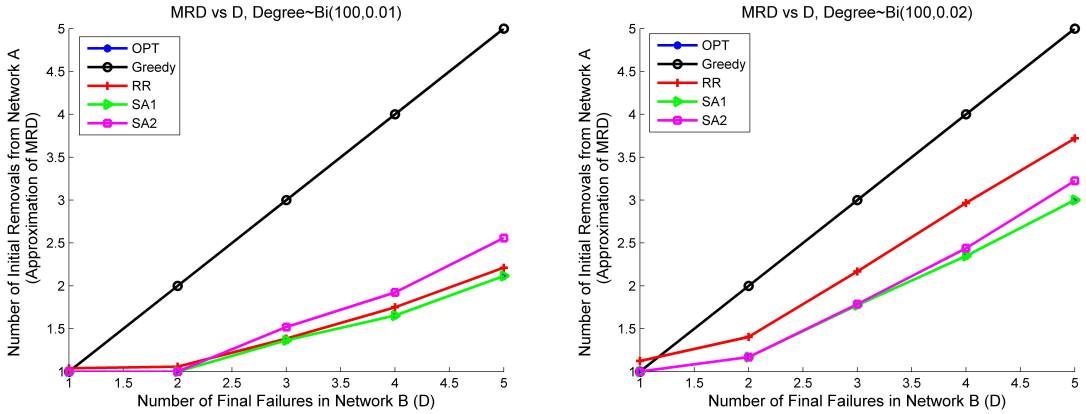

(a) k=1

(b) k=2

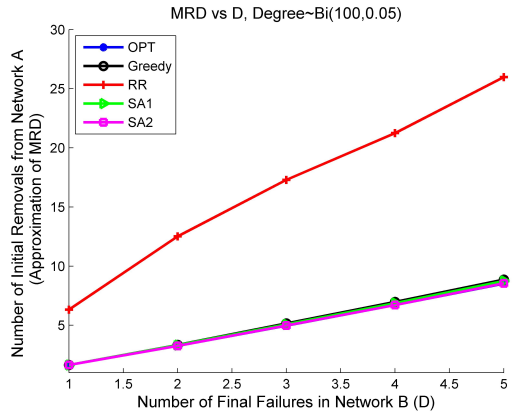

(c) k=3

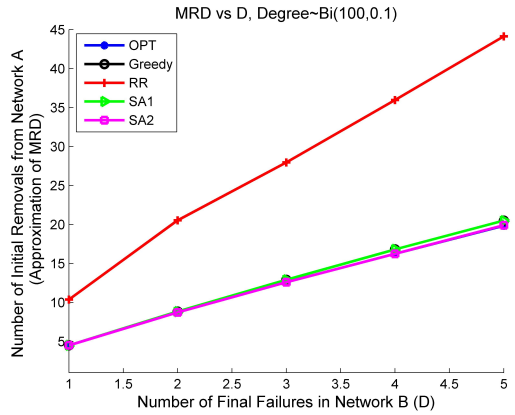

(d) k=4

Figure 2-8: Minimum Node Removal vs Final Failure Size, Type(1) network of size $N = 100$, Failure sizes $D \in [1, 2, 3, 4, 5]$

2-11 that the first simulated annealing algorithm provides the best performance. We also observed that the randomized rounding algorithm performs poorly in this set of networks.

Finally, we consider larger networks of size $N = 1000$. For this size of network, the ILP formulation cannot be solved optimally anymore as the run-time becomes prohibitive. Thus, we only compare the performances of the heuristic algorithms. Figures 2-12 and 2-13 illustrate the results of networks of type(1) and type(2). It can be seen that the simulated annealing algorithms do not provide a significant improvement in the size of initial removals compared to the greedy algorithm, while their run time is much larger than the greedy algorithm.

Another interesting point is that for large networks, the second simulated an-

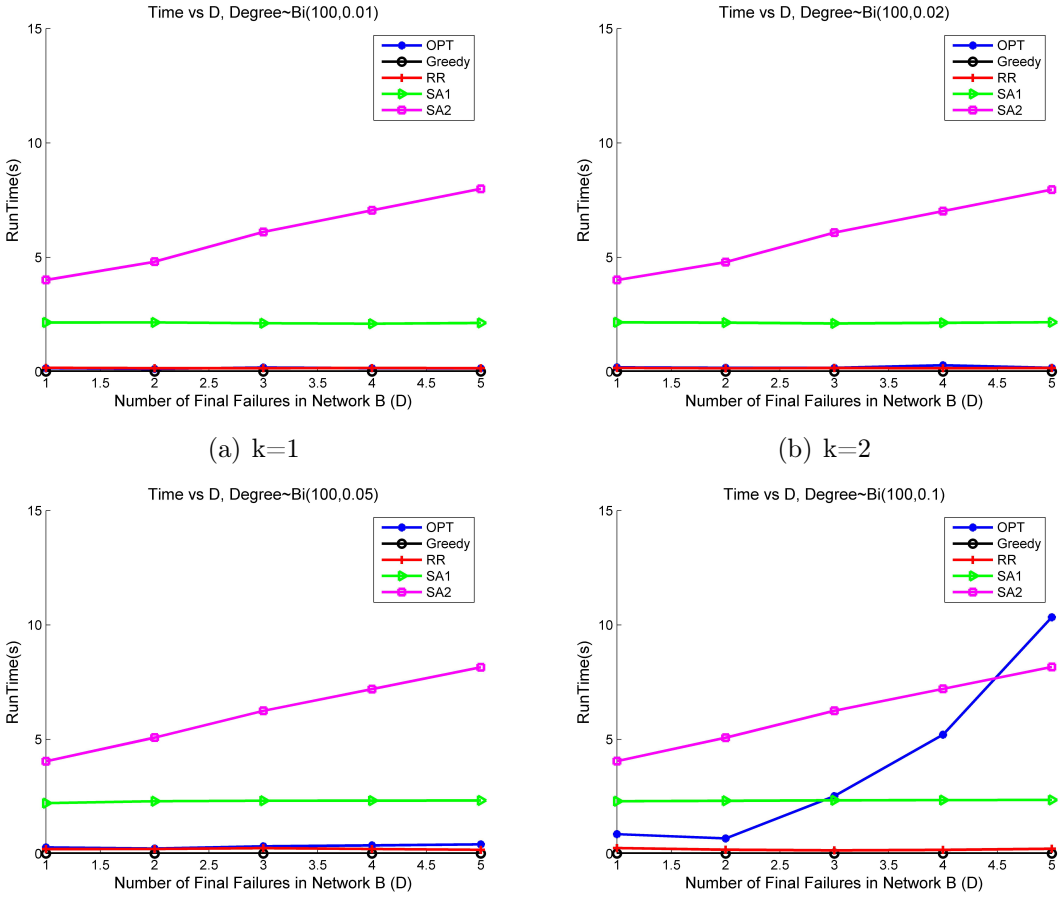

(a) k=1 (b) k=2

(c) k=3 (d) k=4

Figure 2-9: Run-time vs Final Failure Size, Type(1) network of size $N = 100$, Failure sizes $D \in [1, 2, 3, 4, 5]$

nealing algorithm outperforms the first one. Moreover, the run time of the second simulated annealing algorithm remains constant, while the run time of the first simulated annealing algorithm increases as D increases.

2.6 Comparing the interdependency models

We have seen that when networks have unidirectional interdependency, finding the $\mathcal{MRB}(D = N_2)$ is NP-complete; however, it can be solved in polynomial time when the networks have bidirectional interdependency. Here, we try to explain by way of an example why the analysis of unidirectional interdependency is more difficult than bidirectional interdependency. Figures 2-3(a) and 2-3(b) show two networks with the

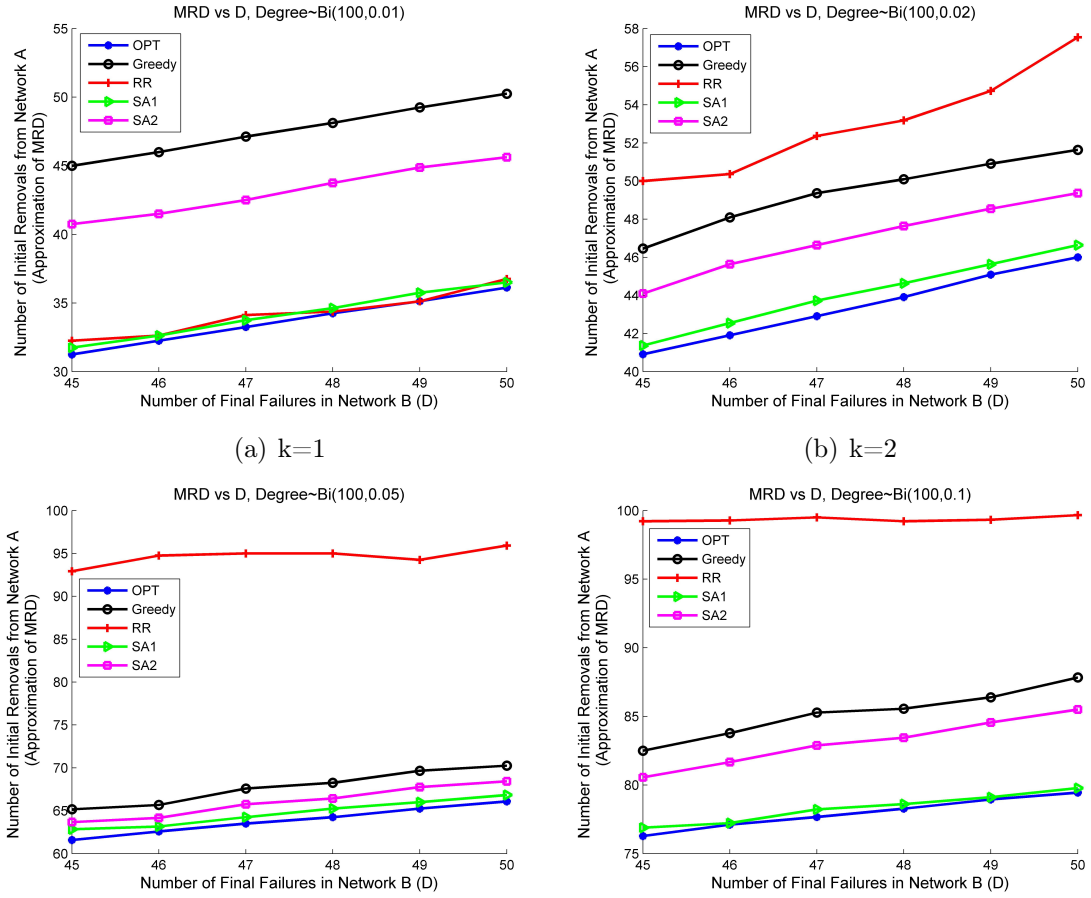

(a) k=1 (b) k=2

(c) k=3 (d) k=4

Figure 2-10: Minimum Node Removal vs Final Failure Size, Type(1) network of size $N = 100$, Failure sizes $D \in [45, 46, 47, 48, 49, 50]$

same topology under the different interdependency models. Suppose that in both networks, node A_1 is intentionally removed. It can be seen that the removal of A_1 in network 2-3(a) leads to the sequential failure of nodes B_2, A_2, and finally B_1. However, removal of A_1 in network 2-3(b) can only cause failure of node A_2. These observations indicate that in the case of unidirectional interdependency, a failure can cascade multiple times between the networks. However, in the case of bidirectional interdependency, a failure cascades only in one stage: either from network A to network B or from network B to network A. This makes the analysis of bidirectional interdependent networks more tractable.

Next we compare the robustness of the interdependency models. We use the random graphs generated in section 2.4.3 to generate a new set of graphs with the

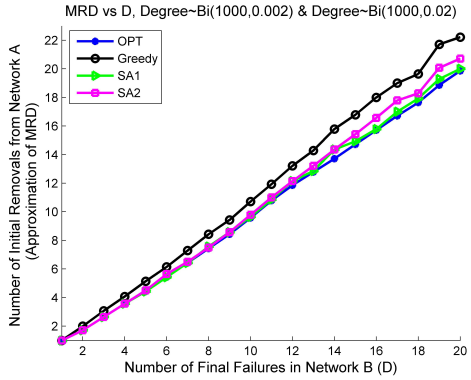

Figure 2-11: Minimum Node Removal vs Final Failure Size, Type(2) network of size $N = 100$ and $k_1, k_2 = [2, 20]$, Failure sizes $D \in [1, \cdots, 20]$

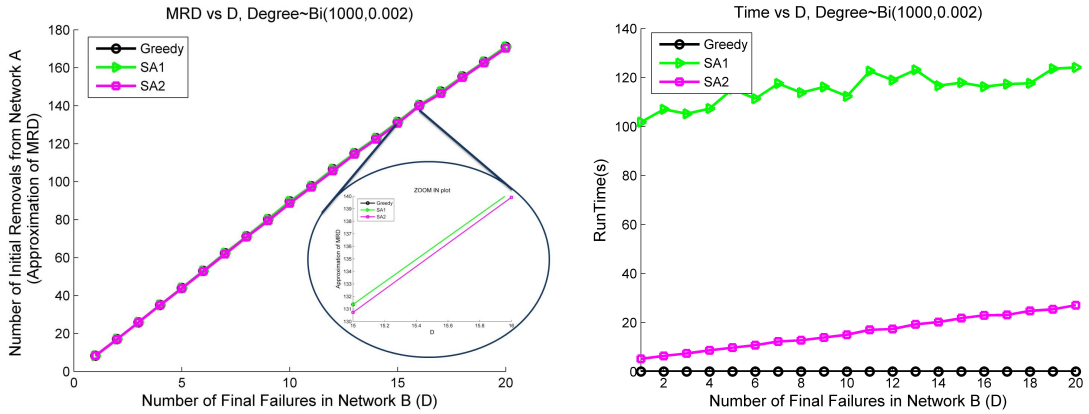

(a) Minimum Node Removal vs Final Failure Size

(b) Run-Time vs Final Failure Size

Figure 2-12: Minimum Node Removal and Run-Time vs Final Failure Size, Type(1) network of size $N = 1000$, Failure sizes $D \in [1, \cdots, 20]$

same number of edges but bidirectional dependency. To compare the robustness of the two models, we find the optimal solution in the unidirectional graphs by solving the hitting set problem using CPLEX, and bidirectional graphs by solving the vertex cover problem. It can be seen from Figure 2-14 that for all values of N, networks with bidirectional dependency need more node removals; therefore, they are more robust to failures. This observation shows that the existence of more disjoint cycles and shorter cycles makes a network more robust.

In the following theorem, we prove that for any two interdependent networks with similar physical properties, the network with bidirectional edges is more robust than the one with unidirectional edges.

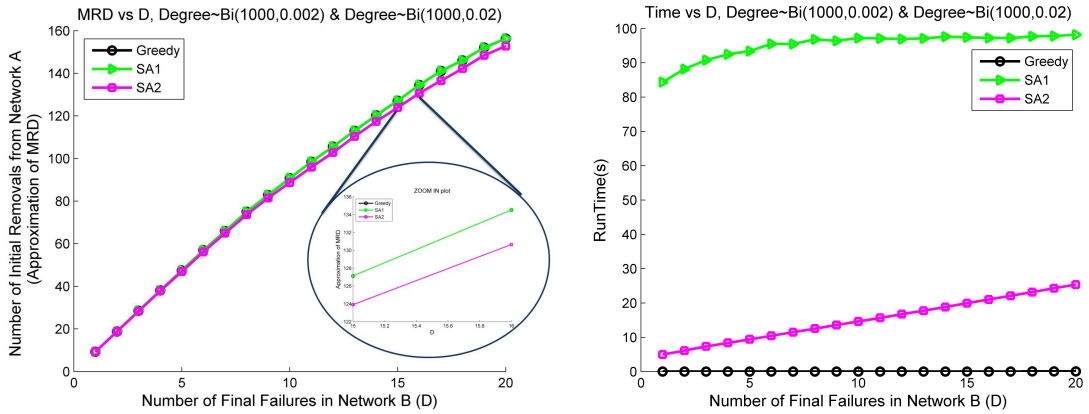

(a) Minimum Node Removal vs Final Failure Size

(b) Run-Time vs Final Failure Size

Figure 2-13: Minimum Node Removal and Run-Time vs Final Failure Size, Type(2) network of size $N = 1000$ and $k_1, k_2 = [2, 20]$, Failure sizes $D \in [1, \cdots, 20]$, Two Binomial Distribution

Theorem 5. Consider the set of all operating interdependent networks, namely G, with N_1 nodes in network A, N_2 nodes in network B, E edges from network A to B and E edges from network B to A, where A and B have star topologies and every node has at least one outgoing edge. For any arbitrary value of D, the network with largest $\mathcal{MR}(D)$ has bidirectional edges.

Proof. By contradiction - Let $G_1 \in G$ be the set of bidirectional interdependent networks and $G_2 \in G$ be the set of unidirectional interdependent networks, where $G_1 \cup G_2 = G$. Moreover, for any subset of D nodes in network B, namely Y_D, let $X(Y_D)$ denote the minimum node removal from network A for the failure of Y_D.

Suppose $G_1^* \in G_1$ is the bidirectional network that has the largest $\mathcal{MR}(D) = X^*$ among all networks in G_1. Next, we prove by contradiction that there exists no unidirectional interdependent network with larger $\mathcal{MR}(D)$.

Consider an arbitrary unidirectional interdependent network in G_2. In order to cause the failure of any subset Y_D with minimum node removal ($X(Y_D)$), one should either remove its direct neighbors $N(Y_D)$ (i.e. the set of nodes in network A that provide direct incoming edges to nodes in Y_D) or the nodes that their failure leads to the failure of $N(Y_D)$. Thus, $X(Y_D) \leq N(Y_D)$. Suppose there exists $G_2^* \in G_2$ with $\mathcal{MR}(D) > X^*$. It means that there exists an allocation of E edges from network A

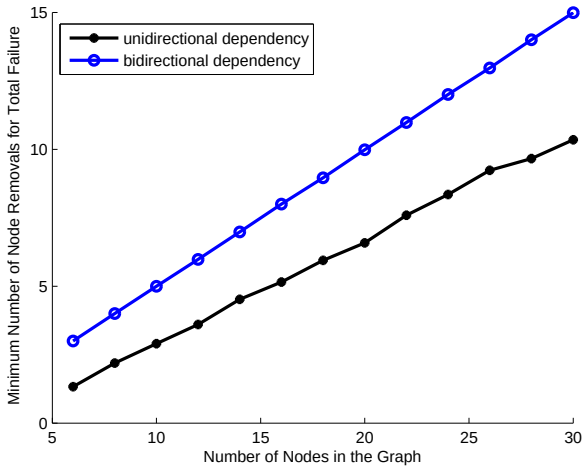

Figure 2-14: Comparing the robustness of interdependency models

to B such that for any $Y_D \in B$, $X^* < X(Y_D) \leq N(Y_D)$. Thus, one can construct a bidirectional network with the same allocation such that $\mathcal{N}(Y_D) > X^*$, for all $Y_D \in B$. Therefore, $\mathcal{MR}(D) = \min\{\mathcal{N}(Y_D) : \forall Y_D \in B\} > X^*$ which is a contradiction.

□

2.7 Robust Design

In this section, our goal is to design the interdependency between two given networks A and B with star topologies such that network B is robust to failures in network A and network A is robust to failures in network B. For simplicity, we assume that both networks have the same number of nodes $N_A = N_B = N$. We also assume that the number of edges between the networks is E.

We introduce two definitions for robustness, and propose algorithms for robust design under each definition.

Definition 4. Lexicographic Robustness: Network G^* is $K-$robust if for every $D \in \{1, \cdots, K\}$, it has the largest $\mathcal{MR}(D)$ among all networks G with the same number of nodes and edges.

Definition 5. Relative Robustness: Network G^* is the most robust network if it has the largest lower bound on the relative $\mathcal{MR}(D)$ for all values of $D \in \{1, \cdots, N\}$;

i.e. largest $\min_{1\leq D\leq N} \frac{\mathcal{MR}(D)}{D}$.

2.7.1 Design Under Lexicographic Definition

Proposition 4. Consider the set of bidirectional interdependent networks with N nodes and kN edges. The k-regular network is the 1-robust network.

Proof. By contradiction - By Proposition 1, in a k-regular network, $\mathcal{MR}(D=1)=k$. Suppose that the 1-robust network is irregular. This means that there exist at least one node with degree less than k; thus, $\mathcal{MR}(D=1)<k$ which is a contradiction. □

Note that for arbitrary values of E, the 1-robust network contains a k-regular subnetwork with $k=\lfloor\frac{E}{N}\rfloor$.

Next, we want to design a 2-robust network. By definition, a 2-robust network is 1-robust, as well. Thus, it is a regular graph by Proposition 4. However, it can be seen from Figure 2-15 that not all regular graphs have the same 2-robustness. In particular, it can be seen that the minimum number of node removals from network A (B) to cause the failure of any two nodes in network B (A) is 3. However, in network G_2 this value is 2. Comparison of the structures of graphs G_1 and G_2 shows that G_2 has a more clustered structure than G_1. Our goal is to find the structure of the most 2-robust network.

In order to find the structural pattern of the 2-robust networks, we formulate the optimal design problem as an ILP (See Appendix 2.10.2 for the formulation details). Figure 2-16 shows the pattern of $\mathcal{MR}(D)$ for networks with different network sizes and node degrees. It can be seen that for any give degree k, as number of nodes N increases, $\mathcal{MR}(D)$ increases until it reaches a threshold. This observation is summarized as follows.

Let $N_0=k(k-1)+1$ where $k\geq 2$. Any 2-robust network with $N\geq N_0$ nodes and degree k has $\mathcal{MR}(D=2)=2k-1$. Moreover, any 2-robust network with $N<N_0$ nodes and degree k has $\mathcal{MR}(D=2)<2k-1$.

In the following, we prove the correctness of our observation.

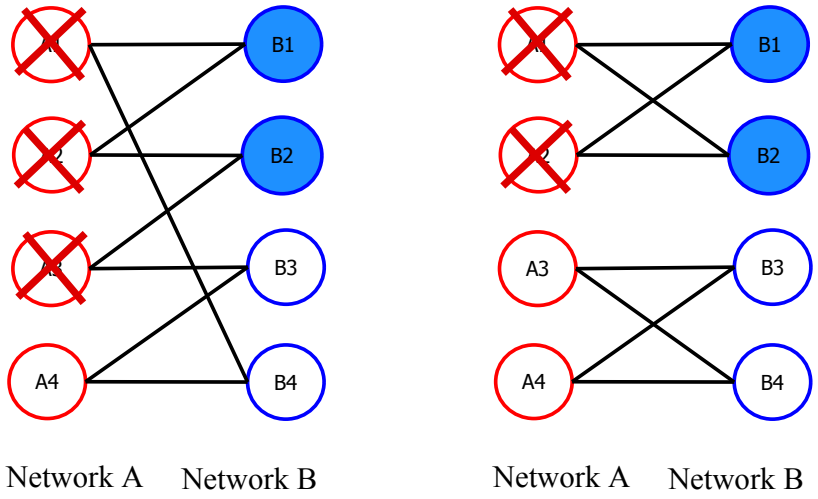

(a) Graph G_1 (b) Graph G_2

Figure 2-15: Regular Interdependent networks with robustness for two failures. In network G_1, minimum node removal to cause the failure of any two nodes is 3, where in network G_2, the minimum node removals is 2.

Lemma 5. For $N = N_0$ and $k \geq 2$, one can construct a 2-robust network with N nodes and degree k such that $\mathcal{MR}(D = 2) = 2k - 1$.

Proof. By construction - Divide the nodes in network A and B into four groups as in Figure 2-17. From left, group 1 has a single node from network A, group 2 has K nodes from network B, group 3 has k batches of $k-1$ nodes from network A, and finally group 4 has $k-1$ batches of $k-1$ nodes from network B. Note that the total number of nodes in both networks A and B is $k(k-1)+1$.

Next, we connect the nodes as follows. Connect the single node in group 1 to all the k nodes in group 2. Next, connect node i in group 2 to all the $k-1$ nodes inside batch i in group 3. Finally, connect node i from the last batch of group 3 to all the $k-1$ nodes of batch i in group 4. So far, all the nodes in group 1, group 2 and the last batch of group 3 has degree k. Moreover, every pair of nodes in group 2 (part of network B) share exactly one neighbor which is the single node in group 1. Next, we connect the nodes in the batches $1, \cdots, (k-1)$ in group 3 to batches $1, \cdots, (k-1)$ in group 4 as follows.

For $i, j \in \{1, \cdots, k-1\}$, connect node i in batch j of group 3 to node $i \pmod{k-1}$ in batch 1 of group 4, node $i + j - 1 \pmod{k-1}$ in batch 2 of group 4, ... , node

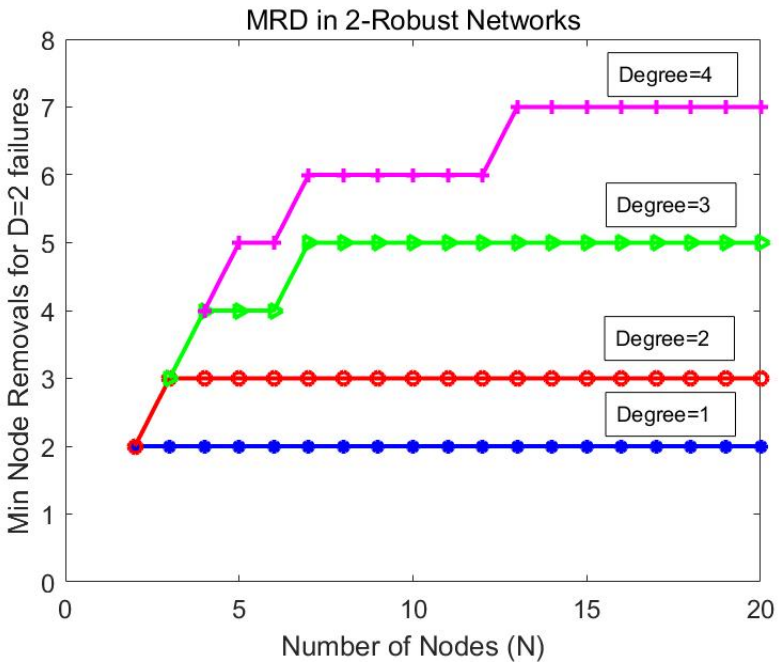

Figure 2-16: $\mathcal{MR}(D)$ for 2-robust networks with different sizes and node-degrees.

$i + j + k - 3 \pmod{k-1}$ *in batch* $k-1$ *of group 4*

This rule satisfies the following conditions:

1. every node is connected to $k-1$ new edges;
2. every node from group 3 is connected to exactly one node inside each batch in group 4;
3. no pair of nodes inside a batch in group 3 share a neighbor in group 4;
4. every pair of nodes from two different batches in group 3 share exactly one neighbor in group 4;
5. every node from group 4 is connected to exactly one node inside each of the first $(k-1)$ batches of group 3;
6. no pair of nodes inside a batch in group 4 share a neighbor in the first $(k-1)$ batches of group 3;
7. every pair of nodes from two different batches in group 4 share exactly one neighbor in the first $(k-1)$ batches of group 3.

Note that conditions (2)-(4) guarantee that every pair of nodes in network A share exactly one neighbor. In addition, conditions (5)-(7) guarantee that any pair of nodes inside group 4 or between groups 2 and 4 share exactly one neighbor.

Therefore, we have constructed a graph with N_0 nodes where every node has degree k, and every pair of nodes in either network A or network B share exactly one neighbor; i.e. $\mathcal{MR}(D) = 2k - 1$.

□

Lemma 6. For $N \geq N_0$ and $k \geq 2$, there exists no regular network with N nodes and degree k such that $\mathcal{MR}(D = 2) > 2k - 1$.

Proof. Since each node has degree k, no two nodes can be connected to more than $2k$ nodes; i.e. $\mathcal{MR}(2) \leq 2k$. Next, suppose that there exists a $k-$regular network with $\mathcal{MR}(D = 2) = 2k$. Thus, every pair of nodes in network B are exactly connected to $2k$ nodes; i.e. each node in network B is connected to k distinct nodes. Equivalently, no node in network A is connected to two nodes in network B; i.e., every node in network A has degree 1, which is a contradiction to $k \geq 2$. □

Lemma 7. For $N < N_0$ and $k \geq 2$, there exists no regular network with N nodes and degree k such that $\mathcal{MR}(D = 2) \geq 2k - 1$.

Proof. Suppose $N = N_0 - 1 = k(k - 1)$. Consider an arbitrary node i from network A. Node i is connected to k nodes in network B, namely set X, where each of these nodes are also connected to $k-1$ nodes in network A, namely set Y. Note that $i \notin Y$. Since the total number of nodes in each network is $k(k-1)$, $|Y| \leq k(k-1)-1$. Thus, there exist at least two nodes in X that share a neighbor in Y. On the other hand, all nodes in X share node i as their neighbor, too. Therefore, there exist at least two nodes in network B that share more than one node in network A. The same argument holds for network A. Thus, $\mathcal{MR}(D = 2) < 2k-1$ for $N = N_0-1$. Clearly, as the total number of nodes decreases, $\mathcal{MR}(D = 2)$ decreases, too. Thus, for any regular network with $N < N_0$, $\mathcal{MR}(D = 2) < 2k - 1$. □

In order to design a 3-robust network under the definition of Lexicographic robustness, one should search among the 2-robust networks which becomes very complicated.

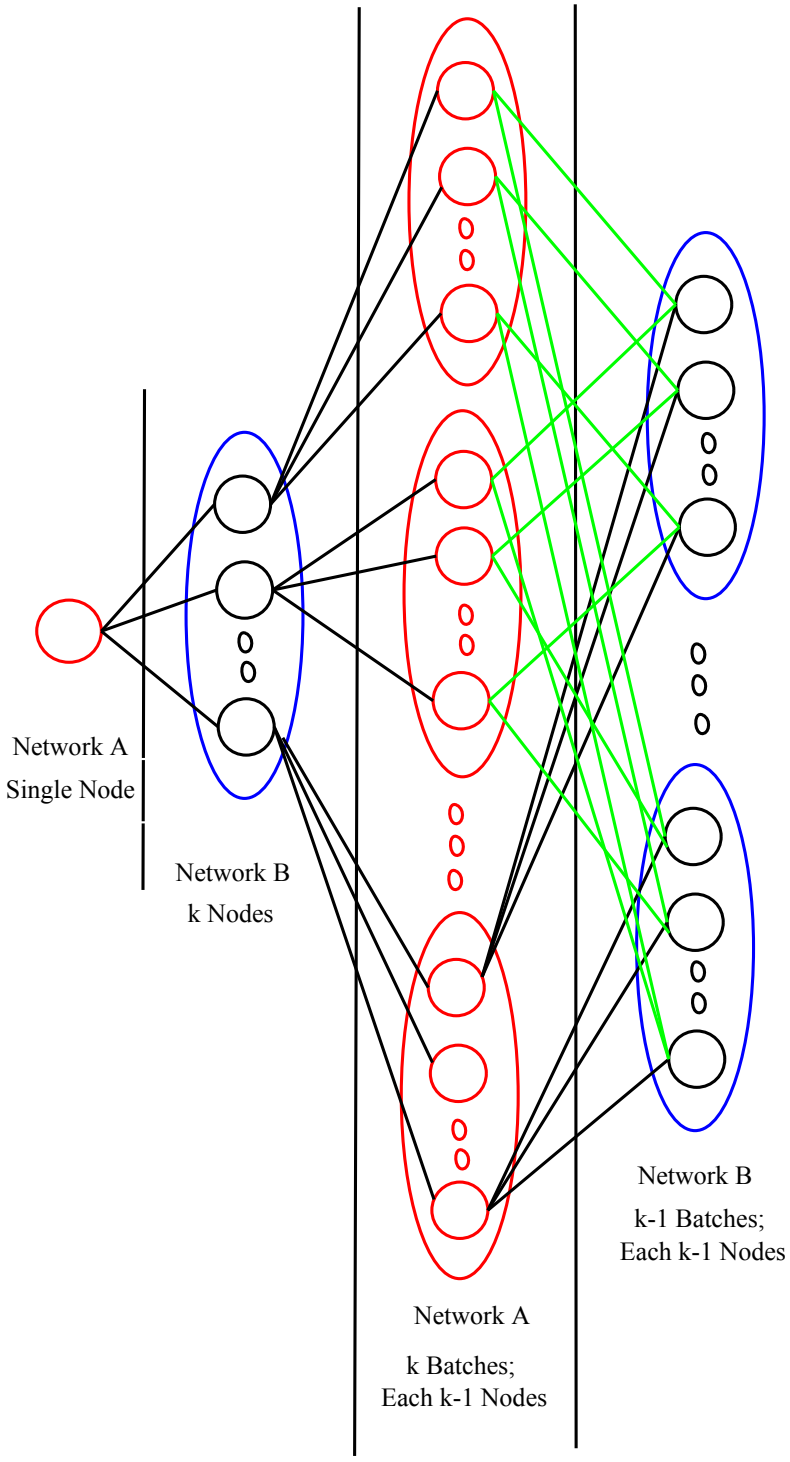

Figure 2-17: An example of construction of a 2-robust network. Black links denote the first set of edges connecting the nodes in group 1, group 2 and the last batch of group 3. Green links denote the set of edges connecting the nodes in group 3 and group 4.

In the next section, we consider the relative robustness and show its relation with expander graphs.

2.7.2 Design under Relative Robustness

First, we show that by definition, a network with large relative $\mathcal{MR}(D)$ has also a large node expansion. Then, we show the construction of expander graphs.

Definition 6. The Node Expansion of a bipartite graph $G = \{A, B\}$, denoted by $h(G)$, is defined as:

$$h(G) = \min_{S \subseteq B} \frac{|\mathcal{N}(S)|}{|S|} \tag{2.7}$$

where $\mathcal{N}(S)$ denotes the neighbor nodes of set S.

Lemma 8. Under relative robustness definition, the most robust network has the largest node expansion.

Proof.

$$\min_{1 \leq D \leq N} \frac{\mathcal{MR}(D)}{D} = \tag{2.8a}$$

$$\min_{1 \leq D \leq N} \frac{\min_{Y_D \subset B, |Y_D| = D} |\mathcal{N}(Y_D)|}{D} = \tag{2.8b}$$

$$\min_{S \subseteq B} \frac{|\mathcal{N}(S)|}{|S|} = h(G) \tag{2.8c}$$

□

Lemma 8 shows that in order to design a robust interdependent network, it is enough to design a network with large node expansion; i.e. an expander bipartite graph. Analysis and design of node and edge expander graphs is a well-studied topic (See [52, 53]). It has been shown that some random graphs share the properties of expander graphs, and they have been used to prove the existence of expander graphs. However, explicit construction of an expander graph is more difficult and there exist only three main strategies for designing them (See [54, 55] for more details).

In the following, we mention one of the main results regarding random graphs and their relation with expander graphs.

Let a bipartite graph $G = \{A, B\}$ be a (D, r) node expander if for all sets $S \subseteq B$ of size at most D, the neighborhood $\mathcal{N}(S)$ is of size at least $r|S|$. Moreover, let $Bip_{N,k}$ be the set of bipartite graphs that have N nodes on each side and are k-Bregular, meaning that every node in network B has degree k.

Theorem 6. For every constant k, there exists a constant $\alpha > 0$ such that for all N, a uniformly random graph from $Bip_{N,k}$ is an $(\alpha N, k-2)$ node expander with probability at least $\frac{1}{2}$.

Proof. See [53] for proof. □

Note that for every $S \subseteq B$, the largest possible neighbor has size of $k|S|$, and Theorem 6 denotes that in a uniform random graph, every $S \subseteq B$ of size αN has neighbors of size $(k-2)|S|$ with probability more than half.

2.8 Discussion

Throughout this chapter, we analyzed the robustness of interdependent networks for star topologies. We defined metric $\mathcal{MR}(D)$ and proved the hardness of evaluating this metric for arbitrary values of D in both unidirectional and bidirectional interdependent networks. We also proved that uniform distribution of edges in a network would result in more robustness. A natural direction of future research would be analyzing more general topologies for interdependent networks which makes the problem more complicated. In fact, we prove that for the tree topologies, evaluating metric $\mathcal{MRB}(D)$ in bidirectional interdependent networks becomes NP-complete even for the special case of total failure in network B; i.e. $D = N_2$. This is due to the fact that failures cascade both inside the networks and between the networks.

Theorem 7. For $D = N_2$, finding the $\mathcal{MRB}(D)$ in a bidirectional interdependent network with tree topology is an NP-complete problem.

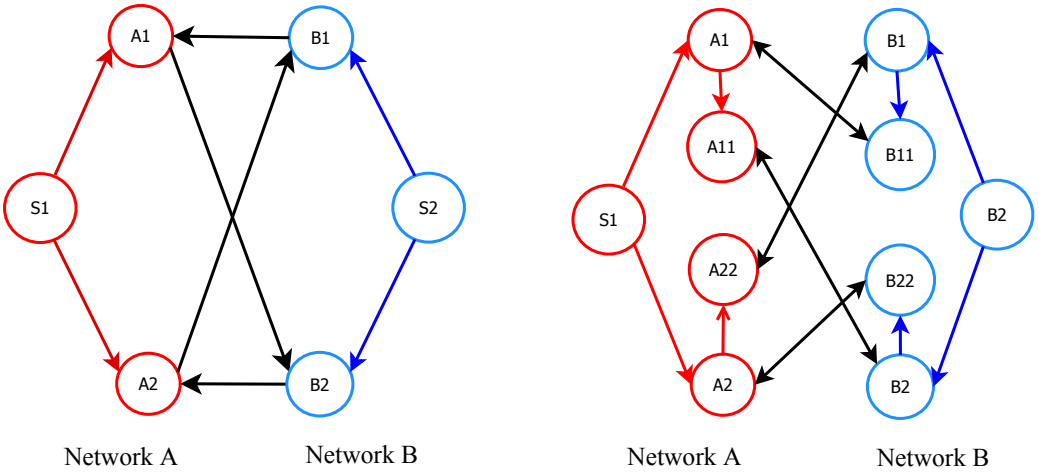

(a) Graph G (b) Graph G'

Figure 2-18: Graph Topologies for Proof of Theorem 7

Proof. The proof is based on a reduction from the problem of finding $\mathcal{MRB}(D)$ in a unidirectional interdependent network with star topology which is proved to be NP-complete [6]. Consider graph G, an arbitrary unidirectional interdependent network with star topology, with nodes $\{A_1, \cdots, A_{N_1}\}$ in network A, nodes $\{B_1, \cdots, B_{N_2}\}$ in network B and two sources S_1 and S_2 which are directly connected to nodes in network A and B, respectively. Let E_{AB} represent the set of edges from network A to network B. Similarly, let E_{BA} represent the set of edges from network B to network A.

Construct graph G', a bidirectional interdependent network with tree topology, using graph G as follows. Generate graph G' similar to graph G, and remove all the edges E_{AB} and E_{BA}. For each node A_i, generate a child node A_{ii} with an edge from A_i to A_{ii}. Similarly, for each node B_j, generate a child node B_{jj} with an edge from B_j to B_{jj}. For every edge in E_{AB} connecting node A_i to node B_j, connect the child node A_{ii} to node B_j . Similarly, for every edge in E_{BA} connecting node B_j to node A_i, connect the child node B_{jj} to node A_i (See Figure 2-18). This construction guarantees that removal of any set of parent nodes X in both graphs G and G' would lead to the failure of the same parent nodes Y in both graphs. Moreover, note that under this construction, failure of any parent node in graph G' guarantees failure of its child.

Next, we show that if $\mathcal{MRB}(D = N_2')$ in graph G' can be found in polynomial time, $\mathcal{MRB}(D = N_2)$ in graph G can also be found in polynomial time which is a contradiction [6].

Suppose R' is the optimal set of node removals that lead to the failure of the entire network B in graph G'. Note that R' could contain both parent and child nodes; however, it is clear that the effect of removal of any parent node A_i (respectively, parent node B_j) is more than or equal to the effect of removal of its child node A_{ii} (respectively, child node B_{jj}). Thus, we replace all the child nodes in R' to the parent nodes, and call the new set R'_P. It is enough to show that R'_P is also the optimal removal set in graph G.

Due to the construction of graph G' from G, removal of R'_P in G leads to the total failure of network B. Next, we prove by contradiction that it is also the optimal solution. Suppose that R is the optimal removal in G where $|R| < |R'_P|$. By construction, removal of nodes R in G' will lead to the total failure of network B; thus, R'_P is not optimal which is a contradiction.

□

In Theorem 7, we proved that finding the optimal removal sets in graph G and G' are equivalent. This was due to the fact that under our construction, parent nodes could replicate the entire cascading failure process. However, this is not true for any arbitrary bidirectional interdependent network with tree topology. Consider the following example.

Example- Consider the network in Figure 2-19. Here, nodes A_1, A_2, A_3 and B_1 are the parent nodes directly connected to the sources, and the rest of nodes are children. Moreover, the nodes between the two networks are connected via bidirectional edges. Suppose parent node A_2 fails. Thus, child nodes A_{21}, B_{21} and B_{22} fail which leads to the failure of parent node A_3.

This example illustrates that the failure of a parent node in network A can lead to the failure of another parent node in network A without affecting any parent node in network B. Therefore, there are no graph structural mapping to replicate the cascade of failures from bidirectional networks to unidirectional ones with star topology.

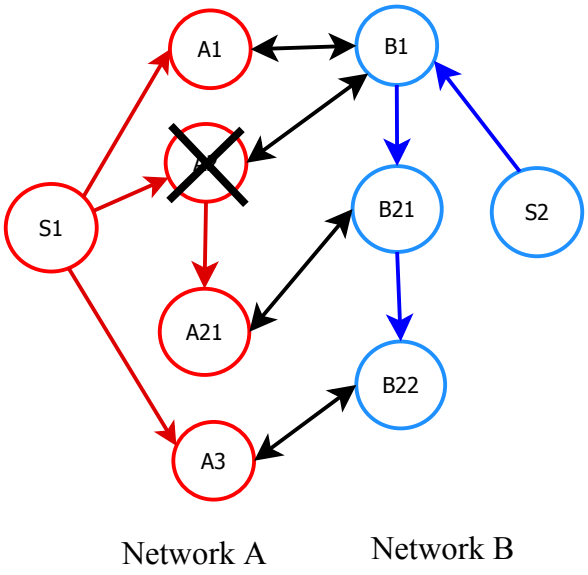

Figure 2-19: An example of bidirectional interdependent networks with tree topology. Here, the failure of parent node A_2 leads to the failure of parent node A_3 without affecting any parent node in network B.

Thus, despite the fact that star topologies illustrate many important properties of interdependent networks, the analysis of general topologies cannot be a direct extension of star topologies and requires extensive analysis.

2.9 Conclusion

In this chapter, we studied the robustness of interdependent networks. We proposed a new model for analyzing interdependent networks with given topologies. We focused on the networks with star topologies to capture the effect of cascading failures due to interdependency. We defined the metrics $\mathcal{MR}(D)$ and $\mathcal{MRB}(D)$ as the minimum number of nodes that should be removed from network A or both networks to cause the failure of D nodes in network B. We proved that evaluating these metrics is not only NP-complete, but also inapproximable. Moreover, we proposed several algorithms based on greedy, randomize rounding and simulated annealing for evaluating our metrics and compared their performances using simulation results. We proved that in the networks with the same number of nodes and edges, those with bidirectional interdependency are more robust than the ones with unidirectional

interdependency. Next, we introduced two closely related definitions for robust interdependent networks, proposed algorithms for explicit design, and showed the relation of robust interdependent networks with expander graphs. Finally, we discussed some ideas about analysis of interdependent networks with general topologies.

2.10 Chapter Appendix

2.10.1 Inapproximability of metric $\mathcal{MR}(D)$

Consider networks G and G' in Figure 2-5. For simplicity, we assume that $N_1 = N_2 = N$. Let W_D be the approximation of $\mathcal{MR}(D)$ in network G where W_D^* is the optimal value. Suppose there exists a PTAS which approximates $\mathcal{MR}(D)$ within factor of $r > 1$; i.e. $W_D^* \leq W_D \leq r \cdot W_D^*$. Moreover, define variables $Z_D = N - W_D$ and $Z_D^* = N - W_D^*$.

Moreover, let X^* be the largest balanced biclique in network G'. It is easy to see that $X^* = \max_{1 \leq D \leq N} \min\{Z_D^*, D\}$. Similarly, let X be the largest balanced biclique in network G' found using the approximated value of metric $\mathcal{MR}(D)$; i.e. $X = \max_{1 \leq D \leq N} \min\{Z_D, D\}$.

Suppose $Z_D^* \geq \frac{N}{k}$ for some constant $k > 1$ [4]. Then, the following equations hold.

Equations (2.9a)-(2.9h) indicate that for any $1 \leq r \leq 1 + \frac{1 - m \cdot . N^{-\epsilon}}{k-1}$ where m and ϵ are some positive constants, if there exists an r-approximation for $\mathcal{MR}(D)$, there exists an $m \cdot N^{-\epsilon}$ approximation for the maximum balanced biclique (MBB) problem which is a contradiction [48, 49].

[4] Note that for constant values of D or Z_D^*, one can find an exact balanced biclique in polynomial time by an argument similar to Proposition 1. Therefore, the difficulty is for non-constant values of D and Z_D^*; i.e. D and Z_D^* are a fraction of network. Thus, k will a constant value.

$$W_D^* \leq W_D \leq r \cdot W_D^* \tag{2.9a}$$

$$\Rightarrow N - r \cdot W_D^* \leq N - W_D \leq N - W_D^* \tag{2.9b}$$

$$\Rightarrow -N(r-1) + r \cdot Z_D^* \leq Z_D \leq Z_D* \tag{2.9c}$$

$$\Rightarrow [r - k(r-1)] \cdot Z_D^* \leq Z_D \leq Z_D* \tag{2.9d}$$

$$\Rightarrow \min\{D, [r - k(r-1)] \cdot Z_D^*\} \leq \min\{D, Z_D\}$$
$$\leq \min\{D, Z_D^*\} \quad \forall D \in \{1 \leq D \leq N\} \tag{2.9e}$$

$$\Rightarrow [r - k(r-1)] \cdot \min\{D, \cdot Z_D^*\} \leq \min\{D, Z_D\}$$
$$\leq \min\{D, Z_D^*\} \quad \forall D \in \{1 \leq D \leq N\} \tag{2.9f}$$

$$\Rightarrow [r - k(r-1)] \cdot \max_{1 \leq D \leq N} \min\{D, \cdot Z_D\}$$
$$\leq \max_{1 \leq D \leq N} \min\{D, Z_D^*\} \leq \max_{1 \leq D \leq N} \min\{D, Z_D^*\} \tag{2.9g}$$

$$\Rightarrow [r - k(r-1)] \cdot X_D^* \leq X_D \leq X_D^* \tag{2.9h}$$

2.10.2 ILP formulation for 2-robust design

Here, we formulate the problem of allocating edges in a 2-robust bidirectional interdependent network. As discussed previously, by definition 4, a 2-robust network is also 1-robust. Thus, we search for the optimal allocation in regular networks.

Let N be the number of nodes in networks A and B, and k be the degree of each node. Let X denote the lower bound on the number of neighbors of any pair of nodes; i.e. $X = \mathcal{MR}(D = 2)$. Let $E \in \{0,1\}^{N \times N}$ be a binary matrix where $E_{ij} = 1$ if node $i \in A$ is connected to node $j \in B$, and $E_{ij} = 0$ otherwise. Moreover, let Z_i^{jr} be a binary variable where $Z_i^{jr} = 1$ if node $i \in A$ is a neighbor of node $j \in B$ or node $r \in B$, and $Z_i^{jr} = 0$ otherwise. Furthermore, let Y_j^{ir} be a binary variable where $Y_j^{ir} = 1$ if node $j \in B$ is a neighbor of node $i \in A$ or node $r \in A$, and $Y_j^{ir} = 0$ otherwise. The ILP formulation is as follows.

$$\max \quad X \tag{2.10a}$$

$$\text{s.t.} \quad \sum_{i=1}^{N} E_{ij} = k \quad j \in 1, \cdots, N \tag{2.10b}$$

$$\sum_{j=1}^{N} E_{ij} = k \quad i \in 1, \cdots, N \tag{2.10c}$$

$$Z_i^{jr} \leq E_{ij} + E_{ik} \quad j \in 1, \cdots, N-1; r \in j+1, \cdots, N \quad i \in 1, \cdots, N \tag{2.10d}$$

$$X \leq \sum_{i=1}^{N} Z_i^{jk} \quad j \in 1, \cdots, N-1; k \in j+1, \cdots, N \tag{2.10e}$$

$$Y_j^{ir} \leq E_{ij} + E_{rj} \quad i \in 1, \cdots, N-1; r \in i+1, \cdots, N \quad j \in 1, \cdots, N \tag{2.10f}$$

$$X \leq \sum_{j=1}^{N} Y_j^{ir} \quad i \in 1, \cdots, N-1; r \in i+1, \cdots, N \tag{2.10g}$$

$$E_{ij} \in \{0, 1\} \quad i \in 1, \cdots, N, j \in 1, \cdots, N \tag{2.10h}$$

$$Z_i^{jr} \in \{0, 1\} \quad i \in 1, \cdots, N; j, r \in 1, \cdots, N \tag{2.10i}$$

$$Y_j^{ir} \in \{0, 1\} \quad j \in 1, \cdots, N; i, r \in 1, \cdots, N \tag{2.10j}$$

Here, the objective is to maximize the lower bound X; i.e. maximize metric $\mathcal{MR}(D = 2)$. Constraints (2.10b) and (2.10b) guarantee that the degree of each node is k. Moreover, Constraints (2.10d) and (2.10e) find the neighbors of any pair of nodes in network B and set X as the lower bound on the number of these neighbors. Similarly, Constraints (2.10f) and (2.10g) find the neighbors of any pair of nodes in network B and set X as the lower bound on the number of these neighbors. Finally, constraints (2.10h-2.10i) sets the variables to be binary.

Chapter 3

Interdependent Power Grid and Communication Networks

In this chapter, we study the interdependency between the power grid and the communication network used to control the grid. A communication node depends on the power grid in order to receive power for operation, and a power node depends on the communication network in order to receive control signals. We demonstrate that these dependencies can lead to cascading failures, and it is essential to consider the power flow equations for studying the behavior of such interdependent networks. We propose a two-phase control policy to mitigate the cascade of failures. In the first phase, our control policy finds the unavoidable failures that occur due to physical disconnection. In the second phase, our algorithm redistributes the power so that all the connected communication nodes have enough power for operation and no power lines overload. In particular, we show that using our mitigation policy, the interdependent power grid is more robust than the isolated one. We also perform a sensitivity analysis to evaluate the performance of our control policy, and show that our control policy achieves close to optimal yield for many scenarios. This analysis can help design robust interdependent grids and associated control policies.

3.1 Introduction

One of the main challenges for sustainability of future power grids is the increased variability and uncertainty caused by integrating renewable sources into the grid. In order to address this challenge, the future grid must be equipped with real-time monitoring and be controlled with fast and efficient control algorithms [56].

The monitoring and control of today's power grid relies on a Supervisory Control and Data Acquisition (SCADA) system. One of the main control operations is the Automatic Generation Control (AGC) which is used to match power supply with demand in the grid through frequency control. This is done both at the local (generator) level, and the wide-area level. AGC systems rely on communication in order to disseminate control information, and the lack of communication, or even delay in communication can cause AGC systems to malfunction and fail, leading to wide-scale power outages [3, 4].

In August 2003, lack of real-time monitoring and rapid control decisions for mitigating failures led to a catastrophic blackout which affected 50 million people in Northeast America. According to the final report of the 2003 blackout [1], this event started with the loss of transmission lines in Ohio due to inadequate tree trimming. However, the operators did not realize these failures due to insufficient monitoring; thus, no remedial action was taken at that time. In the subsequent hour, several transmission lines and generators tripped due to overheating of power lines and local protections in generators[1]. These initial failures triggered a very fast cascade, which occurred in less than 5 minutes and led to a full blackout in the Northeast United States and parts of Canada. The reports in [5] and [2] indicate that the reason for tripping of many generators and transmission lines was power imbalance in the control areas and lack of communication between the operators for mitigating the failures. It is thus essential to design a communication network together with control policies that facilitate widespread monitoring of the power grid, and enables the power grid to react to rapid changes and unexpected failures in the network.

[1]Local protections are systems that trip the generator when abnormal changes such as over/under frequency occur in the grid.

Moreover, for cost and sustainability considerations, the communication equipment often receives the power for operation directly from the power grid. However, this creates a strong interdependency between the two networks, where the operation of the power grid is dependent on receiving control signals from the communication network, and the operation of the communication network is dependent on receiving power from the power grid.

As discussed in the previous chapter, the concept of interdependencies between infrastructures was first introduced in [13]. In [14], Rosato *et al.* studied the impact of failures in the power grid on the performance of communication networks. In [18], Buldyrev et al. presented a model for analyzing the robustness of interdependent random networks and investigated asymptotic connectivity to a "giant component". They showed that interdependent networks are more vulnerable to failures than individual networks in isolation. The authors in [6] modified the model of [18] to account for connectivity to generators and control centers, and studied connectivity in the non-asymptotic regime.

Figure 3-1(a) shows the impact of failures on interdependent networks by considering two random Erdos-Renyi graphs and a one-to-one interdependency between power and communication nodes. Here, we simulated the cascading failure process described by Buldyrev's model in [18]. The result of our simulation shows that indeed the interdependent networks are more vulnerable to failures than isolated networks, and there is a notable drop in the size of the largest connected component when the percentage of initial node removals is more than 50% of total nodes.

However, in a power grid the flows are driven by Kirchoff's laws, and cannot be described by a network flow model. Thus, when a failure occurs in a power grid, the power flow is redistributed on the the rest of the network and some elements could overload and fail, leading to "Cascading Failures". Since this behavior is not captured in the abstract models of [18] and [6], we generated random power grids and implemented the model of cascading failures from [27] in conjunction with the model introduced in [6]. As can be seen from Figure 3-1(b) when taking power failure cascades into account, there exists no large component for any size of initial failure.

Thus, it is critical to consider the actual power flow in analyzing the behavior of the power grid.

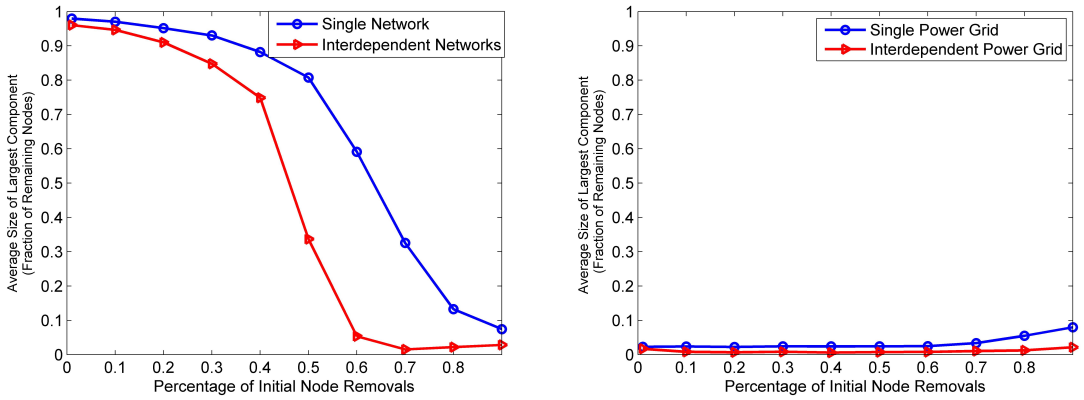

(a) Random Erdos-Renyi Graph - The size of largest component is close to the size of network for small sizes of failure, and there is a drop at a failure rate of about 50%.

(b) Random Power Grid - No large component exists for any size of failure.

Figure 3-1: Ratio of largest component to the number of remaining nodes for different sizes of initial failures; Each network has 500 nodes with expected degree 4. We randomly selected $1/5^{th}$ of the nodes in the power grid and communication network as generators and control centers, respectively, and there is one-to-one interdependency between the two networks. For the power grid, we considered unit reactance for all power lines, and attributed a random amount of power in the range $[1000, 2000]$ to all generators and loads.

Figure 3-1(b) focused on connectivity. However, in power grids, the metric of interest is yield, which is the percentage of served load, not the the size of largest component. Figure 3-2 shows the yield vs the initial node removals in the interdependent Random power grid as described in Figure 3-1(b). It can be seen that the yield in an interdependent power grid is much smaller than the yield in an isolated power grid.

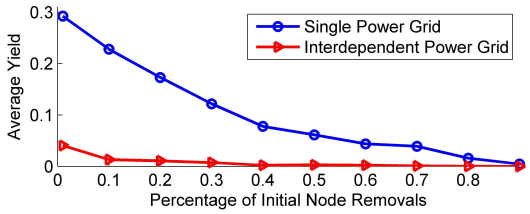

Figure 3-2: Comparing Yield in single and interdependent Power Grid after cascading failures. Increasing the size of failure results in a smaller yield.

As was discussed previously, it is necessary to design a communication network intertwined with the power grid in order to provide real-time monitoring and control for the grid. Therefore, a proper analysis of interdependent networks should account for the availability of control schemes that can mitigate cascading failures. In this chapter, we propose a new load shedding scheme to control the cascade of failures both inside and between the networks. To the best of our knowledge, this work is the first attempt to design control policies for mitigating failures in interdependent networks.

The rest of this chapter is organized as follows. We explain the model of interdependent power grid and communication network in Section 3.2. In Section 3.3, we present a simple control policy followed by a load control policy that mitigate the cascading failures in interdependent networks in one stage. Finally, we perform sensitivity analysis for our load control policy in Section 3.4 and conclude in Section 3.5.

3.2 Model

An interdependent network consists of three subnetworks: the Power grid, the communication network and the interdependency network. In the following, we will explain the model of each subnetwork.

3.2.1 Power Grid

The power grid can be modeled as a graph $G_P = (V_P, E_P)$ where V_P and E_P are power nodes and lines, respectively. There are three types of power nodes in a grid: Generators that generate power, Loads that consume power and Substations that neither generate nor consume power. The flow in power lines cannot be controlled manually; instead, it is determined based on the principles of electricity. In order to analyze the behavior of the power grid, we use the well-known DC power flow model, explained in equation 3.1, that has been widely used in the literature (see [8] for a survey on the power flow models).

Let P be a $|V_P| \times 1$ vector such that P_i denotes the power injection at power node $i \in V_P$. Let $A \in R^{|V_P| \times |E_P|}$ be the adjacency matrix where $A_{ij} = 1$ if link j starts from node i, $A_{ij} = -1$ if link j ends in node i and $A_{ij} = 0$ otherwise. Moreover, let $X \in R^{|E_P| \times |E_P|}$ be the reactance matrix associated to the power grid where X_{ii} denotes the reactance of i^{th} power line and $X_{ij} = 0$ for $j \neq i$. Let $f \in R^{|E_P| \times 1}$ be the vector of power flows in transmission lines and $\theta \in R^{|V_P| \times 1}$ denote the phases at all power nodes. A DC power flow can be modeled as follows.

$$Af = P \tag{3.1a}$$

$$A^T \theta = Xf \tag{3.1b}$$

Constraint 3.1a is a network flow constraint which guarantees that power at every node is balanced. In addition, constraint 3.1b replicates Ohm's law where the amount of power flowing in a power line is equal to the difference in phase angles θ_i and θ_j divided by the reactance of line (i, j).

When a power node or line fails, its load is shifted to other elements of the grid. During this process, the flow in one or more lines may be pushed beyond their capacity which leads to the failure of the overloaded lines. Similarly, failure of these lines redistributes power and may lead to further "Cascading Failures".

The cascade of failures in the power grid is a very complex phenomena, and several models have been introduced for explaining the behavior of cascading failures (see for example [27–30]). In this chapter, we will use the deterministic model explained in [27]. In this model, each power line is associated with a capacity which is considered to be a factor of safety (FoS) typically set to 1.2 times the amount of flow on that line. When a failure occurs, the power will be redistributed to the rest of the grid and the lines with flow more than their capacity will fail. The cascading model can be explained using the following steps.

1. Balance the power in the grid; i.e. if the grid is overloaded, decrease the amount of power at all loads uniformly to match the generation and if the grid is un-

derloaded, decrease the amount of power at all generators to match the load.

2. Resolve the DC power flow model in equations 3.1.

3. Remove all the overloaded power lines; i.e. $f > f^{max}$.

4. If there are no overloaded lines in step 3, the cascade ends. Otherwise, repeat the four steps.

3.2.2 Communication Network

The communication and control network can be modeled as a graph $G_C = (V_C, E_C)$ where V_C and E_C are communication nodes and links, respectively. There are two types of communication nodes: routers that are responsible for transmitting information, and control centers that are responsible for making control decisions.

In order to have a fully monitored and controlled power grid, every power node is equipped with a communication node (router). These nodes receive information from the power nodes and relay it to the control center through other routers. The control center makes the control decisions and sends them back to the routers located at power nodes. In our model, when a communication node fails, all the communication nodes that become disconnected from the control centers can no longer function.

3.2.3 Interdependency

Dependency of Communication Network on the Power Grid

The communication nodes receive the power for their operation from power grid. In order to model this dependency, we associate each communication node C_j with a load P_{C_j} that is connected to the power grid (Figure 3-3). Let P_C^{req} be the required amount of power for operation of the communication node. Thus, communication node C_j operates if $P_{C_j} \geq P_C^{req}$ and it fails otherwise.

In our model, the loads associated to the communication nodes are located in the distribution system and multiple communication nodes can receive power from

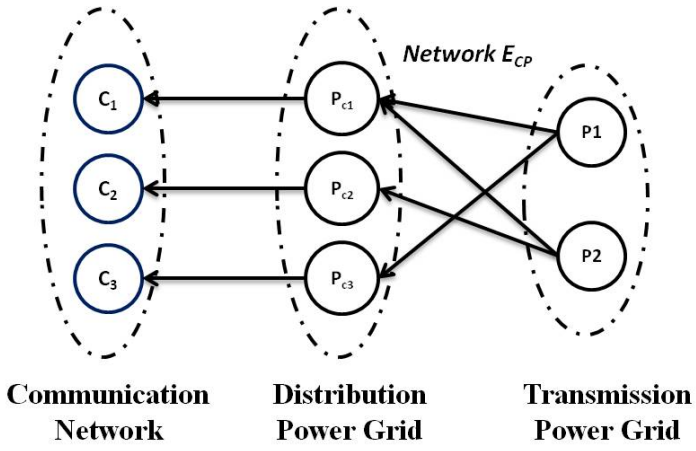

Figure 3-3: Modeling Dependency of Communication Network on Power Grid

one power node in the transmission system (Figure 3-3). We assume that the communication and control nodes have the highest priority in the distribution system; thus, they will receive power as long as the power nodes have sufficient power to meet their demand. We model this part using network flow equations, where the sources are the loads P_i in the power grid and the destinations are loads P_{C_j} located at communication nodes.

Dependency of Power Grid on the Communication Network

Next, we model the impact of loss of communication on the operation of the power grid. As explained in the introduction, AGCs control the operation of generators by setting the amount of power they should generate. If a generator becomes disconnected from the controller, the local controller tries to adjust the generation within a small range of changes in frequency. When the power grid is under stress (e.g. due to failures in the grid), power imbalance can lead to rapid frequency changes; in which case local protection schemes will be activated and trip the generators [1, 3, 4]. Similarly, if a substation loses its control, then the relays cannot be accessed remotely and when the system is under stress, transmission lines will be overloaded and trip. Based on the 2003 blackout report, the large power imbalance in the system and lack of fast control and communication led to tripping of many transmission lines and generators [1].

In this chapter, we analyze the cascade of failures in the power grid when the system is under stress. We say that if a power node loses its correspondent communication and control node(s), it cannot be controlled and fails. This is a deterministic model that can be extended to a probabilistic model where the power node fails randomly with some probability.

In the next section, we will propose control schemes that mitigate cascade of failures by shedding loads and re-dispatching generators. In our analysis, we do not study the transient behaviors of the grid after applying control decisions. Instead, we assume that due to a wide-area control implemented by the communication and control network, all the power nodes are aware of the transient changes in the system and local protections do not activate. This is essential as in the 2003 blackout, many generators tripped due to fluctuations resulting from intentional load sheddings [1].

3.3 Control Policies

3.3.1 Simple Load Shedding Mechanism

In this Section, we apply a simple load shedding control scheme in order to mitigate failures inside the power grid. This control scheme changes the power injection at power nodes so that the total power in the grid is balanced and the flow in transmission lines is below their capacity; thus, no failure cascades in the power grid. Different versions of this algorithm exist in the literature (see for example [57,58]). The simple mitigation policy can be expressed in terms of the linear programming formulation in equation 3.2. Notice that notation “updated" indicates that the power grid and communication network have been updated after initial failure. Let $P^{old}, P^{new} \in R^{|V_P^{updated}|\times 1}$ denote the power injections at power nodes before and after applying the simple mitigation policy. Moreover, let vector f^{max} denote the capacity of power lines.

The objective function 3.2a is to minimize the total change in the power. Constraints 3.2e and 3.2f enforce that the only possible controls are to shed loads and

reduce power at generators. This is due to the fact that generators can ramp down much faster than they can ramp up. Since this control decision should be applied very rapidly in order to keep the network stable, we only allow ramping down; i.e. decreasing generation. Moreover, we assume there is no minimum threshold on the amount of power generation or consumption.

$$\begin{aligned}
\text{minimize} \quad & e^T(|P^{new} - P^{old}|) && \text{(3.2a)}\\
\text{subject to} \quad & A^{updated} f = P^{new} && \text{(3.2b)}\\
& (A^{updated})^T \theta = Xf && \text{(3.2c)}\\
& f \leq f^{max} && \text{(3.2d)}\\
& 0 \leq P_i^{new} \leq P_i^{old} \quad \forall i \in V_{P,gen}^{updated} && \text{(3.2e)}\\
& P_i^{old} \leq P_i^{new} \leq 0 \quad \forall i \in V_{P,load}^{updated} && \text{(3.2f)}
\end{aligned}$$

We apply this mitigation policy to the random interdependent power grid generated in Section 3.1 (Figure 3-1's caption). The only difference is that communication nodes receive power only from loads; thus, it is not a fully one-to-one interdependent topology. However, we try to create as many one-to-one interdependencies as possible; i.e a load is dependent on the communication node that it provides power to. Previous studies have shown that one-to-one interdependent networks are more robust to failures [6]. We observed that although applying this control policy can mitigate failures inside the power grid, the failures still cascade between the communication network and the power grid. Thus, we apply the control algorithm iteratively until no further failures occur. Clearly, the yield in any interdependent topology would be upperbounded by the yield in an isolated power grid. We use this upperbound to examine the performance of our control scheme.

Figure 3-4 shows the yield after applying the simple mitigation policy. It can be seen that although the control policy has improved the yield (when the failure rate is small), there is a dramatic drop in yield when the failure rate exceeds 10%. This is due

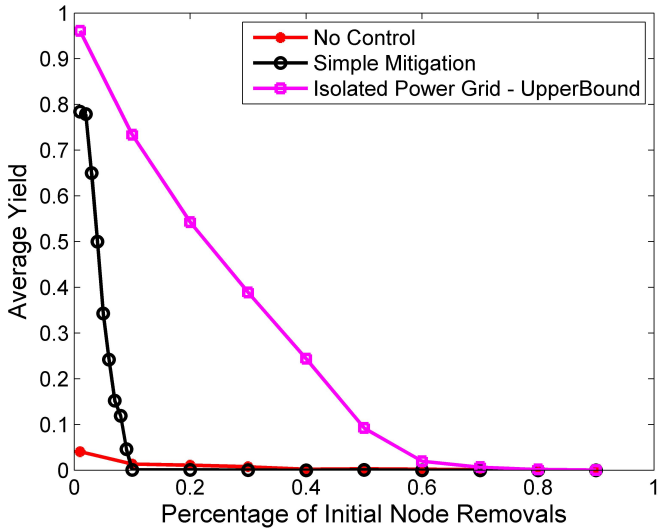

Figure 3-4: Applying Simple Mitigation Policy to Interdependent Power Grids for controlling Cascading failures. Here, the total power required by communication network is 10^{-4} times total load in the power grid.

to the fact that loss of loads leads to the loss of communication nodes that are used to control the generators and thus, the generators fail. Therefore, it is much harder to mitigate the cascading failures in interdependent networks. This simple policy is meant to demonstrate that even simple controls can reduce cascades. Inspired by this observation, we develop a control scheme that aims to keep communication nodes operating.

3.3.2 Load Control Mitigation Policy

It was seen in Section 3.3.1 that a simple mitigation policy cannot mitigate failures in interdependent networks, as failures in the power grid propagate to the communication network and cause additional failures both inside the communication network and in the power grid. In order to avoid such propagations, we propose a novel control policy that consists of two phases: in the first phase, it predicts the unavoidable failures in the power grid and the communication network and removes these nodes from the network. In the second phase, it changes the power injection at power nodes so that (1) power in all transmission lines is below their capacity and (2) all the remaining communication nodes keep operating; i.e. $P_{C_j} \geq P_C^{req}$. This guarantees that

no further failures occur in the power grid and that the failures do not propagate to the communication network. Thus, the cascade of failures will be mitigated in one stage. In the following, we explain these phases in more details.

Phase I

In this phase, we ignore the power flows in the power grid and find the nodes whose failure cannot be avoided by changing the power injection at nodes due to loss of connectivity. Algorithm I describes how to find such failures in polynomial time.

input : Topology of interdependent network and the set of initial node removals
repeat

1. For every power node i, check if there exists a path from a generator to node i and it receives an incoming edge from the communication network;
2. For every communication node j, check if there exists a path from a control center to node j and it receives an incoming edge from power grid;
3. Remove all the nodes that do not satisfy the properties in steps 1 and 2;
4. Remove all isolated generators;
5. Remove all the links connected to the removed nodes.

until *No node can be removed*;
output: Set of all removed nodes

Algorithm 1: Cascade Algorithm

Phase II

In this phase, our objective is to find a set of feasible power injections so that the minimum amount of load is shed and no control node fails due to loss of power. Let E_{CP} denote the adjacency matrix modeling the dependency of the communication network on loads. Let vector h denote the amount of power flowing from loads located in the power transmission grid P_i to loads located in the power distribution grid P_{C_j} that support the communication network (See Figure 3-3). Moreover, let b be a two part power vector. The first part represents the amount of power injection

at loads in the transmission grid with positive sign as these are source nodes; i.e. $-P_i$ since loads P_i are originally modeled with negative values. Similarly, the second part represents the amount of power injection at loads in the distribution grid with negative sign as these are destination nodes; i.e. P_{C_j} since loads P_{C_j} are originally modeled with negative values. Moreover, notice that notation "updated" indicates that the power grid and communication network have been updated by removing the nodes that fail in Phase I.

$$\begin{aligned}
\text{minimize} \quad & e^T(|P^{new} - P^{old}|) && \text{(3.3a)}\\
\text{subject to} \quad & A^{updated} f = P^{new} && \text{(3.3b)}\\
& (A^{updated})^T \theta = Xf && \text{(3.3c)}\\
& f \leq f^{max}, \quad \forall (i,j) \in E_P^{updated} && \text{(3.3d)}\\
& 0 \leq P_i^{new} \leq P_i^{old} \quad \forall i \in V_{P,gen}^{updated} && \text{(3.3e)}\\
& P_i^{old} \leq P_i^{new} \leq 0 \quad \forall i \in V_{P,load}^{updated} && \text{(3.3f)}\\
& P_{C_j} \leq -P_C^{req} \quad \forall j \in V_C^{updated} && \text{(3.3g)}\\
& \sum E_{CP}^{updated} h = b && \text{(3.3h)}\\
& h \geq 0 && \text{(3.3i)}
\end{aligned}$$

Constraint 3.3g guarantees that every remaining communication node receives the minimum amount of power required for operation. Constraint 3.3h models the power flowing from the power grid to the communication network with a network flow model. Constraint 3.3i enforces that the direction of power flow is from power nodes to communication nodes. The combination of these three constraints changes the power injection at power nodes so that the communication nodes remaining from Phase I will continue operating. The rest of constraints are similar to the Simple mitigation policy and set the power injections so that no transmission line is overloaded. Similarly, the objective function is minimizing the total amount of load shedding. Note that this ILP may be infeasible. In such cases the yield would be zero, showing that our control

policy is not capable of controlling the failures in the network.

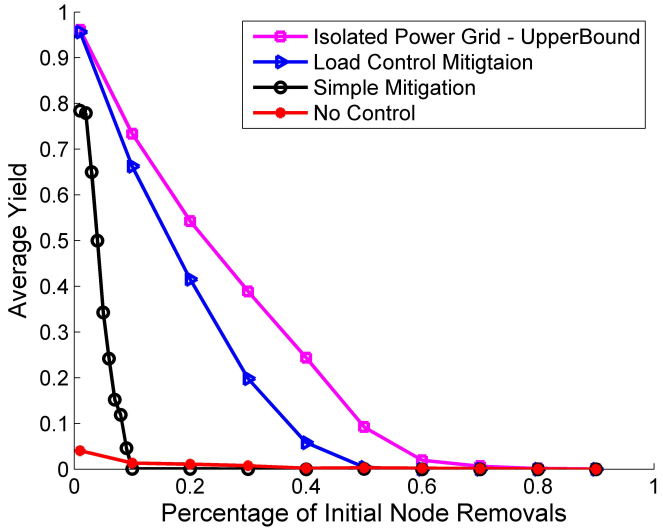

Figure 3-5: Comparing performances of control policies

Figure 3-5 compares the performance of load control mitigation and simple mitigation policies. It can be seen that the yield after applying the load control policy is improved with respect to the simple mitigation policy and it is close to the upper-bound.

Figure 3-6 compares the isolated and interdependent power grids with and without intelligent mitigation policies. As can be seen, the yield (the ratio of served load to the initial load) in interdependent power grid and communication network without control is lower than the isolated power grid (Figure 3-6(a)). However, when intelligent control is applied to the interdependent network, the yield is higher than the isolated power grid (Figure 3-6(b)).

3.4 Sensitivity Analysis

We analyze the performance of our control policy with respect to changes in the communication network and the interdependency between the power grid and communication network. The parameters we study are the amount of power that communication nodes require (P_{C_j}), size of communication network, the average number of

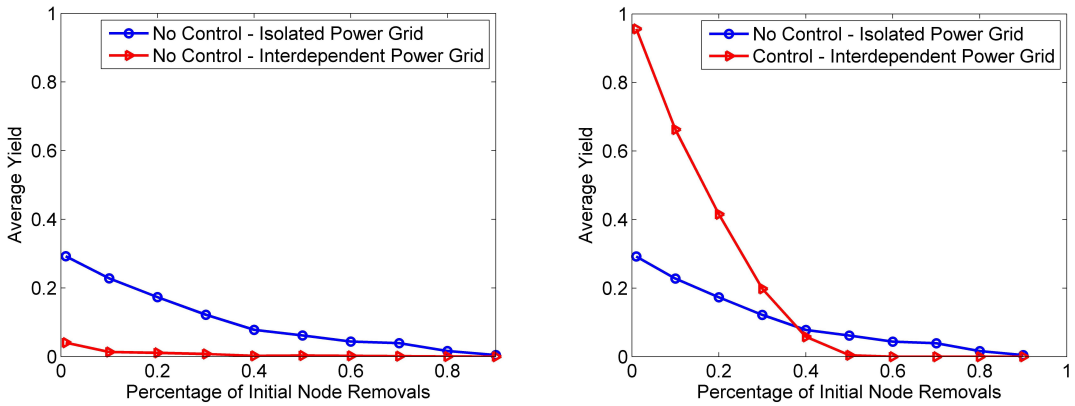

(a) No Control- Interdependent networks are more vulnerable.

(b) Control - Interdependent networks are more reliable.

Figure 3-6: Comparing yield of interdependent and isolated power grids.

power nodes supporting each communication node, namely “Communication Interdependence Degree" and finally, the average number of communication nodes supporting each power node, namely “Power Interdependence Degree".

We generate 30 random networks as in Section 3.1 (Figure 3-1’s caption, where communication nodes receive power only from loads) and test their feasibility by applying our control policy. If the entire network fails in the first phase, the network is not feasible; i.e. no control policy can survive it. We average the yield found by our control policy over the feasible networks.

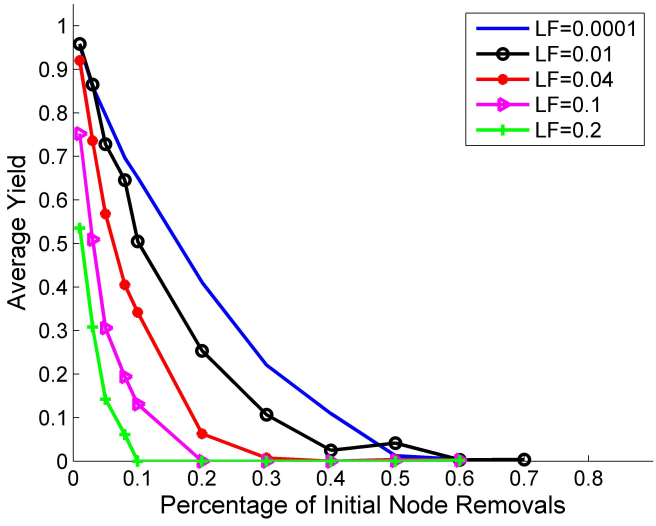

Figure 3-7: Impact of Load Factor on the Yield; 500 communication nodes; 20% of nodes are randomly selected as control centers

We define the “Load Factor" (LF) as the ratio of power required by the communication network to the total load in the power grid. In the previous simulations LF was set to be 10^{-4}. Figure 3-7 shows that by increasing LF, the yield decreases as it is harder to provide the required amount of power for all loads supporting communication network.

We analyze the performance of our policy with respect to the size of communication network; i.e. number of communication nodes. Figure 3-8 shows that for small values of LF, the larger networks have higher yield. However, by increasing LF, the yield of larger networks decreases more; thus, the smaller networks perform better for large LF. This is intuitive as more communication nodes provide more diversity, but also require more power.

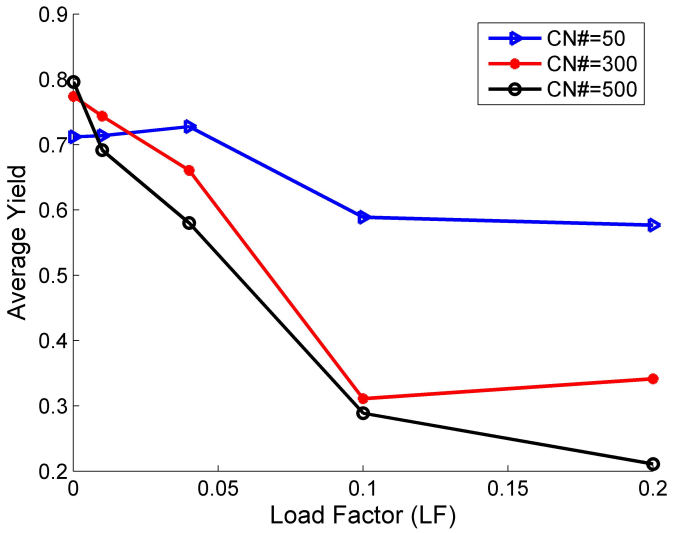

Figure 3-8: Impact of Number of Communication Nodes on the Yield; 20% of communication nodes are randomly selected as control centers; initial removal=5%

The next parameter that we study is the average number of power nodes that support every communication network (interdependence degree). Figure 3-9 shows that the average yield increases by increasing the interdependence degree.

Finally, we investigate the impact of the average number of communication nodes supporting each power node. It can be seen from Figure 3-10 that increasing degree has positive impact on the yield and feasibility; however, it is not as strong as the impact of communication interdependence degree. The reason is due to the structure

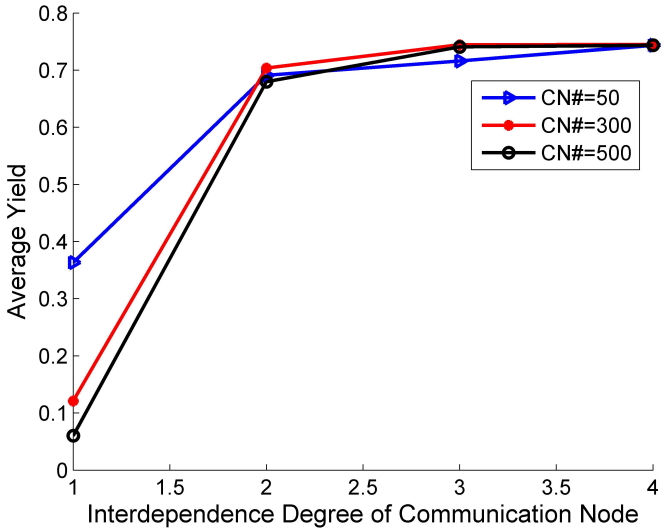

Figure 3-9: Impact of Communication Interdependence Degree on the Yield; initial removal=10%; load factor=0.1

of our control policy that tends to sustain all of the communication network. Thus, if the control policy is feasible, the communication network remains operating, which results in the operation of the power nodes supported by these communication nodes. Therefore, in these scenarios, increasing the support for power grid cannot help. The small improvement that we see here is related to the reduction of failures due to disconnection.

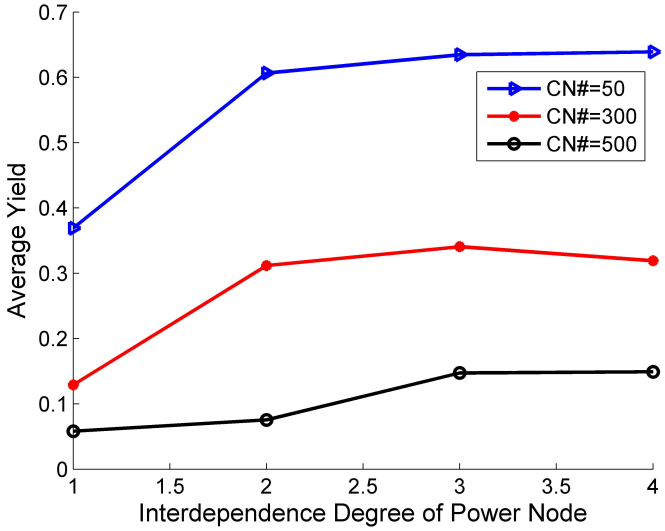

Figure 3-10: Impact of Power Interdependence Degree on the Yield; initial removal=10%; load factor=0.1

3.5 Conclusion

In this chapter, we showed that it is essential to consider the power flow equations for analyzing the behavior of interdependent power grid and communication networks. We argued that in order to analyze the robustness of interdependent networks, one should consider the control schemes for controlling cascading failures both inside and between the power grid and communication network. We proposed a new control scheme that mitigates failures in one stage and keeps the yield close to the maximum possible value. Our policy only allows the failures due to disconnection from generators and control centers. Thus, a connectivity model can be used to describe the process of cascading failures in interdependent topologies. In addition, we tested the performance of our load control policy with respect to changes in several parameters such as load factor (power needed by communication) and interdependence degree.

Chapter 4

Modeling the Impact of Communication Loss on the Power Grid under Emergency Control

In this chapter, we study the interaction between the power grid and the communication network used for its control under emergency situations. We design a centralized emergency control scheme under both full and partial communication support, to improve the performance of the power grid, and use our emergency control scheme to model the impact of communication loss on the grid. We show that unlike previous models used in the literature, the loss of communication does not necessarily lead to the failure of the correspondent power nodes; i.e. the “point-wise" failure model is not appropriate. In addition, we show that the impact of communication loss is a function of several parameters such as the size and structure of the power and communication failure, as well as the operating mode of power nodes disconnected from the communication network. Our model can be used to design the dependency between the power grid and the communication network used for its control, so as to maximize the benefit in terms of intelligent control, while minimizing the risks due to loss of communication.

4.1 Introduction

During normal operation, primary and secondary frequency controls are responsible for stabilizing the grid. In particular, primary frequency control is a local controller which reacts to local changes in frequency and adjusts the generation to keep the frequency within an acceptable range. The secondary controller is responsible for setting the frequency back to its nominal value (e.g. $60Hz$ in US) where it uses the generator's reserves to balance the power. However, during large failures the normal operation controllers cannot stabilize the grid. Therefore, the future smart grid should be equipped with a Communication and Control Network (CCN) that allows rapid monitoring of the power grid and provides intelligent centralized control actions that can mitigate cascade of failures. The centralized control actions to stabilize the grid during catastrophic failures are referred to as "Emergency Control".

There are several studies proposing Emergency control schemes for changing the power generation as well as load shedding so that the grid can be stabilized before any cascading failures occur [28, 57–59]. Although, using this extra information/control improves the performance of the grid, it creates a dependency between the power grid and the communication and control network.

During normal operations, loss of communication is unlikely to lead to significant power failures as local controllers can stabilize the grid. However, when the grid is under stress, lack of situational awareness and control can lead to catastrophic failures. Such events may result from a natural disaster that affects both the communication network and the power grid or the failure of communication components due to loss of power coming from the grid. Therefore, it is very important to study the impact of communication loss on the power grid's stability during a large disturbance.

The impact of communication on the power grid's performance and vice versa was recently studied using an abstract form of interdependency. Buldyrev *et al.* in [18] showed that if there exists a one-to-one interdependency between the nodes of the grid and the communication network, interdependent networks are more vulnerable to failures than isolated networks. In their "point-wise" interdependency model, a

power node fails if it loses its connection to the communication network, and a communication node fails if it loses its connection to the power grid. Similar results were obtained in [6, 20]. Recently, [9] showed that it is critical to use the power flow equations to model the power grid, and interdependency could benefit the power grid if the communication network is used for mitigating the cascade of failures (See Figure 3-6).

In this chapter, we carefully model the function of emergency control of the grid using the communication and control network. Using this model, we show that the loss of any communication network component may lead to the loss of situational awareness and control, and impact the performance of the grid. In particular, we show that the point-wise failure model is not suitable for modeling interdependent power-communication networks. Moreover, we show that the impact of communication loss on the power grid is a function of several parameters such as size and structure of the communication and power failures.

The rest of this chapter is organized as follows. In Section 4.2 we describe the power-communication dependency. In Section 4.3, we formulate the emergency control problem with full and partial communication. Finally, in Section 4.4, we provide simulation results and conclude in Section 4.5.

4.2 Model

4.2.1 PowerGrid-Communication Dependency

Figure 4-1 shows an abstract model of the future control and communication network for an interconnected grid. In this model, each region is supported by a dedicated communication network (intra-region communication network) that monitors all parts of the grid, and sends the information to the control center. The control decisions made by the control center are sent back to the grid via the same communication network. Moreover, the grid regions are connected to each other via several tie lines that allows transmission of power from one region to the other. Therefore, a failure

in one region could cascade to the other regions. In order to avoid such failures, the control centers are connected to each other with an inter-region communication network that allows them to share state information and regional control decisions.

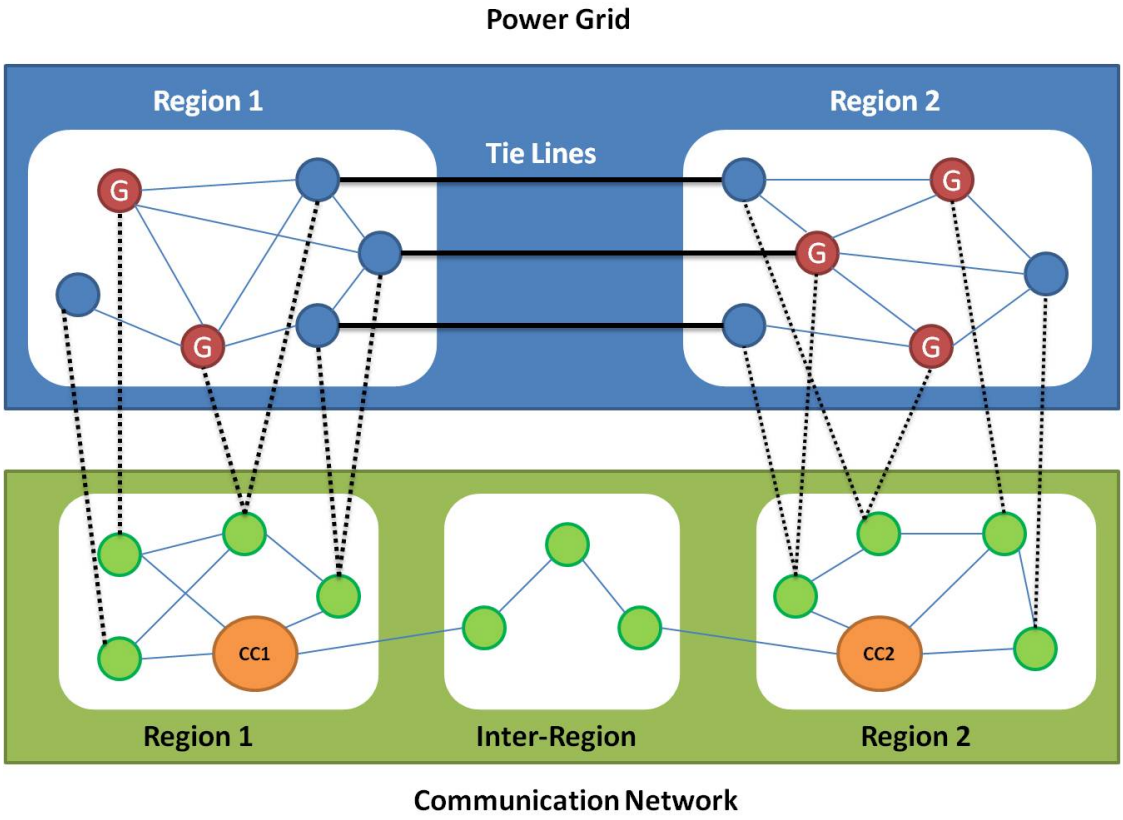

Figure 4-1: Future Power Grid equipped with communication networks and control centers for online monitoring and control; dotted lines indicate dependency of power nodes on communication nodes; G denotes generator, and $CC1$ and $CC2$ denote control centers. Power nodes that have lost their connection to the communication network become “uncontrollable". Note that uncontrollable nodes may operate fine using localized control, but cannot be controlled remotely because they are not reachable.

It can be seen from Figure 4-1 that communication failures could occur either between the regions or inside the regions. **Inter-region** failures can degrade or disconnect the communication between the control centers in different regions. In contrast, **Intra-region** failures can cause some of the power nodes to be disconnected from the communication network and unable to send information to or receive the control decisions from the control center.

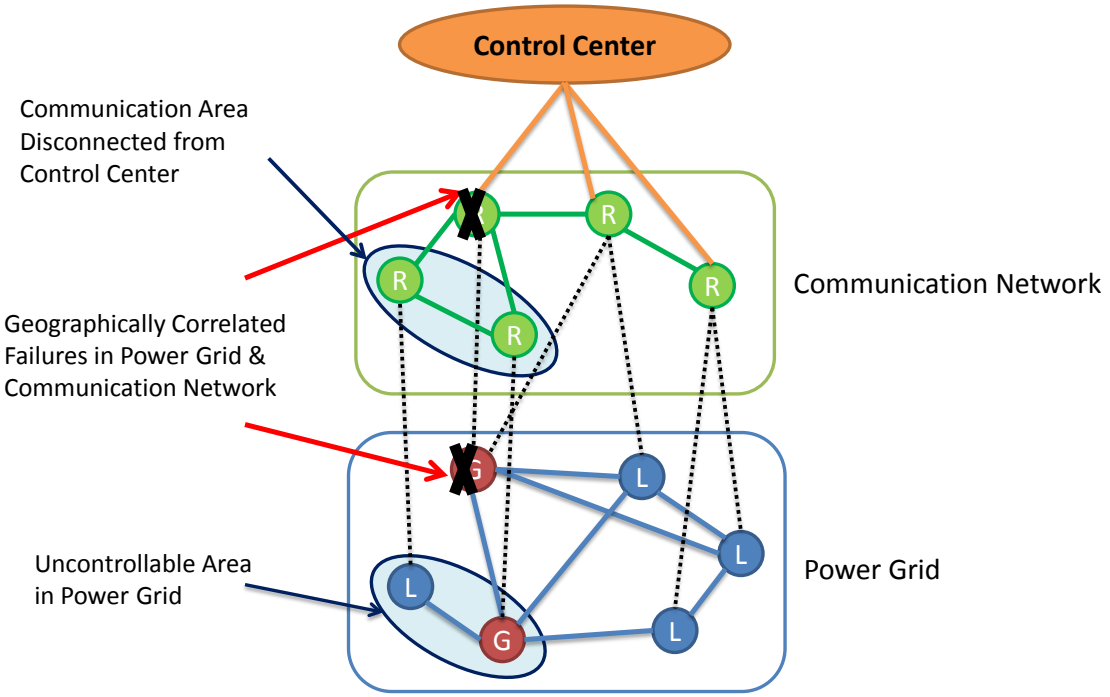

Figure 4-2: Dotted lines indicate dependency of power nodes on communication nodes. Power nodes that have lost their connection to the communication network become "uncontrollable". Note that uncontrollable nodes may operate fine using localized control, but cannot be controlled remotely because they are not reachable.

In this chapter, we study the case of intra-region failures. In particular, we focus on the case where we are able to observe the power failures; i.e. we have communication to the failed power nodes (See Figure 4-2).

4.2.2 Power Grid

The power grid consists of nodes and power lines where power nodes are of three types: Generators (G) that generate power; Loads (L) that consume power and Buses (B) that allow the transmission of power through them, but neither generate nor consume power. In our model, each generator or load is connected to the rest of the grid via a single bus and each bus can be connected to any number of buses. Figure 4-3 shows an example of our system.

In this chapter, we study the steady-state behavior of the grid. We also assume that power lines are loss-less; i.e. can be modeled only by their reactance X. Thus, the flow in a power line is described by a DC model as follows: $f_{ij}X_{ij} = \Delta\theta_{ij}$ where

f_{ij} is the amount of power in line (i, j), X_{ij} is the reactance of line (i, j) and $\Delta\theta_{ij}$ represents the difference in the voltage phase of nodes i and j.

The generators are modeled as synchronous generators with the following swing equation:

$$M_i\dot{\omega}_i = PG_i - D_i(\omega_i - \omega_s) - (\sum_{j\in E} f_{ij} - \sum_{j\in E} f_{ji}) \tag{4.1}$$

where PG_i denotes the mechanical power, and D_i and M_i are generator's damping and inertia, respectively. Moreover, the difference in the flow passing through the generator $(\sum_{j\in E} f_{ij} - \sum_{j\in E} f_{ji})$ denotes the amount of generated electrical power. Finally, ω_i is the frequency of node i and ω_s is the synchronous frequency [see [60] for more details]. Considering the steady-state behavior ($\dot{\omega}_i = 0$), the equation for synchronous generators will reduce to:

$$PG_i - D_i(\omega_i - \omega_s) = \sum_{j\in E} f_{ij} - \sum_{j\in E} f_{ji} \tag{4.2}$$

The damping coefficient D_i is often 0.02 per unit or less (See [61]-pp. 657-663 for more details). This model describes the reaction of generator to the changes in power; if generation is greater than the load, the frequency increases, and if the generation is smaller than the load, the frequency decreases. In order to avoid sharp changes in frequency, we also model the local frequency-droop control (also called primary frequency control) in the grid that is responsible for modifying the amount of power generation based on the changes in frequency; i.e. increases the power generation as frequency drops and decreases the power generation as frequency rises. The droop-control can be written as follows.

$$\Delta PG_i = -\frac{1}{R_i}(\omega_i - \omega_s) \tag{4.3}$$

where R_i is the regulation constant. In a per unit system, the standard value of regulation constant is 0.05 per unit. Thus, in our model of a $60Hz$ system, $R_i = \frac{60*0.05}{PG_i^{initial}}$ where $PG_i^{initial}$ is the initial mechanical power of generator i before any disturbance ([61]-pp. 657-663). The combination of PG_i in equation 4.2 and ΔPG_i

in equation 4.3 models the response of generator i to the changes in power using the local controller:

$$PG_i - (D_i + \frac{1}{R_i})(\omega_i - \omega_s) \quad = \sum_{j \in E} f_{ij} - \sum_{j \in E} f_{ji} \tag{4.4}$$

For the rest of this chapter, we define $\alpha_i = D_i + \frac{1}{R_i}$.

Finally, we consider protection relays located at every power node. The control role of these relays is explained in section 4.2.4.

4.2.3 Communication Network

We consider a zero-delay communication network that supports every power node; i.e. collects synchronous information from every power node, sends it to the control center and sends back the control decision from the control center to all power nodes. The set of collected information by the communication network includes: (i) Magnitude of voltage at node k ($V_k(t)$); (ii) Phase of voltage at node k ($\theta_k(t)$); (iii) Frequency of node k ($\omega_k(t)$); (iv) Flow in power line (k, j) ($f_{kj}(t)$); (v) on/off State of element j ($S_j(t)$).

Note that since we use the DC model in the chapter, the magnitude of voltage $V_k(t)$ is constant and equal to 1 for all nodes. Moreover, the "off" state of an element means that it has failed.

4.2.4 Control Actions

Next, we describe both types of local and centralized control actions needed for operation of the power grid.

Local Control Actions: All power nodes are equipped with local controllers that do not require connection to the communication network and their actions include: (i) *droop control at generators*: Droop control can increase or decrease the amount of generation based on the changes in the frequency as described by equations 4.3 and 4.4; (ii) *Over-frequency generator tripping (protection)*: the protection relays will trip

the generator if the frequency exceeds the maximum threshold ω_{max} due to excess generation in the system; (iii) *Under-frequency load shedding (protection)*: the protection relays will shed the load if the frequency drops below the minimum threshold ω_{min} due to excess load in the system; (iv) *Overloaded line tripping (protection)*: the protection relays will trip the line if the power in that line exceeds the capacity.

Central Control Actions: All power nodes are equipped with sensors/actuators connected to the control center via the communication network. The central control actions include: (i) *Ramping down generators*: if power generation is greater than consumption, the controller decreases the generation to keep the frequency within the acceptable range; (ii) *Intelligent load shedding*: if the power generation is lower than consumption, the controller sheds some load to keep the frequency within the acceptable range; (iii) *Intelligent line tripping*: can be used for changing the topology of the grid or islanding some areas of the power grid. Since in our model every power node is equipped with an actuator, a power line can be tripped by either of its end-nodes.

4.3 Emergency Control

In this Section, we design the optimal emergency control used for mitigation of failures in the power grid in the presence of a fully or partially operational communication network. We can then use these control policies for evaluating the performance of the grid under different communication failure scenarios.

4.3.1 Full Communication

In this case, the power grid is fully supported by a communication network; thus, every generator, load and line can be centrally controlled. The optimal emergency control is the set of central and local control actions that maximizes the served load while keeping the power balanced, maintaining the frequency within an acceptable range and keeping the flows in the power lines within their capacity. We use the control model with full communication as a basis for modeling the control with partial

communication.

In eq. (4.5), we formulate the problem of optimal control with the objective of maximizing served load while stabilizing the grid. Let, V_G, V_L and V_B denote the set of generators, loads and bus nodes after the initial power failure, respectively. Moreover, let ω_i^{min} and ω_i^{max} denoted the minimum and maximum frequency thresholds. In addition, E denotes the set of power lines after the initial failure, and X_{ij} represents the reactance of line (i, j). Finally, let M be a large constant.

The variables f_{ij} and $\Delta\theta_{ij}$ denote the amount of flow in line (i, j) as well as the phase difference of voltages at nodes i and j. In addition, variables PG_i, PL_i and ω_i denote the amount of generation, load and frequency at node i. Note that PG_i and PL_i take positive and negative values, respectively. Finally, z_{ij} is a binary variable associated to line (i, j) that takes value of 1 if line (i, j) is connected and 0 if that line is tripped (modeled in constraint (4.5k)).

As mentioned previously, the objective is to serve the maximum load while stabilizing the grid. Constraints (4.5b,4.5c,4.5d) ensure that the flow conservation is satisfied in generators, loads and buses where generation and load values PG_i and PL_i can change by central controller and term $\alpha_i(\omega_i - \omega_s)$ models the local droop controller at the generators. Constraint (4.5e) models the DC power flow in line (i, j) if it remain connected; i.e. $z_{i,j} = 1$; note that there is no relation between the phases at nodes i and j if the line is tripped ($z_{i,j} = 0$). Constraint (4.5f) guarantees that the flow in line (i, j) is within the capacity if the line is not tripped, and constraint (4.5g) ensures that all nodes in a connected area have the same frequency. Finally, constraints (4.5h, 4.5i, 4.5j) guarantee that the values of frequency, generation and load are maintained within the acceptable range.

$$\min \sum_{i \in V_L} PL_i \tag{4.5a}$$

$$\sum_{j \in E} f_{ij} - \sum_{j \in E} f_{ji} = PG_i - \alpha_i(\omega_i - \omega_s) \quad \forall i \in V_G \tag{4.5b}$$

$$\sum_{j \in E} f_{ij} - \sum_{j \in E} f_{ji} = PL_i \quad \forall i \in V_L \tag{4.5c}$$

$$\sum_{j \in E} f_{ij} - \sum_{j \in E} f_{ji} = 0 \quad \forall i \in V_B \tag{4.5d}$$

$$-M(1 - z_{ij}) \leq X_{ij} f_{ij} - \Delta\theta_{ij} \leq M(1 - z_{ij}) \forall (i,j) \in E \tag{4.5e}$$

$$-z_{ij} f_{ij}^{max} \leq f_{ij} \leq z_{ij} f_{ij}^{max} \quad \forall (i,j) \in E \tag{4.5f}$$

$$-M(1 - z_{ij}) \leq \omega_i - \omega_j \leq M(1 - z_{ij}) \quad \forall (i,j) \in E \tag{4.5g}$$

$$\omega_i^{min} \leq \omega_i \leq \omega_i^{max} \quad \forall i \in V_G \tag{4.5h}$$

$$PG_i^{min} \leq PG_i - \alpha_i(\omega_i - \omega_s) \leq PG_i^{max} \quad \forall i \in V_G \tag{4.5i}$$

$$PL_i^{max} \leq PL_i \leq 0 \quad \forall i \in V_L \tag{4.5j}$$

$$z_{ij} \in \{0, 1\} \quad \forall (i,j) \in E \tag{4.5k}$$

4.3.2 Partial Communication

Next, we consider the case that in addition to the power failure, a part of the communication network fails as well. Thus, parts of the grid lose their connection to the communication network and control center. Our objective is to design an emergency control policy that maximizes the served load and stabilizes the grid using the controllable nodes.

Figure 4-3 shows an example of such power grid with power failures and controllable/uncontrollable areas. In the following, we define each area mathematically, and explain the set of control actions available in each.

The components that have not initially failed in the power grid can be divided into 3 areas described as follows:

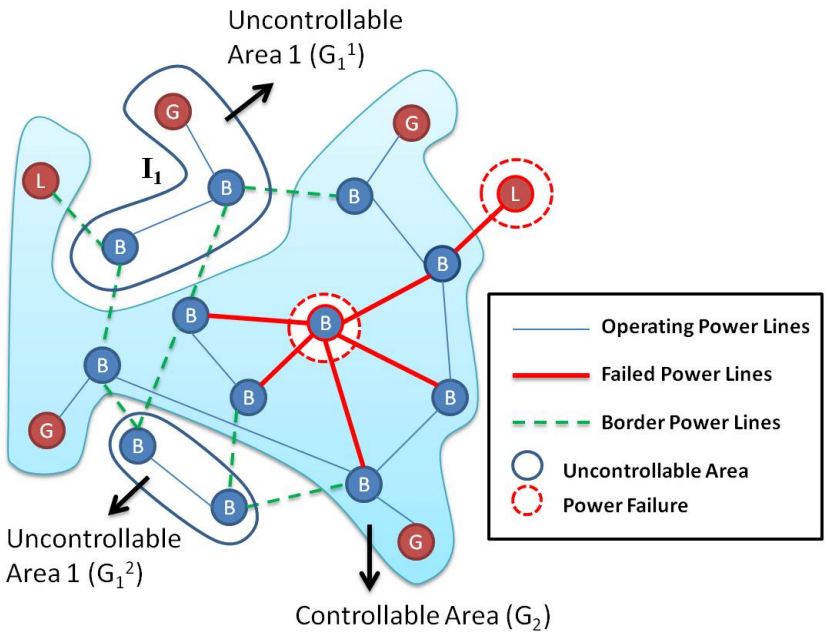

Figure 4-3: Power Grid Model after Communication Loss and Power Failure

Uncontrollable Area: Let $G_1 = \{V_1, E_1\}$ denote the uncontrollable subset of power grid, where V_1 denotes the set of power nodes that are disconnected from the communication network, and E_1 denotes the set of power lines that connect any pair of nodes in V_1. Without loss of generality, we can divide subgraph G_1 into k disjoint subgraphs $G_1^k = \{V_1^k, E_1^k\}$ such that nodes inside $V_1^{k_i}$ are connected and for any $j \neq i$ nodes in $V_1^{k_i}$ and $V_1^{k_j}$ are not connected. Note that depending on the structure of the network, k could be any number equal or greater than 1. The only possible centralized control in these areas is islanding of the entire area by tripping border lines. All of the local controllers described in Section 4.2.4; i.e. droop control and protection schemes, are available. In addition, we have a local controller that switches the nodes in the uncontrollable areas to a pre-defined mode of operation as soon as they are disconnected from the communication network. In this chapter, we consider two possible modes: P_{init} which corresponds to keeping all nodes operating at their last state, and P_{zero} which corresponds to tripping all nodes.

Controllable Area: Let $G_2 = \{V_2, E_2\}$ denote the controllable subset of the power grid, where V_2 is the set of power nodes that are connected to the communication network ($V_2 \cap V_1 = \emptyset$ and $V_2 \cup V_1 = V$ where V is the set of all power nodes), and

E_2 is the set of power lines connecting any pair of nodes in V_2. All central and local controllers described in Section 4.2.4 are available in the controllable areas.

Border Lines: Let E_{12}^k denote the set of power lines that connect the uncontrollable nodes in V_1^k to the controllable nodes in V_2. Border lines can be tripped centrally using the relay in its controllable node. All local controllers at its end-nodes are available.

In eq. (4.6), we formulate the optimal emergency control problem subject to loss of communication. Given the set of control actions, the behavior of the controllable areas can be modeled as described in previous section with Full Control; i.e., eq. (4.6b). However, the nodes in the uncontrollable areas cannot employ centralized control and must rely on localized control and/or islanding as described next. The following ILP shows the general description of optimal emergency control.

$$\min \sum_{i \in V_L} PL_i \tag{4.6a}$$

$$\text{s.t. Constraints}(4.5b - 4.5k) \quad \forall k \in K, i \in V_2, (i,j) \in E_2 \cup E_{12}^k \tag{4.6b}$$

$$\text{Constraints}(4.7a - 4.7i) \quad \forall k \in K, i \in V_1^k, (i,j) \in E_1^k \tag{4.6c}$$

In the following, we describe constraints (4.7a-4.7h) related to the control actions in the uncontrollable areas. Let $\sum_{(i,j) \in E_{12}^k} z_{ij} = 0$ if the uncontrollable area G_1^k is isolated from the rest of grid; i.e. all the border lines are tripped, and $\sum_{(i,j) \in E_{12}^k} z_{ij} > 0$ if it is connected. Moreover, let I^k be a binary variable (modeled in constraint (4.7i)) associated with the uncontrollable area G_1^k where $I^k = 0$ if the isolated uncontrollable area cannot be stabilized just by the local droop controller, and $I^k = 1$ if that area is stabilized (i.e. power is balanced just by using droop control and frequency and power flows are within the acceptable range).

Constraints (4.7a-4.7h) model the control decision in the uncontrollable areas. Note that PG_i^{init} and PL_i^{init} denote the values of generators and loads in uncontrollable area after going to mode P_{init}; i.e. the last values of generators and loads right

before disconnection from communication network. If the mode is set to P_{zero}, PG_i^{init} and PL_i^{init} in constraints (4.7b) and (4.7c) will be set to zero. Constraint (4.7a) denotes that if the uncontrollable area is unstable ($I^k = 0$), it has to be islanded ($\sum_{(i,j)\in E_{12}^k} z_{ij}$).

$$\sum_{(i,j)\in E_{12}^k} z_{ij} \leq MI^k \qquad \forall k \in K \tag{4.7a}$$

$$\begin{aligned} -M(1-I^k) &\leq \sum_j f_{ij} - \sum_j f_{ji} - PG_i^{init} + \alpha_i(\omega_i - \omega_s) \\ &\leq M(1-I^k) \qquad \forall i \in V_{G1}^k, \forall k \in K \end{aligned} \tag{4.7b}$$

$$\begin{aligned} -M(1-I^k) \leq \sum_j f_{ij} - \sum_j f_{ji} - PL_i^{init} &\leq M(1-I^k) \\ \forall i \in V_{L1}^k, \forall k \in K \end{aligned} \tag{4.7c}$$

$$\begin{aligned} -M(1-I^k) \leq \sum_j f_{ij} - \sum_j f_{ji} &\leq M(1-I^k) \\ \forall i \in V_{B1}^k, \forall k \in K \end{aligned} \tag{4.7d}$$

$$\begin{aligned} -M(1-I^k) \leq X_{ij} f_{ij} - \Delta\theta_{ij} &\leq M(1 \ -I^k) \\ \forall (i,j) \in E_1^k, \forall k \in K \end{aligned} \tag{4.7e}$$

$$-f_{ij}^{max} I^k \leq f_{ij} \leq f_{ij}^{max} I^k \qquad \forall (i,j) \in E_1^k, \forall k \in K \tag{4.7f}$$

$$-M(1-I^k) \leq \omega_i - \omega_j \leq M(1-I^k) \quad \forall (i,j) \in E_1^k, \forall k \in K \tag{4.7g}$$

$$\omega_i^{min} I^k \leq \omega_i \leq \omega_i^{max} I^k \qquad \forall i \in V_{G1}^k, \forall k \in K \tag{4.7h}$$

$$I^k \in \{0,1\} \qquad \forall k \in K \tag{4.7i}$$

When an uncontrollable area can be stabilized just by local controllers; i.e. $I^k = 1$, constraints (4.7a-4.7h) will be active. In particular, constraints (4.7b-4.7d) model the power balance in the area using only the droop control at generators, and constraint (4.7e) models the DC power flow in line (i,j). Moreover, constraint (4.7f) guarantees that flow is within the line capacities, constraint (4.7g) forces all the connected nodes to have the same frequency and constraint (4.7h) guarantees that the frequency

remains within the acceptable range.

Note that when $I^k = 0$, the uncontrollable area is unstable; i.e. either power cannot be balanced just by droop controller or some lines are overloaded. Thus, the frequency and line protection relays will be activated to trip the generators, shed the load and trip the lines. This causes extra failures which activates more protection relays. The cascade of failures continue until power is balanced, and frequency and power flows are within their acceptable ranges. We model the cascading failures separately for each uncontrollable area k after observing its correspondent I^k value.

4.4 Simulation Results

We analyze the data from the Italian power grid which consists of 310 buses, 113 generator units and 97 loads. The power failures are considered to be generators. We assume that any arbitrary area in the power grid can lose its connection to the communication network, and investigate the impact of these uncontrollable areas on the performance of the grid. The metric that we use for our analysis is "yield" defined as the ratio of served load [1] to the initial load.

Simulation results show that loss of communication can indeed impact the performance of the power grid and lead to a lower yield. For example, we observed a scenario where loss of 10 power nodes led to 6% load shedding under full communication and 23% load shedding under partial communication (See [11]). In this section, we would like to find the parameters that have the greatest impact on performance.

4.4.1 Effect of size and structure of uncontrollable areas

We consider different number of uncontrollable nodes with different clusterings. In particular, we define a cluster as a set of connected nodes where a cluster of size 1 means that no two uncontrollable nodes are connected and a cluster of size 10 means that the uncontrollable area can be divided into disjoint subareas, each with

[1] Served Load is considered to be the sum of power from controllable areas, stable uncontrollable areas and unstable uncontrollable areas that have experienced cascading failures.

10 connected nodes.

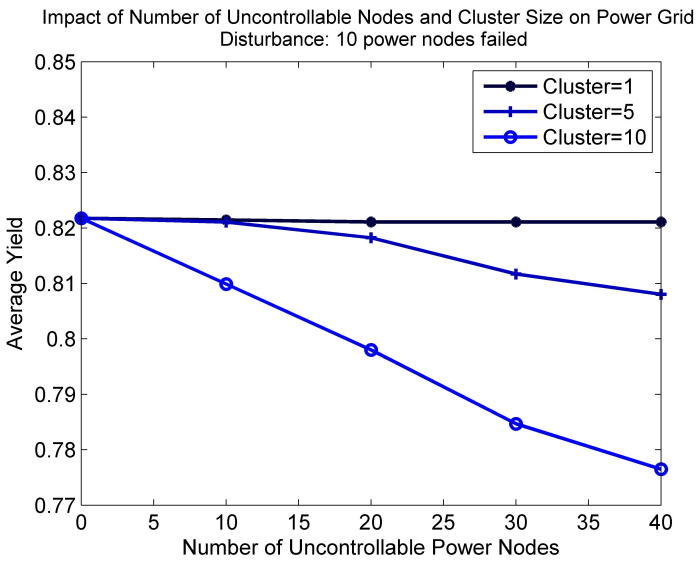

Figure 4-4: Average yield vs. Number of uncontrollable power nodes; P_{init} mode.

Figure 4-4 shows that for a given size of power disturbance, the average yield (over 100 scenarios) decreases as the number of uncontrollable nodes increases. In addition, it shows that for the same number of uncontrollable nodes, the average yield decreases as the size of cluster increases. We observed that for the cases that all the uncontrollable areas can be stabilized using droop control; i.e. $I^k = 1$, the yield of partial communication is very close to the yield of full communication. However, for the cases that at least one uncontrollable area is unstable, the yield decreases significantly. Since large clusters could contain more generators and loads, the effect of loss of such clusters is more severe. Moreover, Figure 4-5 shows the impact of size and structure of uncontrollable areas on their stability. It can be seen that as the size of uncontrollable area increases the fraction of unstable cases increases. In addition, it can be seen that as the size of clusters increases, it is less probable to lose a cluster. This is due to the fact that a large cluster could contain more power, and losing it could cause a significant loss of power. Finally, observations from Figures 4-4 and 4-5 show that every uncontrollable power node does not fail; i.e. “point-wise" failure model is not appropriate for power-communication interdependency.

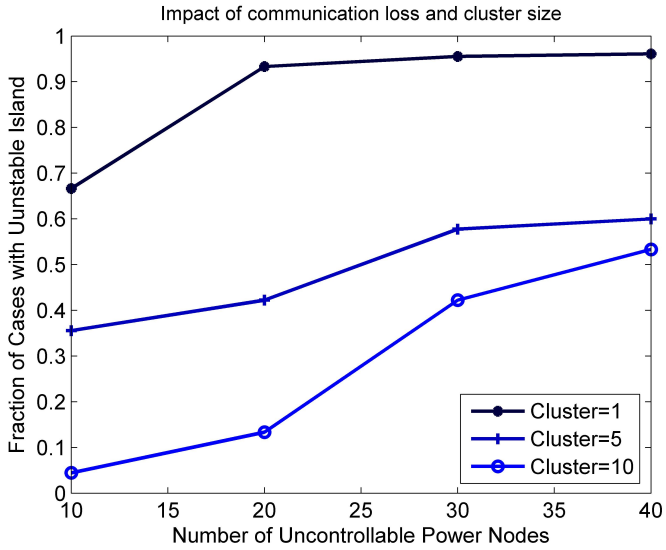

Figure 4-5: Fraction of cases with unstable islands vs. Number of uncontrollable power nodes; P_{init} mode.

4.4.2 Effect of Size of Power Loss

Next, we consider the effect of size of power failure on performance. Figure 4-6 shows that as the size of power failure increases, the average yield decreases. Moreover, it shows that the impact of communication loss increases as the number of power failures increases. This is due to the fact that for larger sizes of uncontrollable areas, it is harder to control a power disturbance and the impact on the yield is more severe.

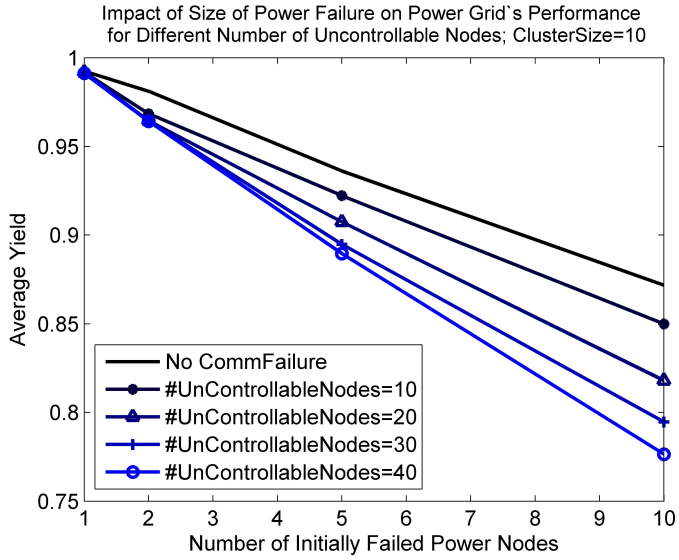

Figure 4-6: Average yield vs. Number of initially failed power nodes; P_{init} mode.

4.4.3 Effect of Different Modes

Finally, we compare the impact of different predefined modes P_{init} and P_{zero} described in Section 4.3.2. By simulating different failure scenarios under both modes, we observed that there exist scenarios where controlling the grid under P_{zero} mode leads to higher yield than P_{init} mode. In fact, in such scenarios, keeping the uncontrollable area operating at the P_{init} mode was infeasible; thus, they were islanded due to instability. But, under P_{zero} mode, it is possible to keep an uncontrollable area and use the buses in that area for transmitting power. Figure 4-7 shows that although in most cases the P_{init} mode results in a higher yield, the fraction of scenarios with $Y(P_{zero}) > Y(P_{init})$ increases as the number of uncontrollable nodes or failed power nodes increases. In particular, we observed that for the cases where P_{init} has the higher yield, the average difference in yield is 7% and for the cases where P_{zero} has the higher yield, the average difference is 8%.

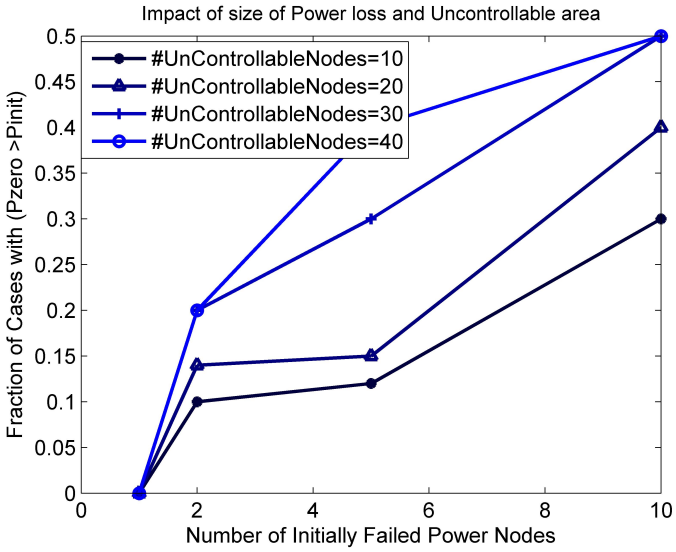

Figure 4-7: Fraction of cases with $(Y(P_{zero}) > Y(P_{init}))$ vs. Number of initially failed power nodes.

4.5 Conclusion

In this chapter, we showed that although controlling the power grid using the communication network could be very beneficial, it could be harmful if we lose part of

the control and communication network. Therefore, it is essential to have a thorough analysis on the impact of communication network on power grid to identify the vulnerabilities of the system. In particular, we showed that this impact is a function of several parameters including the size and structure of the communication loss. Therefore, it is very important to not only design a robust communication network, but also allocate the communication nodes to the power grid so that the negative impact of communication loss is minimized. Another direction of research is to design more intelligent local controllers so that in the lack of communication, the nodes can stabilize the grid even during large disturbances.

Chapter 5

Distributed Frequency Control in Power Grids under Limited Communication

In this chapter, we analyze the impact of communication failures on the performance of optimal distributed frequency control. We consider a consensus-based control scheme, and show that it does not converge to the optimal solution when the communication network is disconnected. We propose a new control scheme that uses the dynamics of power grid to replicate the information not received from the communication network, and prove that it achieves the optimal solution under any single communication link failure. In addition, we show that this control improves cost under multiple communication link failures.

Next, we analyze the impact of discrete-time communication on the performance of distributed frequency control. In particular, we show that the convergence time increases as the time interval between two messages increases. We propose a new algorithm that uses the dynamics of the power grid, and show through simulation that it improves the convergence time of the control scheme significantly.

5.1 Introduction

The main objective of a power grid is to generate power, and transmit it to the consumers. The power grid balances supply and demand through frequency control. This is done both at the local (generator) level, and the wide-area level as follows.

1. **Primary Frequency Control (Droop Control):** A local frequency controller that balances the power by speeding up or slowing down the generators; i.e. creating deviation from the 60Hz nominal frequency; this controller responds to the changes in power within milliseconds to seconds.

2. **Secondary Frequency Control (AGC):** AGC is a centralized frequency controller that re-adjusts the set points of generators to balance the power and restores the nominal frequency; this is a close-loop automatic controller that is applied every 2-4 seconds and requires communication network between AGC and generators.

3. **Economic Dispatch:** This is a centralized controller that reschedules the generators to minimize the cost of generation; this control decision is made by the ISO every 10-15 minutes, and requires communication network between ISO and generators.

The future power grid is going to integrate renewable energy resources. This will increase the fluctuations in the generation, and requires more reserve capacity to balance the power. One of the approaches to balancing power without having large reserve capacities is demand response, where loads are "adjustable" and participate in balancing the power. Since the number of loads is large, they cannot be controlled in a centralized manner. Thus, it is essential to use "distributed" control for demand response that incorporates all three stages of traditional frequency control.

Recently, there have been many attempts to develop distributed frequency control mechanisms. In [62], the authors consider the case that the total amount of required power is known, and designed a distributed algorithm that determines the amount of load participation to minimize the cost. In [33], the authors design a distributed

frequency controller which balances the power under unknown changes in the amount of generation and load, and compare its performance with a centralized controller.

In [34], the authors propose a primary control mechanism, similar to the droop control, for microgrids leading to a desirable distribution of power among the participants, and propose a distributed integral controller to balance the power. These results are extended in [35], where the authors use a similar averaging-based distributed algorithm to incorporate all three stages of frequency control in microgrids. Moreover, in [36], the authors propose a similar consensus-based algorithm for optimal frequency control in transmission power grid.

In [63], the authors use a primal-dual algorithm to design a primary frequency control for demand response in power grids. The results are extended in [64] and [65], where the authors design a primal-dual algorithm to model all three stages of a traditional frequency control in the power grid.

Although there exist several different distributed frequency control mechanisms in the literature, they all rely on the use of communication to exchange control information (e.g., Lagrangian multipliers). Moreover, convergence to an optimal solution requires the underlying communication network to be connected. In addition, in the design and analysis of all these controllers, it is assumed that the communication messages between neighboring nodes are transmitted in continuous time; however, in practice, these messages will be transmitted in discrete time. In this chapter, we analyze the performance of a consensus-based control scheme under communication failures. We show that when the communication network is disconnected, the control scheme balances the power by retrieving the normal frequency; however, its cost is not optimal. Moreover, we analyze the effect of discrete-time communication on the convergence time of this control scheme.

Next, we propose a novel control algorithm which uses the information from the power flow to replicate the direct information received from the communication network. We prove that our algorithm achieves the optimal solution under any single communication link failure. We also show via simulation results that our algorithm improves the cost under multiple communication failures. Finally, we propose a se-

quential algorithm based on our control mechanism, and show that it improves the convergence time under discrete-time communication.

The rest of this chapter is organized as follows. In Section 5.2, we describe the power grid's model. In Section 5.3, we describe a consensus-based distributed frequency control, and analyze it under communication link failures and discrete-time communication. In Section 5.4, we will propose a novel decentralized control for a two-node system and prove its optimality and stability, and in Section 5.5, we extend our control mechanism for multi-node systems under disconnected communication networks. Next, in Section 5.6, we propose a sequential control algorithm that improves the convergence time under discrete-time communication. Finally, we conclude in Section 5.7.

5.2 System Model

Let $\mathcal{G}_{\mathcal{P}} = \{\mathcal{N}_{\mathcal{P}}, \mathcal{E}_{\mathcal{P}}\}$ be the power grid, where $\mathcal{N}_{\mathcal{P}}$ denotes the set of power nodes, and $\mathcal{E}_{\mathcal{P}}$ denotes the set of power lines. The power at every node j, whether it is a generator or a load, consists of adjustable and unadjustable parts. The unadjustable part is the amount of power that cannot be changed; i.e. fixed demand or generation. The adjustable part is the amount of power that can be changed; i.e. controllable load or generation. The sum of the total power determines the amount of power imbalance in the grid, which leads to the frequency deviation. The role of a controller is to balance the power by using the adjustable power at all nodes with minimum cost. Next, we describe the dynamics of the power grid which translate the power imbalance to frequency deviation. Then, we describe the optimal control policy.

Let M_j be the inertia of node j, and D_j be the droop coefficient of node j. Moreover, let $p_j(t)$ be the unadjustable power and $u_j(t)$ be the adjustable power (control) at node j and at time t. In addition, let B_{jk} be the susceptance of power line (j,k), and $f_{jk}(t)$ be the amount of power flow from node j to node k at time t. We can describe the dynamics of the power grid using the swing equation at every node and the power flow equation at every line as follows.

$$M_j\dot{\omega_j}(t) = -D_j\omega_j(t) + p_j(t) + u_j(t) - \sum_{k:(j,k)\in\mathcal{E}_\mathcal{P}} f_{jk}(t)$$

$$j \in \mathcal{N}_\mathcal{P} \tag{5.1a}$$

$$\dot{f_{jk}}(t) = B_{jk}(\omega_j(t) - \omega_k(t)) \qquad (j,k) \in \mathcal{E}_\mathcal{P} \tag{5.1b}$$

The objective of our control is to minimize the total cost of adjustable power at steady-state while balancing power. Let p_j^* be the steady-state unadjustable power, and u_j^* be the steady-state adjustable power (control) at node j. Moreover, let f_{jk}^* be the steady-state power flow from node j to node k. The optimal steady-state control can be formulated as follows.

$$\min_{u^*,f^*} \quad \sum_{j\in\mathcal{N}_\mathcal{P}} \frac{1}{2} C_j u_j^{*2} \tag{5.2a}$$

$$s.t. \quad p_j^* + u_j^* - \sum_{k:(j,k)\in\mathcal{E}_\mathcal{P}} f_{jk}^* = 0 \quad j \in \mathcal{N}_\mathcal{P} \tag{5.2b}$$

It was shown in [36] and [35] that the optimal solution to equation (5.2) has the form of $C_i u_i^* = C_j u_j^*$, where $\sum_{j\in\mathcal{N}} u_j^* = -\sum_{j\in\mathcal{N}} p_j^*$ [1].

5.3 Distributed Control

Let the power grid be supported by a connected communication network $\mathcal{G}_\mathcal{C} = \{\mathcal{N}_\mathcal{C}, \mathcal{E}_\mathcal{C}\}$, where $\mathcal{N}_\mathcal{C}$ denotes the set of communication nodes, and $\mathcal{E}_\mathcal{C}$ denotes the set of communication links. The optimal distributed frequency control can be described by the following differential equation.

$$C_i\dot{u}_i(t) = -\omega_i(t) - C_i \sum_{j:(i,j)\in\mathcal{E}_\mathcal{C}} (C_i u_i(t) - C_j u_j(t)) \quad i \in \mathcal{N}_\mathcal{P} \tag{5.3}$$

[1] Note that satisfying condition $C_i u_i^* = C_j u_j^*$ can also be interpreted as fairness in sharing the loads.

Accordingly, the distributed control works as follows: node i measures the local frequency ω_i, receives the information $C_j u_j(t)$ from the neighbor nodes via the communication network, and updates the local control value $u_i(t)$. It is shown in [36] and [35] that if the communication network is connected, the control mechanism in equation (5.3) converges to the optimal solution, which is globally asymptotically stable.

5.3.1 Impact of Communication Link Failures

The control mechanism in equation (5.3) will achieve the optimal solution if the communication network is connected. However, if the communication network is disconnected, while power will be balanced, optimal cost may not be achieved; i.e. it cannot guarantee that $C_i u_i^* = C_j u_j^*$ for all i, j nodes. Next, we show via an example that the impact on the cost could be significant.

Consider the power grid in Figure 5-1 (The data of the grid and the costs can be found in Appendix 5.8.1). In this example, the communication network has the same topology as the power grid. The total load in this grid is 25 p.u., and we increase the load in node 3 by 5 p.u. (20% total increase). Simulation results show that the optimal cost, by applying control mechanism 5.3 under a fully connected communication network, is 23.27. If the communication link between nodes 2 and 7 fails, the cost increases to 35.69, while the cost under no communication is 39.11. This example shows that the failue of only one communication link could have a significant impact on the cost of distributed control.

5.3.2 Impact of Discrete-time Communication

In the design and analysis of the distributed control mechanism described in equation (5.3), it is assumed that the communication messages are updated in continuous time. However, in reality, the communication messages will be updated in discrete time. Let T be the time interval between two communication messages. Then, the distributed control can be described as follows.

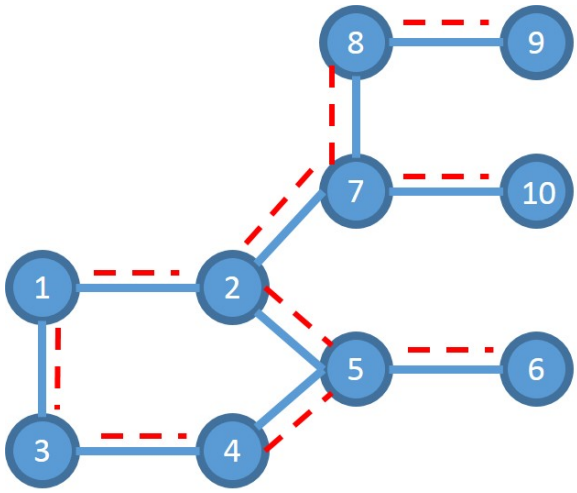

Figure 5-1: Power Grid Toy Example - Solid lines are power lines and dashed lines are communication lines.

$$C_i\dot{u}_i(t) = -\omega_i(t) - C_i \sum_{j:(i,j)\in\mathcal{E}_\mathcal{C}} (C_i u_i(t) - C_j u_j(KT))$$
$$i \in \mathcal{N}_\mathcal{P}, \quad KT \leq t \leq (K+1)T \tag{5.4}$$

Define the convergence time t^* to be the first time such that $|(Cost(t^*) - Cost^*)| < 0.01$, where $Cost(t^*)$ is the cost at time t^* and $Cost^*$ is the optimal cost. By running the control in equation (5.4) on the power grid in Figure 5-1 for different values of T, it can be seen that the time of convergence increases as T increases (See Figure 5-2).

5.4 Decentralized Control for Two-node System

In this section, we consider a two-node system connected by a power line and communication link as in Figure 5-3(a). As described, when the communication link fails, node i does not receive information $C_j u_j(t)$ and node j does not receive information $C_i u_i(t)$. Therefore, the optimal cost cannot be achieved. Next, we propose a control algorithm that uses the dynamics of the power grid instead of direct information $C_i u_i(t)$ and $C_j u_j(t)$, and still achieves the optimal solution.

Previously, the adjustable power at both nodes i and j was updated based on

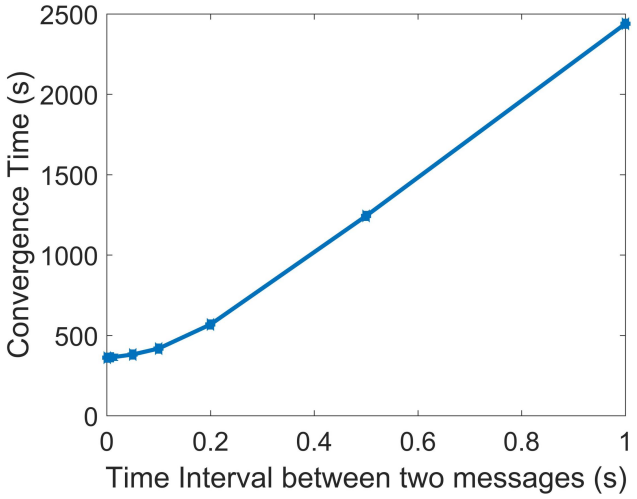

Figure 5-2: Convergence Time increases as T increases.

the local frequency and the information received from the neighboring node. In our control scheme, we update the adjustable power at every node based on the local frequency and a local artificial variable, where this variable is updated based on the power flow dynamics between the two nodes. Since the changes in the flow is a function of the frequency at both nodes, it contains some indirect information about the adjustable control as well as the cost of the neighbor node. We prove that this information is enough to guarantee the optimality of the our control scheme.

Let q_i and q_j be the two artificial variables at nodes i and j, respectively. Our decentralized control for the two-node system can be described as follows.

$$C_i \dot{u}_i(t) = -\omega_i(t) - q_i(t) \tag{5.5a}$$

$$C_j \dot{u}_j(t) = -\omega_j - q_j(t) \tag{5.5b}$$

$$\dot{q}_i(t) = -\frac{\dot{f}_{ij}}{B_{ij}} - 2q_i(t) \tag{5.5c}$$

$$\dot{q}_j(t) = \frac{\dot{f}_{ij}}{B_{ij}} - 2q_j(t) \tag{5.5d}$$

As described, control at node i is updated only based on the local frequency ω_i

and the value of artificial variable q_i. Moreover, value of q_i is updated based on the derivative of flow f_{ij} which can be observed locally. Similarly, control at node j depends on the local frequency ω_j and the derivative of flow f_{ji} which can be observed locally. Thus, there is no need to a communication network between nodes i and j. Next, we claim that the new control achieves the optimal solution (See Figure 5-3).

(a) Two-Node System with Communication (b) Two-Node System without Communication

Figure 5-3: Let t_0 be the time failure: node i knows $c_j u_j(t_0)$ and node j knows $c_i u_i(t_0)$; Nodes i and j can initialize $q_i(t_0)$ and $q_j(t_0)$ properly to guarantee optimality

Using the new control as in equations (5.5), the dynamics of the system can be written as follows.

$$M_i\dot{\omega}_i(t) = -D_i\omega_i(t) + p_i(t) + u_i(t) - f_{ij}(t) \tag{5.6a}$$

$$M_j\dot{\omega}_j(t) = -D_j\omega_j(t) + p_j(t) + u_j(t) + f_{ij}(t) \tag{5.6b}$$

$$\dot{f}_{ij}(t) = B_{ij}(\omega_i(t) - \omega_j(t)) \tag{5.6c}$$

$$C_i\dot{u}_i(t) = -\omega_i(t) - q_i(t) \tag{5.6d}$$

$$C_j\dot{u}_j(t) = -\omega_j(t) - q_j(t) \tag{5.6e}$$

$$\dot{q}_i(t) = -(\omega_i(t) - \omega_j(t)) - 2q_i(t) \tag{5.6f}$$

$$\dot{q}_j(t) = -(\omega_j(t) - \omega_i(t)) - 2q_j(t) \tag{5.6g}$$

In the following, we will prove the optimality and stability of the dynamical system described in equation (5.6).

5.4.1 Optimality

Theorem 8. Let $q_i(t_0) = -q_j(t_0) = C_i u_i(t_0) - C_j u_j(t_0)$. Then, the equilibrium point of the system described in equation (5.6) achieves the optimal cost.

Proof. In order to prove the optimality, we need to show that equation (5.6) guarantees $\omega_i^* = \omega_j^* = 0$ and $C_i u_i^* = C_j u_j^*$ at the equilibrium point; i.e. power is balanced, and cost is minimized.

At the equilibrium, all of the derivatives in equation (5.6) are equal to zero. Therefore, we will have the following equations.

$$\omega_i^* - \omega_j^* = 0 \tag{5.7a}$$

$$\omega_i^* - q_i^* = 0 \tag{5.7b}$$

$$\omega_j^* - q_j^* = 0 \tag{5.7c}$$

$$-(\omega_i^* - \omega_j^*) - 2q_i^* = 0 \tag{5.7d}$$

$$-(\omega_j^* - \omega_i^*) - 2q_j^* = 0 \tag{5.7e}$$

Solving equations (5.7) results in $\omega_i^* = \omega_j^* = 0$, which guarantees that power is balances at the equilibrium point. In addition, we will have $q_i^* = q_j^* = 0$.

Equations (5.6f) and (5.6g) show that $\dot{q}_i(t) = -\dot{q}_j(t)$ for all time $t \geq t_0$. Since we have initialized $q_i(t_0) = -q_j(t_0)$, it is easy to see that $q_i(t) = -q_j(t)$ for $t \geq t_0$.

Next, we subtract equation (5.6e) from equation (5.6d). Thus, we will have $C_i \dot{u}_i - C_j \dot{u}_j = -(\omega_i - \omega_j) - 2q_i$ which is equal to the equation (5.6f). Therefore, $\dot{q}_i = C_i \dot{u}_i - C_j \dot{u}_j$.

By taking integral over both sides from $t = t_0$ to infinity, we will have $(C_i u_i^* - C_i u_i(t_0)) - (C_j u_j^* - C_j u_j(t_0)) = q_i^* - q_i(t_0)$, and assumption $q_i(t_0) = C_i u_i(t_0) - C_j u_j(t_0)$ results in $c_i u_i^* - C_j u_j^* = q_i^*$. Since $q_i^* = 0$, $C_i u_i^* = C_j u_j^*$ which guarantees the optimality of the equilibrium point.

□

5.4.2 Stability

Next, we prove that the equilibrium point of the dynamical system described in equation (5.6) is globally asymptotically stable. Since our dynamical system is linear, it is enough to show that the roots of the characteristic polynomial of the system are all located in the negative side of the plane.

Let $D, M, C \in R^{2\times 2}$ be diagonal matrices denoting the droop coefficient, inertia and cost at nodes i and j, respectively. Let B be the susceptance of the power line between nodes i and j. Moreover, let $A_p \in R^{2\times 1}$ be the node-edge incidence matrix, $L_p^B = A_p B A_p^T$ be the weighted laplacian matrix of the power grid, and $L_c \in R^{2\times 2}$ be the laplacian matrix of the communication network. Finally, let $s(\lambda)$ be the characteristic polynomial of the system.

Let the state vector of the two-node system be $[\omega_i, \omega_j, f_{ij}, u_i, u_j, q_i, q_j]$. We can rewrite the state matrix of our dynamical system as follows.

$$A = \begin{bmatrix} -M^{-1}D & -M^{-1}A_p & M^{-1}I^{2\times 2} & 0^{2\times 2} \\ BA_p^T & 0^{1\times 1} & 0^{1\times 2} & 0^{1\times 2} \\ -C^{-1} & 0^{2\times 1} & 0^{2\times 2} & -C^{-1} \\ -L_c & 0^{2\times 1} & 0^{2\times 2} & -2I^{2\times 2} \end{bmatrix}$$

Let $s(\lambda) = det(A - \lambda I)$ be the characteristic polynomial of matrix A.

$$s(\lambda) = det \begin{bmatrix} -M^{-1}D - \lambda I^{2\times 2} & -M^{-1}A_p & M^{-1}I^{2\times 2} & 0^{2\times 2} \\ BA_p^T & -\lambda & 0^{1\times 2} & 0^{1\times 2} \\ -C^{-1} & 0^{2\times 1} & -\lambda I^{2\times 2} & -C^{-1} \\ -L_c & 0^{2\times 1} & 0^{2\times 2} & -(2+\lambda)I^{2\times 2} \end{bmatrix}$$

By schur complement formula,

$$s(\lambda) = (2+\lambda)^2 det \begin{bmatrix} -M^{-1}D - \lambda I^{2\times 2} & -M^{-1}A_p & M^{-1} \\ BA_p^T & -\lambda & 0^{1\times 2} \\ C^{-1}[\frac{L_c}{2+\lambda} - I^{2\times 2}] & 0^{2\times 1} & -\lambda I^{2\times 2} \end{bmatrix}$$

Next, we take $(2+\lambda)^2$ into the matrix by multiplying the last row with $(2+\lambda)I^{2\times 2}$.

Thus, $s(\lambda) = det \begin{bmatrix} -M^{-1}D - \lambda I^{2\times 2} & -M^{-1}A_p & M^{-1} \\ BA_p^T & -\lambda & 0^{1\times 2} \\ C^{-1}[L_c - (\lambda+2)I] & 0^{2\times 1} & -\lambda(\lambda+2)I^{2\times 2} \end{bmatrix}$

Next, we take out $[L_c - (\lambda+2)I]$ from the big matrix as follows.

$$s(\lambda) = det(-[L_c-(\lambda+2)I])det \begin{bmatrix} -M^{-1}D - \lambda I^{2\times 2} & -M^{-1}A_p & M^{-1} \\ BA_p^T & -\lambda & 0^{1\times 2} \\ -C^{-1} & 0^{2\times 1} & \lambda(\lambda+2)[L_c - (\lambda+2)I]^{-1} \end{bmatrix}$$

By simplifying the matrices, we will get the following.

$$s(\lambda) = \lambda(\lambda+2)det \begin{bmatrix} -M^{-1}D - \lambda I & -M^{-1}A_p & M^{-1} \\ BA_p^T & -\lambda & 0^{1\times 2} \\ -C^{-1} & 0^{2\times 1} & -L_c - \lambda I \end{bmatrix}$$

By schur complement formula,

$$s(\lambda) = \lambda(\lambda+2)det(L_c+\lambda)det \begin{bmatrix} -M^{-1}D - \lambda I - M^{-1}(L_c+\lambda I)^{-1}C^{-1} & -M^{-1}A_p \\ BA_p^T & -\lambda \end{bmatrix}$$

We apply the schur complement formula, one more time.

$$s(\lambda) = \lambda^2(\lambda+2)det(L_c+\lambda)det \left[-M^{-1}D - \lambda I - M^{-1}(L_c+\lambda I)^{-1}C^{-1} - \tfrac{1}{\lambda}M^{-1}A_pBA_p^T\right]$$

$$s(\lambda) = (\lambda+2)det(M^{-1})det(L_c+\lambda)det \left[\lambda D + \lambda^2 M + \lambda(L_c+\lambda I)^{-1}C^{-1} + L_p^B\right]$$

$$s(\lambda) = (\lambda+2)det(M^{-1})det \left[\lambda(L_c+\lambda)D + \lambda^2(L_c+\lambda)M + \lambda C^{-1} + (L_c+\lambda)L_p^B\right]$$

$s(\lambda) = (\lambda+2)det(M^{-1})det(H(\lambda))$, where

$$H(\lambda) = \left[(\lambda^2 D + \lambda^3 M + \lambda C^{-1}) + (\lambda L_c D + \lambda^2 L_c M + (2+\lambda)L_p^B)\right]$$

Since the system is linear, it is enough to show that the real parts of all roots of characteristic polynomial $s(\lambda)$ are negative.

Theorem 9. The conditions in equation (5.8) are sufficient to guarantee that the equilibrium point of the system described in equation 5.6 is globally asymptotically stable.

$$M \succ 0 \tag{5.8a}$$

$$\frac{1}{2}(L_c M + M L_c) + D \succ 0 \tag{5.8b}$$

$$\frac{1}{2}(L_c D + D L_c) + L_P^B + C^{-1} \succ 0 \tag{5.8c}$$

$$\lambda_{min}[(L_p^B + \frac{1}{2}(L_c D + D L_c) + C^{-1})] \times$$
$$\lambda_{min}[(\frac{1}{2}(L_c M + M L_c) + D)] > 4B \max\{M_1, M_2\} \tag{5.8d}$$

Proof. Roots of $s(\lambda)$ are 0, -2 and roots $det(H(\lambda))$. Thus, it is enough to show that under the conditions in equations 5.8, $det(H(\lambda))$ does not have a root on the right-hand side of the plane.

The necessary condition for $det(H(\lambda)) = 0$ is that there exists eigenvector $y \neq 0$ such that $H(\lambda)y = 0$. Therefore, $y^* H(\lambda) y = 0$.

We show that under the conditions in equations 5.8, for any $x \neq 0$, roots of $x^* H(\lambda) x = 0$ will be in the left-hand side of the plane; thus, it is a sufficient condition for the stability of our system.

Without loss of generality, we assume $x^* x = 1$, and rewrite $x^* H(\lambda) x$ as follows.

$x^* H(\lambda) x = a_0 + a_1\lambda + a_2\lambda^2 + a_3\lambda^3 = 0$, where $a_0 = x^*(2L_p^B)x$, $a_1 = x^*(L_p^B + L_c D + C^{-1})x$, $a_2 = x^*(L_c M + D)x$ and $a_3 = x^*(M)x$.

Under the conditions in equations 5.8, coefficients a_1, a_2, a_3 are all positive.

- $a_1 = x^*(L_p^B + L_c D + C^{-1})x = x^*(L_p^B + \frac{1}{2}(L_c D + D L_c) + C^{-1})x$; L_p^B is positive semidefinite, and C^{-1} is positive definite. $\frac{1}{2}(L_c D + D L_c)$ is also positive definite by conditions in 5.8.

- $a_2 = x^*(L_c M + D)x = x^*(\frac{1}{2}(L_c M + M L_c) + D)x$; D is a positive definite matrix; $\frac{1}{2}(L_c M + M L_c)$ is also positive definite by conditions in 5.8.

- $a_3 = x^*(M)x > 0$, since M is a positive definite matrix.

However, since L_p^B, the laplacian matrix of the power grid, is a positive semidefinite matrix, the coefficient a_0 will be nonnegative; i.e. $a_0 = x^*(2L_p^B)x \geq 0$. We consider both cases where $a_0 = 0$ and $a_0 > 0$, and show that in each case, the roots of $det(H(\lambda))$ will be in the left-hand side of the plane.

Case I: Let $a_0 = 0$; Thus, $x^*H(\lambda)x = a_1\lambda + a_2\lambda^2 + a_3\lambda^3 = \lambda(a_1 + a_2\lambda + a_3\lambda^2) = 0$. One root of the above equation is $\lambda = 0$, and since $a_1, a_2, a_3 > 0$, the other two roots will be in the left-hand side of the plane by the Routh-Hurwitz stability criteria.

Case II: Let $a_0 > 0$. By Routh-Hurwitz stability criteria, roots of $x^*H(\lambda)x$ will have negative real values, if $a_i > 0$ for $i = 0, 1, 2, 3$, and $a_0a_3 < a_1a_2$.

$a_1a_2 = [x^*(L_p^B + L_cD + C^{-1})x][x^*(L_cM + D)x] > [x^*(2L_p^B)x][x^*(M)x] = a_0a_3$ if and only if

$[\lambda_{min}(L_p^B + L_cD + C^{-1})][\lambda_{min}(L_cM + D)] > \lambda_{max}(2L_p^B)\lambda_{max}(M)$

□

Next, we argue that sufficient conditions in equations (5.8a)-(5.8d) often hold in practice. Condition (5.8a) holds as inertia is a positive value. Condition (5.8b) holds as the inertia of nodes in a distribution network is very small; and the matrix becomes strictly diagonally dominant. Conditions (5.8c) and (5.8d) hold if the cost values are scaled down; i.e. increase C^{-1}. Note that the only requirement for optimality of the control is that the ratio of power distribution be proportional to the inverse ratio of costs. Thus, scaling all the cost values will not affect the solution.

5.5 Control under Communication Link Failures

In this section, we extend the idea in Section 5.4 to multi-node systems. In particular, we introduce a new control mechanism that uses the dynamics of the power flow between adjacent nodes to replicate the direct information transmitted between them via a communication link. We show that our new control mechanism achieves the optimal solution under single communication link failure, and improves the cost under multiple communication link failures.

5.5.1 Single Communication Link Failure

Consider the power grid and communication network in Figure 5-4. Suppose the communication link between nodes i and j fails. We claim that if nodes i and j update their local control decision only based on the power flow between nodes i and j, and the rest of the nodes keep their previous control rule, the dynamical system will converge to the optimal solution. The new control mechanism can be described as follows.

$$C_k \dot{u}_k(t) = -\omega_k(t) - C_k \sum_{l:(k,l)\in\mathcal{E}_C} (C_k u_k(t) - C_l u_l(t))$$

$$k \in \mathcal{N}\backslash\{i,j\} \tag{5.9a}$$

$$C_i \dot{u}_i(t) = -\omega_i(t) - q_i(t) \tag{5.9b}$$

$$C_j \dot{u}_j(t) = -\omega_j(t) - q_j(t) \tag{5.9c}$$

$$\dot{q}_i(t) = -(\omega_i(t) - \omega_j(t)) - 2q_i(t) \tag{5.9d}$$

$$\dot{q}_j(t) = -(\omega_j(t) - \omega_i(t)) - 2q_j(t) \tag{5.9e}$$

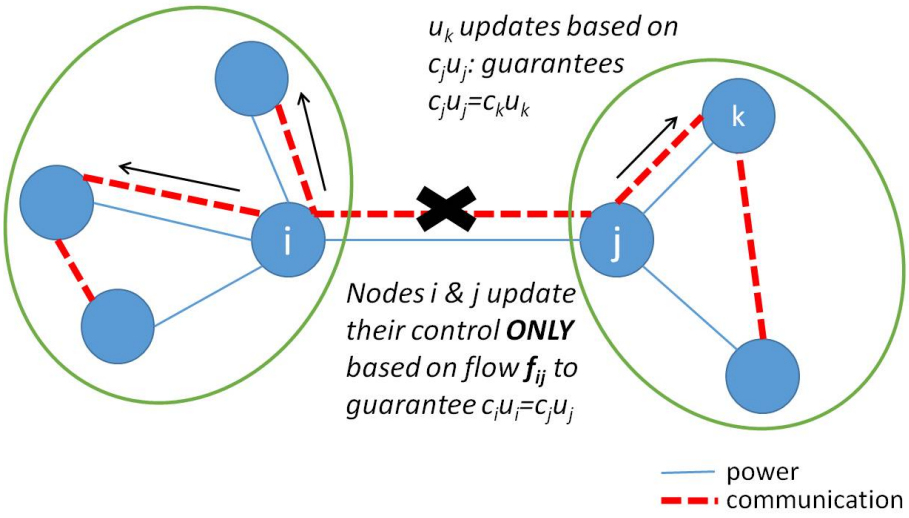

Figure 5-4: Power Grid and Communication Network - Solid lines are power lines and dashed lines are communication lines.

According to equation (5.9), all the nodes that are connected to node i via the communication network, receive the information $c_i u_i(t)$ from node i; however, node i does not update its control based on the information received from other nodes via communication network. Similarly, all the nodes connected to node j via the communication network, update their control based on the information $C_j u_j$ they receive from node j; however, node j does not use the information it receives from other nodes via the communication network. Instead, nodes i and j update their control only based on their local frequency and the power flow between nodes i and j. This control rule can be interpreted as a master/slave algorithm, where nodes i and j are the master nodes that guarantee $C_i u_i^* = C_j u_j^*$, and the rest of nodes are the slave nodes that follow the changes in nodes i and j.

Theorem 10. Suppose the communication link between nodes i and j fails at time t_0, but they are connected via a power line. By updating the control mechanism according to equation (5.9), and initializing $q_i(t_0) = -q_j(t_0) = C_i u_i(t_0) - C_j u_j(t_0)$, the optimal solution will be achieved.

Proof. Equation (5.9a) guarantees that $C_k u_k^* = C_l u_l^*$ for all $k \in \mathcal{N} \backslash \{i, j\}$. In particular, for any node k connected to node i, $C_k u_k^* = C_i u_i^*$, and for any node k connected to node j, $C_k u_k^* = C_j u_j^*$. On the hand, equations (5.9b)-(5.9e) guarantee that $C_i u_i^* = C_j u_j^*$ (See Theorem 8 for optimality of a two-node system). Therefore, the equilibrium point is optimal. □

Corollary 5. Suppose the power grid has a connected topology, and the original communication network contains a subtree of the power grid. Then, the control mechanism described in equation (5.9) achieves the optimal solution, under any single communication link failure.

Proof. Let an arbitrary communication link (i, j) fail. If there does not exist a power line between nodes i and j, the communication topology is guaranteed to remain connected as it still contains a subtree of the power grid. Thus, the control mechanism will not be updated, and the optimal solution will be achieved. If there exists a power

line between nodes i and j, the control mechanism will be updated as in equation (5.9), which guarantees to achieve the optimal solution. □

Similar to the two-node system, one can find sufficient conditions under which the updated control mechanism in equation (5.9) is globally asymptotically stable for a multi-node system. For more details See Appendix 5.8.2.

Consider Figure 5-1, and suppose that the communication link between nodes 2 and 7 fail. Under the original control mechanism, the cost increases from 23.27 to 35.69. However, the new control mechanism will achieve the optimal solution.

We compare the frequency response of the original control under full communication and the new control under single communication link failure. For simplicity, we only show the angular velocities at nodes 2 and 7 in Figures 5-5(a) and 5-5(b); however, the same results hold for all the other nodes. We observed that for all nodes, the frequency response of the two control mechanisms are very similar, indicating that the new control mechanism will not create any abrupt changes in the frequency of the system.

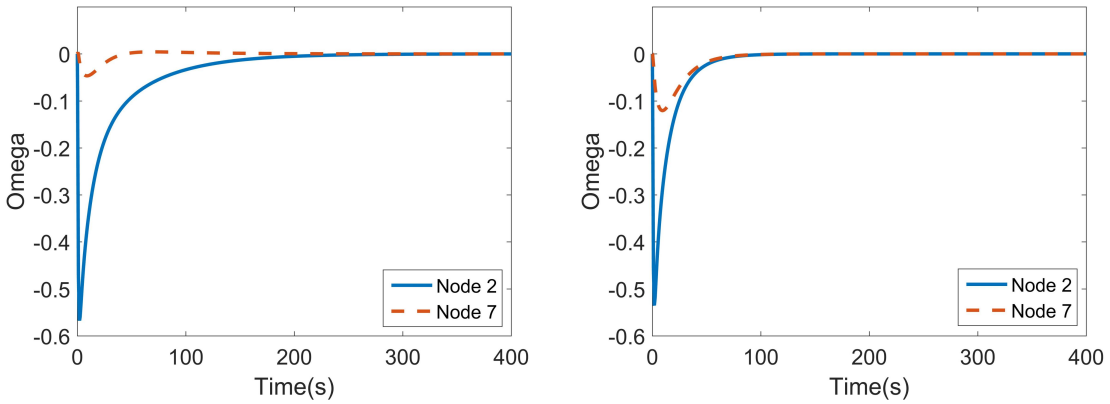

(a) Frequency Response of Original Control under Full Communication

(b) Frequency Response of New Control under Single Link Communication Failure

Figure 5-5: Comparing the frequency responses

5.5.2 Multiple Communication Link Failures

In this section, we consider the case that multiple communication links fail (See Figure 5-6 as an example.) We generalize the control mechanism described for the

single communication link failures as follows.

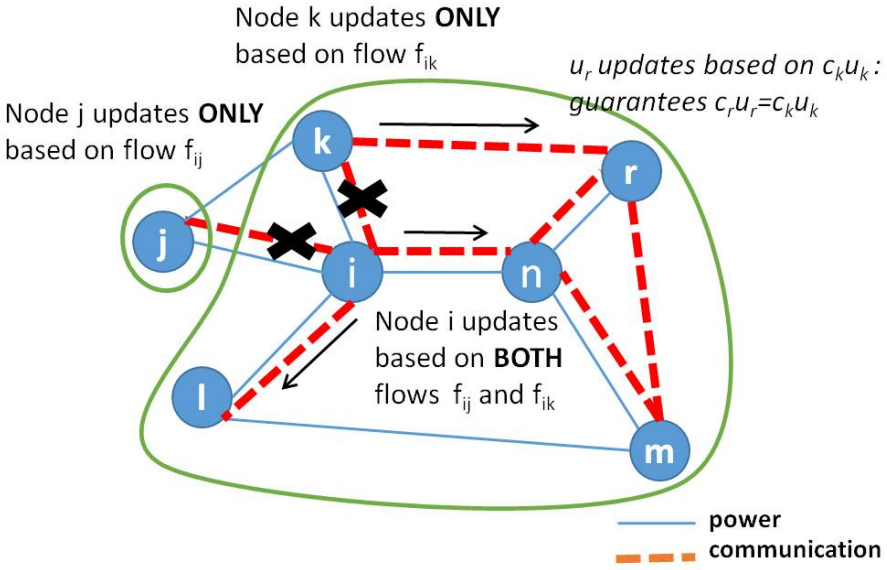

Figure 5-6: Power Grid and Communication Network - Solid lines are power lines and dashed lines are communication lines.

Consider pairs of nodes that have lost their communication links, but they are connected via power lines. Let F be the set of such nodes. Moreover, let q_i be the artificial variable for every node $i \in F$, and initialize it as $q_i(t_0) = \sum_{j \in F:(i,j) \in E_P} (C_i u_i(t_0) - C_j u_j(t_0))$.

The update control rule can be written as follows.

$$C_r \dot{u}_r(t) = -\omega_r(t) - C_r \sum_{l:(r,l) \in \mathcal{E}_C} (C_r u_r(t) - C_l u_l(t)) \quad r \in \mathcal{N} \backslash F \tag{5.10a}$$

$$C_i \dot{u}_i(t) = -\omega_i(t) - q_i(t) \quad i \in F \tag{5.10b}$$

$$\dot{q}_i(t) = - \sum_{j \in F:(i,j) \in E_P} (\omega_i(t) - \omega_j(t)) - 2q_i(t) \tag{5.10c}$$

It can be seen from equation (5.10) that every pair of node i and j that have lost their communication link, but are connected via a power line will switch to the new control rule, where the control rule at the rest of nodes remains the same. This control rule does not guarantee to achieve the optimal solution; however, we show

that in practice it improves the cost.

Consider the power grid in Figure 5-1, and assume that the communication links between nodes 1 and 2 and nodes 2 and 5 have failed. Under the original control, the cost increases from 23.27 to 36.87 which is 58% increase in the optimal cost. However, our control described in equation (5.10) achieves a cost of 25.45, which is only 9% increase in the optimal cost (49% improvement). In addition, we observed that the new control policy will not lead to any unacceptable changes in the frequency response.

5.6 Control with Discrete-Time Communication

In this Section, we study the impact of discrete-time communication on the performance of distributed frequency control. As discussed in Section 5.3.2, when the time interval between communication messages increases, the convergence time increases. In this Section, we propose an algorithm that sequentially updates the control of pairs of nodes using the dynamics of the power flow between them. Using simulation results, we show that the new algorithm converges much faster than the original one.

Let T be the time interval between communication messages. Let $\mathcal{E}_{\mathcal{S}} = \{e_1, \cdots, e_m\} = \mathcal{E}_{\mathcal{P}} \cap \mathcal{E}_{\mathcal{C}}$ be the set of pairs of nodes that share the power lines and communication links. The algorithm is as follows.

Let communication messages update at time instants KT, where $K \geq 0$. At each time interval $KT \leq t < (K+1)T$, the algorithm selects a link $e_r \in E_S$, and updates the control according to equations (5.9), where i and j are the end-nodes of the selected link e_r. The only difference is in equation (5.9a), where the control should be updated based on the most recent communication message received at time KT; i.e. $C_k \dot{u}_k(t) = -\omega_k(t) - C_k \sum_{l:(k,l)\in\mathcal{E}_{\mathcal{C}}} (C_k u_k(t) - C_l u_l(KT)) \quad \forall k \neq i, j$. At the beginning of next time interval, new communication messages will be received, and the algorithm selects the next link in E_S. The algorithm keeps iterating on the links in sequence until convergence is achieved.

Figure 5-7 shows the sequence of link selection and control updates at nodes.

This algorithm improves the convergence rate because during each interval, it uses the additional information from the dynamics of the power grid to update the control at each node.

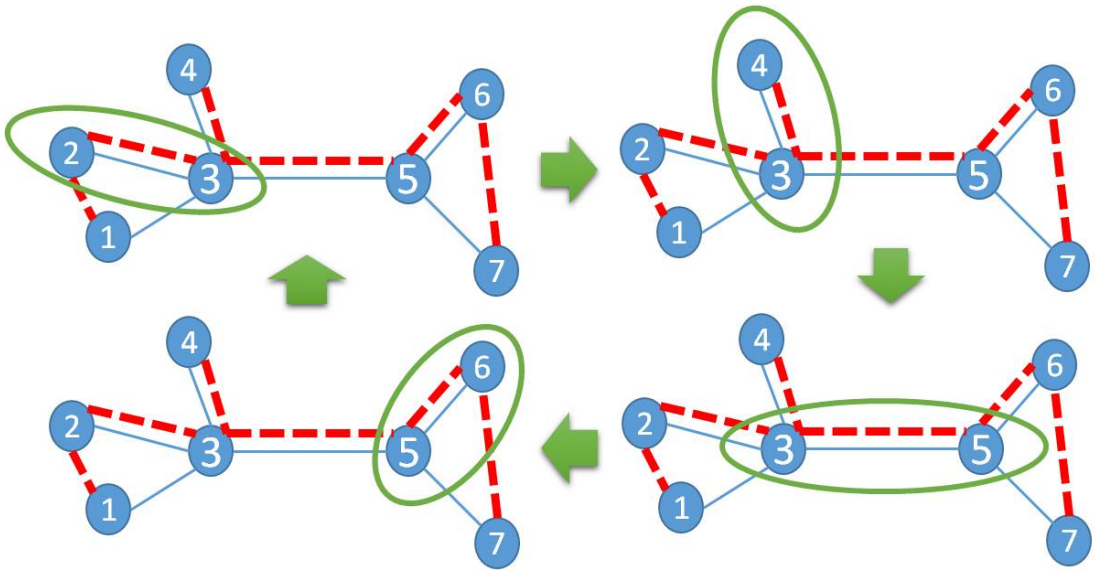

Figure 5-7: Power Grid and Communication Network - Solid lines are power lines and dashed lines are communication lines. The shared edges between the power grid and communication network are $(2,3),(3,4),(3,5),(5,6)$, and the algorithm sequentially selects one of these edges, and uses its power flow to control the power changes at nodes.

We applied the original control scheme as well as the new control scheme to the power grid in Figure 5-1. For simplicity, we only show the results for two nodes 1 and 5; however, the results are the same for the rest of nodes. Figures 5-8(a) and 5-8(b) show that increasing the value of T increases the convergence time under the original control. Figures 5-8(c) and 5-8(d) indicate that by applying the new control mechanism, the convergence time for $T = 1s$ is similar to the convergence time of the original control for $T = 1ms$. In addition, it can be seen that although the general behavior of the power under both control mechanisms are similar, there are some fluctuations in the value of power under the new control algorithm. However, by comparing the frequency response of the control mechanisms in Figures 5-8(e) and 5-8(f), it can be seen that the fluctuations in the frequency response of nodes under the new algorithm are negligible.

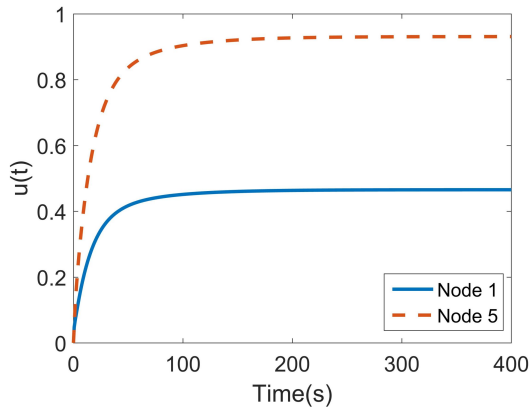

(a) T=1ms; Original Control

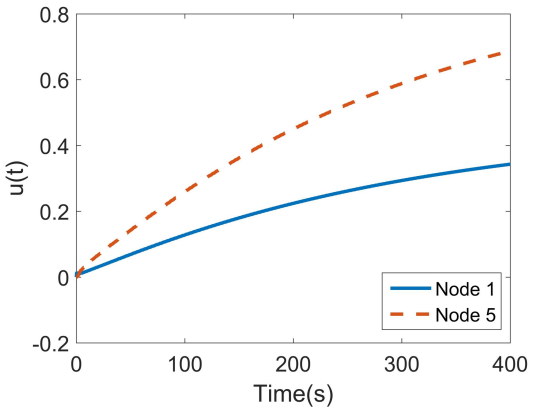

(b) T=1s; Original Control

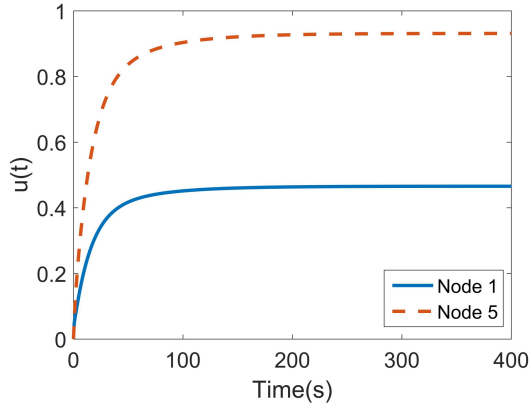

(c) T=1ms; Original Control

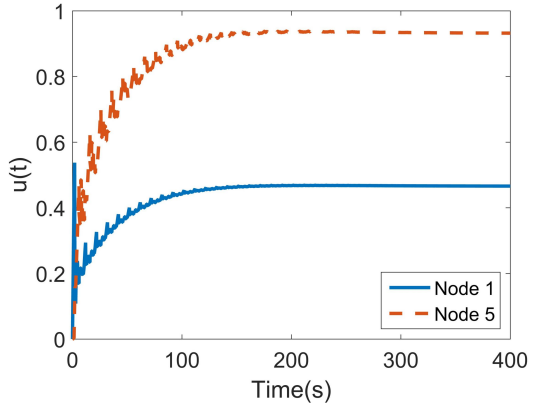

(d) T=1s; New Control Algorithm

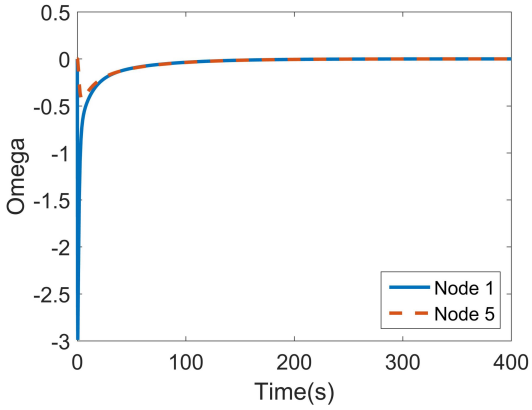

(e) Frequency Response of Original Control for T=1ms

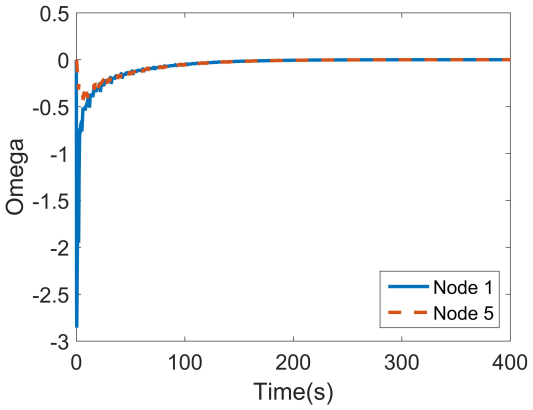

(f) Frequency Response of New Control for T=1s

Figure 5-8: Comparing the power and frequency response for large T under new control with small T under the original control

5.7 Conclusion

In this chapter, we analyzed the impact of communication failures as well as discrete-time communication messages on the performance of optimal distributed frequency control. We considered the consensus-based algorithm proposed in [36] and [35], and showed that although the control mechanism can balance the power, it will not achieve the optimal solution under communication failures.

Next, we proposed a novel control mechanism that uses the dynamics of the power flow between two nodes instead of the information received directly from the communication link between them. We proved that our algorithm achieves the optimal solution under any single communication link failure. We also used simulation results to show that the new control improves the cost under multiple communication link failures.

Finally, we showed that the convergence time of the distributed control increases as the time between two communication messages increases. We proposed a sequential control scheme which uses the dynamics of the power grid, and using simulation results, we showed that it improves the convergence time significantly.

5.8 Chapter Appendix

5.8.1 Data of the power grid in Figure 5-1

Inertia, initial power, droop control and cost of adjustable control at nodes 1 to 10 are as follows.

$M = [0.01, 0.02, 0.01, 0.1, 0.05, 0.8, 0.05, 1, 0.1, 0.01]$

$P_0 = [1, 5, -2, 6, -5, -10, -4, 8, 5, -4]$

$D = \frac{|P_0|}{3}$

$\sim [0.33, 1.67, 0.67, 2, 1.67, 3.33, 1.33, 2.67, 1.67, 1.33]$

$Cost = [10, 10, 100, 100, 5, 10, 7, 9, 5, 10]$

Reactance of lines 1 to 10 are as follows.

$Reactance = [1, 2, 3, 1, 5, 4, 6, 1, 9, 1]$

5.8.2 Stability of Multi-Node System

Simplifying $s(\lambda)$ for Multi-Node System

Let $D, M, C \in R^{N_P \times N_P}$ be the diagonal matrices of droop, inertia and cost values of the all nodes in the power grid. Moreover, let $I \in R^{N_P \times N_P}$ be the identity matrix.

Suppose that we label the nodes such that nodes N_P and $N_P - 1$ be the nodes that have lost their communication link. Let A_p be the adjacency matrix of the power grid. Moreover, let L_c be the laplacian matrix of the communication network. Finally, define $L_c^* = \begin{bmatrix} L_{c_1} \\ 0^{2\times N-2} | L_{c_2} C_2^{-1} \end{bmatrix}$, where

$L_{c_1} = L_c[1 : N_P - 2, 1 : N_P - 2]$ and $L_{c_2} = \begin{bmatrix} 1 & -1 \\ -1 & 1 \end{bmatrix}$ be the laplacian matrix of a two-node system.

Then, the characteristic polynomial of our multi-node system is as follows.

$$s(\lambda) = \lambda(\lambda + 2)$$
$$det \begin{bmatrix} -M^{-1}D - \lambda I^{N\times N} & -M^{-1}A_p & M^{-1}I^{N\times N} \\ BA_p^T & -\lambda I^{E\times E} & 0^{E\times N} \\ -C^{-1} & 0^{N\times E} & -L_c^*C - \lambda I^{N\times N} \end{bmatrix}$$

Using the same techniques as in Section 5.4, the characteristic polynomial can be simplified as follows.

$$s(\lambda) = \lambda^{1+E}(\lambda + 2) det(L_c^*C + \lambda)$$
$$det \left[-M^{-1}D - \lambda I - M^{-1}(L_c^*C + \lambda I)^{-1}C^{-1} - \tfrac{1}{\lambda} M^{-1}A_p B A_p^T \right]$$

Let L_p^B be the weighted laplacian matrix of the power grid, where $L_p^B = A_p B A_p^T$.

Therefore,

$s(\lambda) = (-1)^N \lambda^{1+E-N}(\lambda + 2) det(M^{-1}) det(H(\lambda))$,

where $H(\lambda) = (\lambda^2 D + \lambda^3 M + \lambda C^{-1})$

$+ (\lambda L_c^* C D + \lambda^2 L_c^* C M + (L_c^* C + \lambda) L_p^B)$

Proof of Stability

In this section, we claim that the following conditions are sufficient for the stability of the multi-node system.

$$M \succ 0 \tag{5.11a}$$

$$\frac{1}{2}(L_c^* CM + MCL_c^{*T}) + D \succ 0 \tag{5.11b}$$

$$L_p^B + \frac{1}{2}(L_c^* CD + DCL_c^{*T}) + C^{-1} \succ 0 \tag{5.11c}$$

$$[\lambda_{min}(L_p^B + L_c^* CD + C^{-1})][\lambda_{min}(L_c^* CM + D)]$$
$$> \lambda_{max}(L_c^* CL_p^B)\lambda_{max}(M) \tag{5.11d}$$

Similar to the two-node system, in order to prove the stability of the multi-node system, it is enough to show that the real-parts of all eigenvalues are negative. This is due to the fact that we have a linear system. Thus, we need to prove that the all the roots of $s(\lambda)$ are in the negative-side of the plane.

Since the power grid is a connected network, it contains a subtree; thus, $E \geq N-1$. Therefore, the roots of $s(\lambda)$ are 0, -2 and roots $det(H(\lambda))$. Thus, it is enough to show that $det(H(\lambda))$ does not have a root on the right-hand side of the plane.

Similar to the two-node system, the necessary condition for $det(H(\lambda)) = 0$ is that there exists eigenvector $y \neq 0$ such that $H(\lambda)y = 0$. Therefore, $y^* H(\lambda) y = 0$.

We show that under conditions 5.11, for any $x \neq 0$, roots of $x^* H(\lambda) x = 0$ will be in the left-hand side of the plane; thus, these conditions are sufficient for the stability of our system.

Without loss of generality, we assume $x^* x = 1$, and rewrite $x^* H(\lambda) x$ as follows.

$x^* H(\lambda) x = a_0 + a_1\lambda + a_2\lambda^2 + a_3\lambda^3 = 0$, where $a_0 = x^*(L_c^* CL_p^B)x$, $a_1 = x^*(L_p^B + L_c^* CD + C^{-1})x$, $a_2 = x^*(L_c^* CM + D)x$ and $a_3 = x^*(M)x$.

Similar to the two-node system, we first show that under conditions 5.11, coefficients a_1, a_2, a_3 are positive.

- $a_1 = x^*(L_p^B + L_c^* CD + C^{-1})x = x^*(L_p^B + \frac{1}{2}(L_c^* CD + DCL_c^{*T}) + C^{-1})x > 0$. This

is guarantees under condition 5.11c.

- $a_2 = x^*(L_c^* CM + D)x = x^*(\frac{1}{2}(L_c^* CM + MCL_c^{*T}) + D)x > 0$. This is guarantees under condition 5.11b.

- $a_3 = x^*(M)x > 0$, which is guaranteed under condition 5.11a.

However, since L_p^B, the laplacian matrix of the power grid, is a positive semidefinite matrix, the coefficient a_0 will be nonnegative; i.e. $a_0 = x^*(L_c^* CL_p^B)x \geq 0$. We consider both cases where $a_0 = 0$ and $a_0 > 0$, and find the sufficient conditions for each case under which the roots of $det(H(\lambda))$ are in the left-hand side of the plane.

Case I: Let $a_0 = 0$; Thus, $x^*H(\lambda)x = a_1\lambda + a_2\lambda^2 + a_3\lambda^3 = \lambda(a_1 + a_2\lambda + a_3\lambda^2) = 0$. One root of the above equation is $\lambda = 0$, and since $a_1, a_2, a_3 > 0$, the other two roots will be in the left-hand side of the plane by the Routh-Hurwitz stability criteria.

Case II: Let $a_0 > 0$. By Routh-Hurwitz stability criteria, roots of $x^*H(\lambda)x$ will have negative real values, if $a_i > 0$ for $i = 0, 1, 2, 3$, and $a_0a_3 < a_1a_2$.

$a_1a_2 = [x^*(L_p^B + L_c^* CD + C^{-1})x][x^*(L_c^* CM + D)x] > [x^*(L_c^* CL_p^B)x][x^*(M)x] = a_0a_3$ if and only if

$[\lambda_{min}(L_p^B + L_c^* CD + C^{-1})][\lambda_{min}(L_c^* CM + D)] > \lambda_{max}(L_c^* CL_p^B)\lambda_{max}(M)$

Chapter 6

Conclusion

In this thesis we modeled and analyzed the robustness of interdependent networks.

First, we proposed a new abstract model for analyzing interdependent networks with known topologies. We considered two types of unidirectional and bidirectional interdependency. We defined several metrics for finding the most critical nodes in such interdependent networks, evaluated their complexity and proposed heuristics for their evaluation. We introduced two closely related definitions for robust design of interdependent networks; proposed algorithms for explicit design, and demonstrated the relation between robust interdependent networks and expander graphs.

Next, we studied the interdependency between the power grid and the communication network used to control the grid. We considered the case where a communication node depends on the power grid in order to receive power for operation, and a power node depends on the communication network in order to receive control signals. We demonstrated that these dependencies can lead to cascading failures, and it is essential to consider the power flow equations for studying the behavior of such interdependent networks. We proposed a two-phase control policy to mitigate the cascade of failures. In the first phase, our control policy finds the unavoidable failures that occur due to physical disconnection. In the second phase, our algorithm redistributes the power so that all the connected communication nodes have enough power for operation and no power lines overload. In particular, we showed that using the intelligent mitigation policy, the interdependent power grid is more robust than the isolated one. We also

performed a sensitivity analysis to evaluate the performance of our control policy, and showed that our control policy achieves close to optimal yield for many scenarios.

Next, we studied the impact of communication loss on the power grid under emergency control in more details. We designed a centralized emergency control scheme under both full and partial communication support, to improve the performance of the power grid. We used our emergency control scheme to model the impact of communication loss on the grid. We showed that unlike previous models used in the literature, the loss of communication does not necessarily lead to the failure of the correspondent power nodes; i.e. the "point-wise" failure model is not appropriate. In addition, we showed that the impact of communication loss is a function of several parameters such as the size and structure of the power and communication failure, as well as the operating mode of power nodes disconnected from the communication network.

Finally, we analyzed the impact of communication failures on the performance of optimal distributed frequency control. We considered a consensus-based control scheme, and showed that it does not converge to the optimal solution when the communication network is disconnected. We proposed a new control scheme that uses the power dynamics to replicate the information not received from the communication network, and proved that it achieves the optimal solution under any single communication link failure. In addition, we showed that this control improves cost under multiple communication link failures. We also analyzed the impact of discrete-time communication on the performance of distributed frequency control. In particular, we showed that the convergence time increases as the time interval between two messages increases. We proposed a new algorithm that uses the dynamics of the power grid, and showed through simulation that it improves the convergence time of the control scheme significantly.

Bibliography

[1] US Canada Power System Outage Task Force. Final Report on the August 14, 2003 Blackout in the United States and Canada: Causes and Recommendations. [Online]. Available: http://energy.gov/sites/prod/files/oeprod/DocumentsandMedia/BlackoutFinal-Web.pdf

[2] (2004, Jan) NY-ISO Interim Report on the August 14, 2003 Blackout. [Online]. Available: http://www.hks.harvard.edu/hepg/Papers/NYISO.blackout.report.8.Jan.04.pdf

[3] NERC Resources Subcommittee. (2011, Jan) Balancing and Frequency Control. [Online]. Available: http://www.nerc.com/docs/oc/rs/NERCBalancingandFrequencyControl040520111.pdf

[4] Generator Protection. [Online]. Available: http://www.ee.siue.edu/~smuren/ECE545Notes/Ch11-GeneratorProtection.pdf

[5] U.S./Canada Power Outage Task Force. (2003, Sep.) August 14, 2003 Outage, Sequence of Events. [Online]. Available: http://www.nerc.com/docs/docs/blackout/BlackoutSummary-Draft-6b.pdf

[6] M. Parandehgheibi and E. Modiano, "Robustness of interdependent networks: The case of communication networks and the power grid," *IEEE Conference on Global Communications Conference (GLOBECOM)*, pp. 2164 – 2169, 2013.

[7] M. Parandehgheibi and E. Modiano, "Robustness of bidirectional interdependent networks: Analysis and design," *arXiv preprint arXiv:1605.01262*, 2016.

[8] A. R. Bergen and V. Vittal, *Power system analysis.* Prentice-Hall, 1999.

[9] M. Parandehgheibi, E. Modiano, and D. Hay, "Mitigating cascading failures in interdependent power grids and communication networks," *IEEE International Conference on Smart Grid Communications (SmartGridComm)*, pp. 242–247, 2014.

[10] M. Parandehgheibi, K. Turitsyn, and E. Modiano, "Modeling the impact of communication loss on the power grid under emergency control," *IEEE International Conference on Smart Grid Communications (SmartGridComm)*, pp. 356 – 361, 2015.

[11] M. Parandehgheibi, K. Turitsyn, and E. Modiano. (2015) Investigating the impact of communication loss on power grid stability during a large disturbance. Grid Science Winter School and Conference. [Online]. Available: http://cnls.lanl.gov/gridscience/media/Posters/Parandehgheibi.pdf

[12] M. Parandehgheibi, K. Turitsyn, and E. Modiano, "Distributed frequency control in power grids under limited communication," *arXiv preprint arXiv:1605.00947*, 2016.

[13] S. M. Rinaldi, J. P. Peerenboom, and T. K. Kelly, "Identifying, understanding, and analyzing critical infrastructure interdependencies," *Control Systems, IEEE*, vol. 21, no. 6, pp. 11–25, 2001.

[14] V. Rosato, L. Issacharoff, F. Tiriticco, S. Meloni, S. Porcellinis, and R. Setola, "Modelling interdependent infrastructures using interacting dynamical models," *International Journal of Critical Infrastructures*, vol. 4, no. 1-2, pp. 63–79, 2008.

[15] M. Parandehgheibi, H.-W. Lee, and E. Modiano, "Survivable paths in multi-layer networks," in *Information Sciences and Systems (CISS), 2012 46th Annual Conference on.* IEEE, 2012, pp. 1–6.

[16] M. Parandehgheibi, H.-W. Lee, and E. Modiano, "Survivable path sets: A new approach to survivability in multilayer networks," *Journal of Lightwave Technology*, vol. 32, no. 24, pp. 4139–4150, 2014.

[17] S. Neumayer and E. Modiano, "Assessing the effect of geographically correlated failures on interconnected power-communication networks," in *Smart Grid Communications (SmartGridComm), 2013 IEEE International Conference on*. IEEE, 2013, pp. 366–371.

[18] S. V. Buldyrev, R. Parshani, G. Paul, H. E. Stanley, and S. Havlin, "Catastrophic cascade of failures in interdependent networks," *Nature*, vol. 464, no. 7291, pp. 1025–1028, 2010.

[19] R. Parshani, S. V. Buldyrev, and S. Havlin, "Interdependent networks: reducing the coupling strength leads to a change from a first to second order percolation transition," *Physical review letters*, vol. 105, no. 4, p. 048701, 2010.

[20] J. Gao, S. V. Buldyrev, H. E. Stanley, and S. Havlin, "Networks formed from interdependent networks," *Nature physics*, vol. 8, no. 1, pp. 40–48, 2012.

[21] X. Huang, J. Gao, S. V. Buldyrev, S. Havlin, and H. E. Stanley, "Robustness of interdependent networks under targeted attack," *Physical Review E*, vol. 83, no. 6, p. 065101, 2011.

[22] O. Yagan, D. Qian, J. Zhang, and D. Cochran, "Optimal allocation of interconnecting links in cyber-physical systems: Interdependence, cascading failures, and robustness," *Parallel and Distributed Systems, IEEE Transactions on*, vol. 23, no. 9, pp. 1708–1720, 2012.

[23] D. T. Nguyen, Y. Shen, and M. T. Thai, "Detecting critical nodes in interdependent power networks for vulnerability assessment," *IEEE Trans. Smart Grid*, vol. 4, no. 1, pp. 151–159, 2013.

[24] A. Sen, A. Mazumder, J. Banerjee, A. Das, and R. Compton, "Identification of k most vulnerable nodes in multi-layered network using a new model of interde-

pendency," in *Computer Communications Workshops (INFOCOM WKSHPS), 2014 IEEE Conference on*. IEEE, 2014, pp. 831–836.

[25] A. Das, J. Banerjee, and A. Sen, "Root cause analysis of failures in interdependent power-communication networks," in *Military Communication Conference (MILCOM)*, 2014.

[26] G. Ranjan and Z.-L. Zhang, "How to glue a robust smart-grid?: a finite-network theory for interdependent network robustness," in *Proceedings of the Seventh Annual Workshop on Cyber Security and Information Intelligence Research*. ACM, 2011, p. 22.

[27] A. Bernstein, D. Bienstock, D. Hay, M. Uzunoglu, and G. Zussman, "Power grid vulnerability to geographically correlated failuresŮanalysis and control implications," in *INFOCOM, 2014 Proceedings IEEE*. IEEE, 2014, pp. 2634–2642.

[28] J. Chen, J. S. Thorp, and I. Dobson, "Cascading dynamics and mitigation assessment in power system disturbances via a hidden failure model," *International Journal of Electrical Power & Energy Systems*, vol. 27, no. 4, pp. 318–326, 2005.

[29] I. Dobson, B. A. Carreras, and D. E. Newman, "A probabilistic loading-dependent model of cascading failure and possible implications for blackouts," in *System Sciences, 2003. Proceedings of the 36th Annual Hawaii International Conference on*. IEEE, 2003, pp. 10–pp.

[30] I. Dobson, B. A. Carreras, and D. E. Newman, "A branching process approximation to cascading load-dependent system failure," in *System Sciences, 2004. Proceedings of the 37th Annual Hawaii International Conference on*. IEEE, 2004, pp. 10–pp.

[31] P. Rezaei, P. D. Hines, and M. Eppstein, "Estimating cascading failure risk: Comparing monte carlo sampling and random chemistry," in *PES General Meeting| Conference & Exposition, 2014 IEEE*. IEEE, 2014, pp. 1–5.

[32] E. B. Fisher, R. P. O'Neill, and M. C. Ferris, "Optimal transmission switching," *Power Systems, IEEE Transactions on*, vol. 23, no. 3, pp. 1346–1355, 2008.

[33] M. Andreasson, D. V. Dimarogonas, K. H. Johansson, and H. Sandberg, "Distributed vs. centralized power systems frequency control," in *2013 12th European Control Conference, ECC 2013; Zurich; Switzerland; 17 July 2013 through 19 July 2013*, 2013, pp. 3524–3529.

[34] J. W. Simpson-Porco, F. Dörfler, and F. Bullo, "Synchronization and power sharing for droop-controlled inverters in islanded microgrids," *Automatica*, vol. 49, no. 9, pp. 2603–2611, 2013.

[35] F. Dorfler, J. Simpson-Porco, and F. Bullo, "Breaking the hierarchy: Distributed control & economic optimality in microgrids," 2014.

[36] C. Zhao, E. Mallada, and F. Dörfler, "Distributed frequency control for stability and economic dispatch in power networks," in *Proceedings of American Control Conference*, 2015.

[37] S. V. Buldyrev, N. W. Shere, and G. A. Cwilich, "Interdependent networks with identical degrees of mutually dependent nodes," *Physical Review E*, vol. 83, no. 1, p. 016112, 2011.

[38] A. Bashan, Y. Berezin, S. V. Buldyrev, and S. Havlin, "The extreme vulnerability of interdependent spatially embedded networks," *Nature Physics*, vol. 9, no. 10, pp. 667–672, 2013.

[39] Y. Berezin, A. Bashan, M. M. Danziger, D. Li, and S. Havlin, "Spatially localized attacks on interdependent networks: the existence of a finite critical attack size," *arXiv preprint arXiv:1310.0996*, 2013.

[40] E. M. Shahrivar, M. Pirani, and S. Sundaram, "Robustness and algebraic connectivity of random interdependent networks," *IFAC-PapersOnLine*, vol. 48, no. 22, pp. 252–257, 2015.

[41] C. M. Schneider, N. Yazdani, N. A. Araújo, S. Havlin, and H. J. Herrmann, "Towards designing robust coupled networks," *Scientific reports*, vol. 3, 2013.

[42] M. Stippinger and J. Kertész, "Enhancing resilience of interdependent networks by healing," *Physica A: Statistical Mechanics and its Applications*, vol. 416, pp. 481–487, 2014.

[43] M. R. Garey and D. S. Johnson, *Computers and intractability*. wh freeman New York, 2002, vol. 29.

[44] M. Yannakakis, "Node-deletion problems on bipartite graphs," *SIAM Journal on Computing*, vol. 10, no. 2, pp. 310–327, 1981.

[45] J. Guo, F. Hüffner, and H. Moser, "Feedback arc set in bipartite tournaments is np-complete," *Information processing letters*, vol. 102, no. 2, pp. 62–65, 2007.

[46] V. Chvatal, "A greedy heuristic for the set-covering problem," *Mathematics of operations research*, vol. 4, no. 3, pp. 233–235, 1979.

[47] R. K. Ahuja, T. L. Magnanti, and J. B. Orlin, "Network flows," DTIC Document, Tech. Rep., 1988.

[48] U. Feige and S. Kogan, "Hardness of approximation of the balanced complete bipartite subgraph problem," *Dept. Comput. Sci. Appl. Math., Weizmann Inst. Sci., Rehovot, Israel, Tech. Rep. MCS04-04*, 2004.

[49] S. Khot, "Ruling out ptas for graph min-bisection, dense k-subgraph, and bipartite clique," *SIAM Journal on Computing*, vol. 36, no. 4, pp. 1025–1071, 2006.

[50] L. A. Wolsey, Ed., *Integer programming*. New York: Wiley, 1998, vol. 42.

[51] J.-L. Guillaume and M. Latapy, "Bipartite graphs as models of complex networks," *Physica A: Statistical Mechanics and its Applications*, vol. 371, no. 2, pp. 795–813, 2006.

[52] S. Hoory, N. Linial, and A. Wigderson, "Expander graphs and their applications," *Bulletin of the American Mathematical Society*, vol. 43, no. 4, pp. 439–561, 2006.

[53] S. P. Vadhan, *Pseudorandomness*. Now, 2012.

[54] A. Yehudayoff, "Proving expansion in three steps," *ACM SIGACT News*, vol. 43, no. 3, pp. 67–84, 2012.

[55] Ryan O'Donnel. Exapnders. [Online]. Available: http://www.cs.cmu.edu/~odonnell/toolkit13/lecture12.pdf

[56] IEC MSB - Market Strategy Board. (2012, Oct.) Grid integration of large capacity renewable energy sources and use of large-capacity electrical energy storage. [Online]. Available: http://www.iec.ch/whitepaper/pdf/iecWP-gridintegrationlargecapacity-LR-en.pdf

[57] S. Koch, S. Chatzivasileiadis, M. Vrakopoulou, and G. Andersson, "Mitigation of cascading failures by real-time controlled islanding and graceful load shedding," in *Bulk Power System Dynamics and Control (iREP)-VIII (iREP), 2010 iREP Symposium*. IEEE, 2010, pp. 1–19.

[58] D. Bienstock, "Optimal control of cascading power grid failures," in *Decision and control and European control conference (CDC-ECC), 2011 50th IEEE conference on*. IEEE, 2011, pp. 2166–2173.

[59] S. Pahwa, C. Scoglio, S. Das, and N. Schulz, "Load-shedding strategies for preventing cascading failures in power grid," *Electric Power Components and Systems*, vol. 41, no. 9, pp. 879–895, 2013.

[60] A. Chakrabortty and P. P. Khargonekar, "Introduction to wide-area control of power systems," in *American Control Conference (ACC), 2013*. IEEE, 2013, pp. 6758–6770.

[61] J. D. Glover, M. Sarma, and T. Overbye, *Power System Analysis & Design, SI Version*. Cengage Learning, 2011.

[62] A. D. Dominguez-Garcia and C. N. Hadjicostis, "Coordination and control of distributed energy resources for provision of ancillary services," in *Smart Grid*

Communications (SmartGridComm), 2010 First IEEE International Conference on. IEEE, 2010, pp. 537–542.

[63] C. Zhao, U. Topcu, N. Li, and S. Low, "Design and stability of load-side primary frequency control in power systems," *Automatic Control, IEEE Transactions on*, vol. 59, no. 5, pp. 1177–1189, 2014.

[64] E. Mallada and S. Low, "Distributed frequency-preserving optimal load control," in *World Congress*, vol. 19, no. 1, 2014, pp. 5411–5418.

[65] E. Mallada, C. Zhao, and S. Low, "Optimal load-side control for frequency regulation in smart grids," in *Communication, Control, and Computing (Allerton), 2014 52nd Annual Allerton Conference on*. IEEE, 2014, pp. 731–738.